Application of NHSi and NHGe supported Cu(I) halide complexes as efficient catalysts for A^3 and KA^2 coupling reaction: Solvent-free approach in a microwave reactor

A Thesis

submitted to

Indian Institute of Science Education and Research, Pune

In partial fulfillment of the requirements for the M.Sc. Degree Programme

by

Kashish

Registration No. 20226212

Under the guidance of

Dr. Shabana Khan

Indian Institute of Science Education and Research, Pune, Dr. Homi Bhabha Road, Pashan, Pune 411008, INDIA.

April, 2024

Certificate

This is to certify that the thesis titled "*Application of NHSi and NHGe supported Cu(I) halide complexes as efficient catalysts for A^3 and KA^2 coupling reactions: Solvent-free approach in a microwave reactor*" represents the research work carried out by **Kashish (20226212)** at the Indian Institute of Science Education and Research, Pune, towards the partial fulfillment of the MSc. degree program. The research was conducted under Dr. Shabana Khan's supervision, Department of Chemistry, during the academic year 2023-2024.

Dr. Shabana Khan

TAC Committee Members:

Dr. Shabana Khan (Associate Professor)

Dr. Sujit K. Ghosh (Professor)

This thesis is dedicated to my parents,

Mr. Om Parkash and Mrs. Veena Rani

Declaration

I hereby declare that the document entitled "*Application of NHSi and NHGe Supported Cu(I) Halide Complexes as Efficient Catalysts for A^3 and KA^2 Coupling Reaction: Solvent-Free Approach in a Microwave Reactor*" comprises the findings of my research conducted at the Department of Chemistry, Indian Institute of Science Education and Research, Pune. The research was carried out under the guidance of **Dr. Shabana Khan**, and I affirm that it has not been presented for any other degree program. Wherever others contribute, every effort is made to indicate this clearly, with due reference to the literature and acknowledgment of collaborative research and discussions.

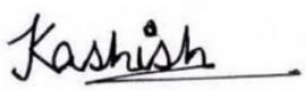

Kashish

20226212

Date: 9th April, 2024

Acknowledgments

I extend my deepest gratitude to Dr. Shabana Khan (Associate Professor) for the opportunity to conduct research under her expert guidance within her laboratory. The exceptional research environment provided by her has been instrumental in shaping my academic journey. Her valuable guidance, insightful discussions, and unwavering support have been crucial in completing my thesis project. I am extremely thankful to my expert member, Dr. Sujit Ghosh (Professor), for their valuable suggestions and advice during my project. I sincerely thank Mr. Md Jabed Hossain for his consistent support and guidance throughout my project, always being available to assist me in every aspect. My gratitude also extends to Mr. Brij Shah for his invaluable help during the lab work. I would also like to thank Ms. Moushakhi and Ms. Ruksana Akhtar for their assistance whenever I needed it. Special thanks to Ms. Prachi Gothe and Mr. Kumar Gaurav for their continuous support, making my lab experience enjoyable. I would also like to acknowledge the contributions of my other lab members, including Ms. Nilanjana, Mr. Sandeep Kaulage, Mr. Vijay Mandal, Parth, Prabhakar, and Ahan Nag, for their valuable assistance.

I express my gratitude to IISER Pune for providing a conducive research environment and also for giving me the IISER Pune IDeaS Tuition fee waiver. Special thanks to Dr. Sandeep Mishra, Mr. Nitin, and Mr. Karan for doing the NMR and to Dr. Sandeep Kanade for conducting the HRMS analysis.

Special thanks to all my friends for making this IISER journey memorable, and lastly, I extend my heartfelt thanks to my beloved family, including my parents (Mr. Om Parkash and Mrs. Veena Rani) and my brother Lovish Mehta, for their unwavering belief in me and their continuous support and assistance throughout my journey.

Table of Contents

List of Schemes

List of Charts

List of Figures

List of Tables

Table of Abbreviations

Notation	Name
A^3	Aldehyde-Amine-Alkyne
KA^2	Ketone-Amine-Alkyne
NHC	N-heterocyclic carbene
NHSi	N-heterocyclic silylene
NHGe	N-heterocyclic germylene
NMR	Nuclear magnetic resonance
RT	Room temperature
bs	Broad spectra
equiv.	equivalent
ppm	Parts per million
h	Hour
$CDCl_3$	Chloroform-D
HRMS	High-Resolution Mass Spectroscopy
TON	Turnover number
Dipp	2,6-Diisopropylphenyl
Mes	1,3,5-Trimethylphenyl
TOF	Turnover frequency

1. Abstract

N-heterocyclic silylenes (NHSis), the heavier analogs of carbenes, have been demonstrated to possess strong *σ*-donation properties and, in some cases, *π*-acceptance properties as well. These highly reactive species have attracted significant interest due to their remarkable chemistry. Though the chemistry of NHSis has been well explored in metal complexation and small-molecule activation, their activity as catalytic agents has received less attention. The reaction between a carbonyl component, an alkyne, and a secondary amine, resulting in the formation of a propargylamines, is of wide-ranging importance due to its utility in drug discovery and pharmaceutical applications. Previous reports have explored the use of NHC-supported Cu(I) complexes for catalysis of the A^3 and KA^2 coupling reactions; however, there is no report on the catalytic activity of NHSi-supported Cu(I) complexes for the same reaction.

In this thesis, we report a novel approach to the KA^2 and A^3 coupling reactions using an NHSi-supported copper (I) catalyst. The catalyst incorporates an earth-abundant and nontoxic first-row transition coinage metal, copper(I), within a silylene ligand, and its use in the KA^2 and A^3 coupling reactions affords the corresponding propargyl amines in excellent yield with low catalyst loading and fast reaction times. We have thoroughly expounded on the substrate scope of the reaction and tested the catalyst's reactivity with challenging substrates. In addition, we have also tested the catalytic activity of the corresponding N-heterocyclic germylene (NHGe) complexes and compared their utility as catalysts. The NHSi-based complex effectively catalyzes both the facile A^3 reaction and the comparatively more challenging KA^2 reaction with near-quantitative yield. (**Figure 1**).

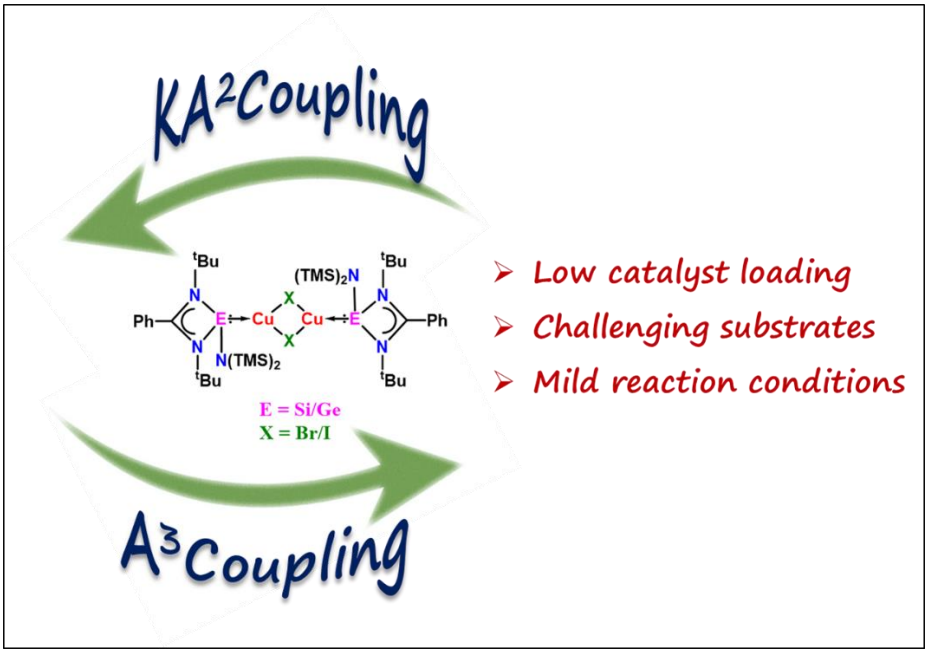

Figure 1: A^3 and KA^2 coupling by NHSi and NHGe supported Cu(I) halide complexes.

2. Introduction

Carbenes are low-valent carbon species characterized by the presence of six-valence electrons on a carbon atom. Long considered to be mere intermediates in organic reactions, the chemistry of these fleeting compounds was solidly established in 1991 when Arduengo successfully isolated carbenes using nitrogen-containing backbones, leading to the development of N-heterocyclic carbenes (NHCs).[1] The highly electrophilic carbon center in NHCs is stabilized by conjugation with the lone pairs of the neighboring N-atoms, and these species exist in the singlet configuration with a lone pair and an empty *p*-orbital on the same atom. Because of their lone pairs and vacant orbitals, these NHCs have garnered attention for their stability and dual functionality as both Lewis acids and bases. These characteristics enable NHCs to form robust transition metal complexes, whose strength often surpasses that of complexes with traditional ligands like phosphines.[2] As we go down the members of Group 14, encountering elements like silicon, germanium, tin, and lead, a decrease in the extent of hybridization becomes apparent. This phenomenon is due to the larger atomic radii and reduced overlap between *s* and *p*-orbitals,[3] resulting in higher energy gaps between singlet and triplet states. Even though carbenes and tetrylenes (their heavier congeners) have been successfully isolated and are stable under an inert atmosphere, they exhibit highly unfavorable oxidation states, making them extremely

reactive and prone to oligomerization or polymerization.[4] This reactivity poses challenges in handling and isolating these compounds, necessitating both kinetic and thermodynamic stabilization strategies. Thermodynamic stabilization involves appending the carbene nucleus with heteroatoms that donate electron-density into its vacant orbital *via* the mesomeric effect. In contrast, kinetic stabilization is achieved by employing bulky substituents, which prevent dimerization and protect against external nucleophile attacks (**Figure 2**).

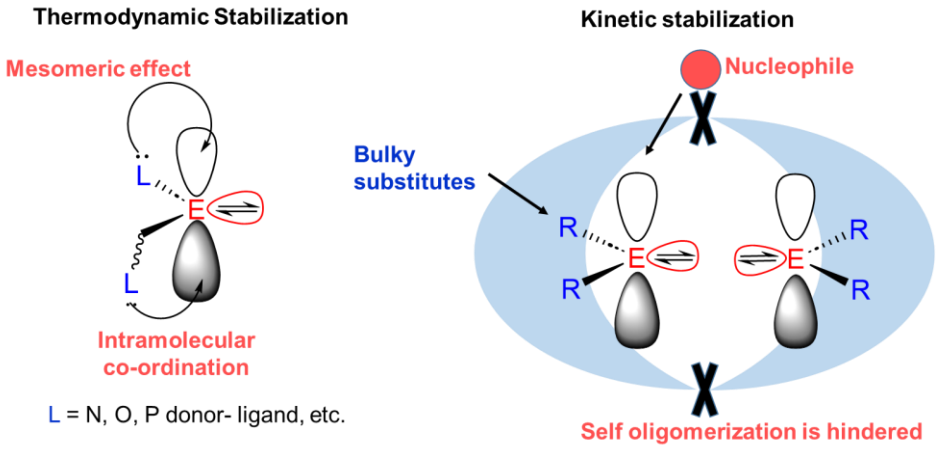

Figure 2: Thermodynamic and Kinetic stabilization of tetrylenes. (E= group-14 elements).

The investigation of coinage metal complexes, particularly those possessing d^{10} electronic configurations such as copper (Cu), silver (Ag), and gold (Au), has garnered considerable attention within the field of transition metal chemistry. The chemistry of these complexes has undergone a paradigm shift in recent years, and their photophysical properties, strong metal binding capabilities, and promising catalytic applications are areas of active research. NHCs have emerged as crucial ligands for stabilizing low-valent main group elements and forming transition metal complexes.[5] Despite significant advancements in exploring NHCs and their applications, a research gap exists concerning the catalytic potential of heavier tetrylene complexes, particularly in conjunction with coinage metals like copper, silver, and gold. NHSis, the heavier analogs of carbenes, have demonstrated utility in activating small molecules and forming transition metal complexes, facilitating C-C and C-X bond formations and reduction reactions.[6] However, the catalytic applications of NHSi-supported coinage metal complexes have received comparatively lesser scholarly attention. This

emphasizes the imperative requirement to explore the catalytic potential of heavier tetrylenes to fully exploit their capabilities and propel the advancements in this field.

The metals in group 11 tend to form weak complexes with arenes and usually do not coordinate in the η^6 mode. However, our group has isolated Cu(I) arene complexes in the η^6 mode for the first time.[7] The Si(II)→Cu(I) complexes have demonstrated potential as effective homogeneous catalysts in crucial reactions such as the hydrosilylation of ketones reported by the group of Barceiredo and Kato[8] (**Chart 1a**) and alkyne-azide cycloaddition reactions reported by Stalke and co-workers (**Chart 1b**).[9] Our group has contributed to this area by reporting CuAAC reactions facilitated by NHSi-supported Cu(I) cationic **(Chart 1c)**[10] and NHSi-supported Cu(I) halide complexes (**Chart 1f**).[11] Notably, the literature on the use of NHSi-supported gold and silver complexes as homogeneous catalysts is limited, with our group being among the few to investigate such applications, including the use of NHSi-supported gold cationic complexes in glycosidation reactions (**Chart 1d**)[12] and NHSi-stabilized low-coordinate Ag(I)···Arene cationic complex (**Chart 1e**) in A^3 coupling reactions.[13]

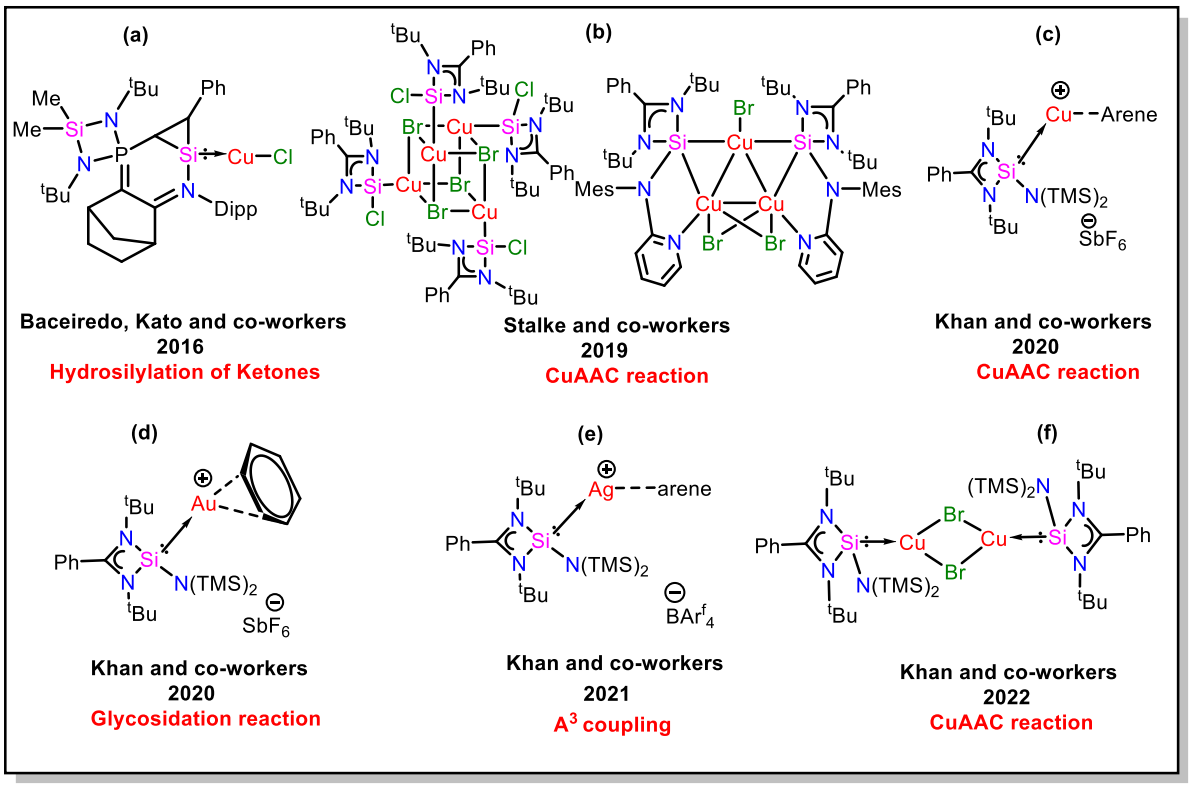

Chart 1: Application of NHSi-supported coinage metal complexes (Dipp= 2,6-Diisopropylphenyl, Mes= 1,3,5-Trimethylphenyl).

The potential demonstrated by NHSi-supported coinage metal complexes has led us to focus on NHSi-supported coinage metal complexes, particularly copper, due to its cost-effectiveness and widespread availability compared to other coinage metals. The primary motivation for this study is to fill the current gap in knowledge about these complexes and to investigate their catalytic capability thoroughly. Our research focused on a benzamidinato-ligated silylene featuring a four-membered ring architecture. This selection was based on its straightforward synthesis, high thermodynamic stability, and the ability to adjust its *σ*-donation and *π*-acceptance properties by modifying the group attached to the silicon center.[14] Among the available variants, we selected PhC(N^{t}Bu)$_2$SiN(TMS)$_2$ due to its greater *σ*-donation capabilities compared to other substitutions (**Figure 3**).[15] It showed the smallest HOMO-LUMO gap among N-donors attached to the silicon center. In choosing the catalytic reaction, we considered reactions relevant to industrial and commercial applications. Propargylamines are particularly interesting due to their extensive applications in drug delivery and pharmaceuticals.[16] As a result, we have decided to concentrate on synthesizing propargylamines as part of our investigation into the versatile applications of NHSi complexes.

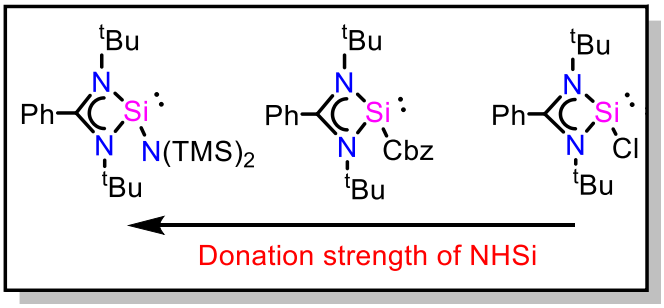

Figure 3: Comparison of donor strength of silylenes (Cbz= carbazole).

2.1 Catalysis involving Multicomponent reaction

Propargylamines are a class of compounds of significant importance due to their utility in biological contexts, drug delivery, and pharmaceutical applications. The conventional approach for synthesizing propargylamines involves generating metal acetanilides using stoichiometric amounts of harsh bases or organometallic reagents, followed by their reaction with *in situ* generated imines.[17] However, this method suffers from drawbacks, such as the need for purification at each stage, as it is a multistep synthesis that compromises its environmental sustainability.

A cleaner and more efficient route to synthesize propargylamines is through a multicomponent reaction (MCR) that combines three or more reactants. MCRs promote green chemistry principles by reducing waste with increasing efficiency. As such, they have become an important focus of modern synthetic chemistry research, with numerous applications in the fields of organic synthesis and drug discovery. The three-component A^3 (aldehyde-amine-alkyne) and KA^2 (ketone-amine-alkyne) coupling reactions are efficient methods for synthesizing propargylamines, which employ transition metal catalysts to activate the alkyne C-H bond, enabling the reaction to occur under mild conditions.[18]. Various transition metals, including Cu, Ag, and Au, have been explored for the A^3 coupling reaction, with copper being favored for its cost-effectiveness.

Wei and co-workers in 2002 demonstrated an A^3 coupling reaction catalyzed by a combination of $RuCl_3$ and CuBr, which showed a substantial increase in yield compared to using CuBr alone.[19] Following this, Tye and co-workers showcased another approach for catalyzing the A^3 coupling reaction in 2003, utilizing copper chloride (CuCl) in dioxane at 150 °C.[20] Building on these findings, Fan, and co-workers (2004) introduced a rapid microwave-assisted A^3 coupling method using copper Iodide (CuI) (15 mol %) and water as a solvent, reducing reliance on organic solvents.[21] Similarly, Nagaiah and co-workers offered an environment-friendly alternative with an ionic liquid as a solvent and copper bromide (CuBr) as a catalyst.[22] Yadav and co-workers also corroborated this method (2004), using 8 mol% of CuBr under neat conditions at 100 °C.[23] Eycken and co-workers (2010) further contributed to this field by utilizing CuBr (20 mol %) as a catalyst.[24] Additionally, other studies explored the use of copper cyanide (CuCN) [25] and copper(II) trifluoromethanesulfonate [$Cu(OTf)_2$] [26] as a catalyst. In 2015, Eycken and co-workers employed a mixture of copper (I) chloride (CuCl) and copper (II) chloride ($CuCl_2$) as catalysts at 110 °C, further diversifying the range of catalysts explored for the A^3 coupling reaction.[27] Despite these advancements, challenges persist, such as high catalyst loading, elevated temperature requirements, and higher reaction times. This necessitates investigating modifications to the ligand or copper center properties to enable the A^3 coupling reaction to occur under milder conditions, which would contribute significantly to the advancement of this field. In 2013, Navarro and co-workers utilized NHCs in the A^3 coupling reaction, employing a homogenous NHC-supported Cu(I) complex (**Chart**

2a).[28] However, similar progress has not been made for the analogous NHSi-supported Cu(I) complex.

The KA^2 coupling reaction remains a challenging reaction in organic synthesis. The KA^2 coupling reaction involves the combination of a ketone, an alkyne, and an amine, presenting significant hurdles due to the lower reactivity of ketimines compared to aldimines, which is attributed to factors like a steric hindrance and electronic effects.[29] Recent advancements have addressed these challenges. Eycken and co-workers pioneered the use of CuI at 100 °C,[30] while Larsen and co-workers employed $Cu(OTf)_2$ with cyclohexanone[31] and $CuCl_2$ with $Ti(OEt)_4$ as an additive at 110 °C to improve ketone electrophilicity.[32] Ma and co-workers successfully used CuBr with molecular sieves as additives.[33] However, these methods often require higher catalyst loadings, increased temperatures, longer reaction times, and additives. In 2023, Vougioukalakis and co-workers utilized 4 mol % Cu(I) NHC as a catalyst and $Ti(OEt)_4$ as an additive for enhancing the ketone electrophilicity in KA^2 coupling reactions (**Chart 2b**)[34]. However, as is the case for the A^3 reaction, there are no reports on the analogous NHSi-supported Cu(I) complex for catalysis of the KA^2 reaction.

Based on the available literature and in pursuit of our research focus on silylene complexes in catalysis, we have strategically chosen to employ our NHSi-supported Cu(I) bromide complex for catalyzing the A^3 and KA^2 coupling reactions (**Chart 2c**). This project aims to comprehensively investigate silylene complexes' catalytic capabilities and explore their potential applications in organic synthesis.

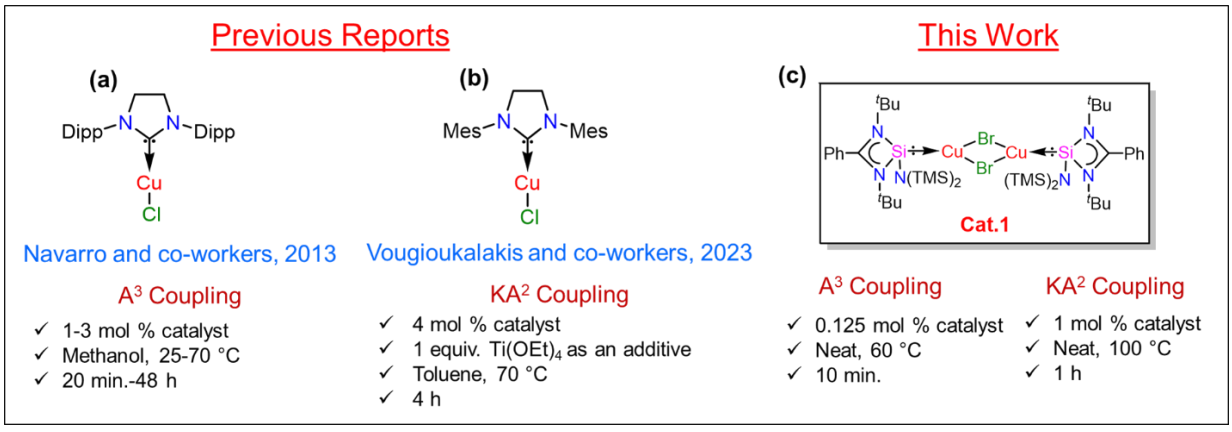

Chart 2: Reported NHC-supported Cu(I) complexes for A^3 and KA^2 coupling reactions.

3. Experimental Section

3.1 Material and Instrumentations

All experimental procedures were conducted under inert gas conditions using the standard Schlenk technique within an argon-filled MBRAUN MB 150-GI glovebox. The solvents used in the experiments were purified using the MBRAUN MB SPS-800 solvent purification system. Chemicals used in the study were sourced from reputable suppliers, including Sigma Aldrich, Alfa-Aesar, ChemScene, and BLD Pharma. The synthetic procedure for silylene and germylene-supported Cu(I) complexes was followed as reported in the literature.

3.2 Analytical Methods

The ^{1}H and ^{13}C NMR spectra were recorded in $CDCl_3$ solvents using a Bruker 400 MHz spectrometer. Mass spectrometry data were acquired using an AB Sciex 4800 plus HRMS instrument.

4. Results and Discussion

In 2021, our group initially attempted the A^3 coupling reaction using the [Ag(I)-η^2-arene]$^+$ complex. However, we pursued an alternative catalyst due to its inherent instability as a cationic species. We explored the potential of silylene-based complexes in coupling reactions and turned to silylene-based copper complexes for the A^3 and KA^2 coupling reactions. Notably, silylene-supported copper halide complexes have been successfully employed in click chemistry reactions. Therefore, we utilized our previously reported NHSi-supported Cu(I) bromide complex for A^3 and KA^2 coupling reactions. This complex was synthesized by reacting NHSi with CuBr in a 1:1 ratio, followed by overnight stirring and vacuum filtration to obtain Cat. 1 (**Scheme 1**)

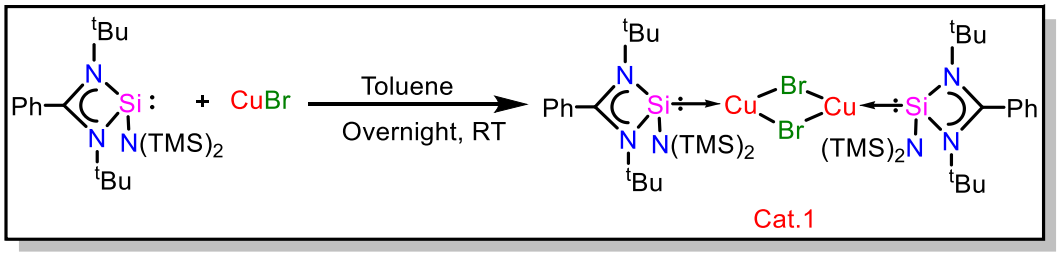

Scheme 1: Synthesis of NHSi- Cu(I) bromide complex.

4.1 Optimization of A^3 coupling reaction

Our investigation commenced with the selection of paraformaldehyde, phenylacetylene, and piperidine as reactants for the A^3 coupling reaction, conducted with the help of microwave irradiation. The aim was to systematically evaluate the reaction conditions by varying catalyst loadings and reaction temperatures.

Initially, 0.5 mol% of the catalyst was employed at a temperature of 100°C in neat conditions under microwave irradiation for 10 minutes. Subsequently, the product was purified using column chromatography, resulting in a product yield of >99%. We obtained a nearly quantitative yield of the product, which was also obtained upon reducing the reaction temperature to 60 °C while maintaining the same catalyst loading and reaction time. Conversely, conducting the reaction at room temperature diminished the yield by 40 %. Further optimization involved maintaining the reaction temperature at 60 °C while decreasing the catalyst loading to 0.25 mol % and then to 0.12 mol %, yielding a product yield over 99 % within 10 minutes. However, subsequent reductions in catalyst loading led to decreased product yield.

Ultimately, we established the optimized conditions for the reaction, achieving the highest yield (>99 %) with 0.12 mol % of catalyst at 60 °C within 10 minutes of the reaction (Entry-8) (**Table 1**). These findings demonstrate the effectiveness of silylene-supported Cu(I) bromide complexes in catalyzing the A^3 coupling reaction under controlled reaction conditions.

Table 1: Optimization of reaction conditions for A^3 coupling reaction catalyzed by NHSi-supported Cu(I) complex.

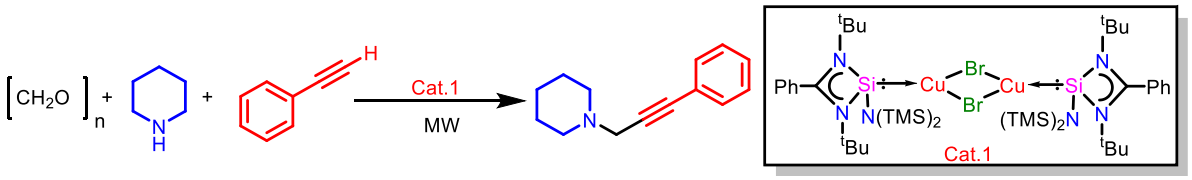

Entry	Catalyst	Mol (%)	Temp (°C)	Time (min)	Yield* (%)
1	Cat. 1	0.5	80	60	>99
2	Cat. 1	0.5	100	10	>99
3	Cat. 1	0.5	100	5	92
4	Cat. 1	0.5	60	10	>99

5	Cat. 1	0.5	RT	30	40
6	Cat. 1	0.1	120	30	88
7	Cat. 1	0.25	60	10	>99
8	Cat. 1	0.125	60	10	>99

*Isolated yields were calculated after column chromatography by performing the reaction at 0.5 mmol scale

4.2 Substrate Scope

With the optimized conditions established, we aimed to explore the utility of our catalyst in catalyzing the A^3 coupling reaction for a diverse range of substrates. Our investigation delved into investigating the effect of different combinations of the alkyne, amine, and aldehyde components. Remarkably, we found that our catalytic system exhibited excellent compatibility with both cyclic and acyclic secondary amines. Specifically, diethylamine and bulky diisopropylamine yielded good to excellent product yields when combined with alkynes and aldehydes. Furthermore, variations in the alkyne substrates were explored, and it was noted that both electron-donating and withdrawing groups led to moderate to excellent product yields. In addition, the impact of changing the aldehyde substrate from paraformaldehyde to benzaldehyde was studied by reacting benzaldehyde with piperidine and phenylacetylene, which resulted in an excellent yield of >99 %. These observations highlight the versatility and efficiency of our catalyst across a broad range of amine, alkyne, and aldehyde substrates.

Moreover, we tested our catalytic system by utilizing dialkynes and trialkynes, the use of which as substrates has not yet received much scholarly attention. Treating 1,4-diethynylbenzene with 2 equiv. Paraformaldehyde and piperidine yielded product **1i** (**Scheme 2**) in >99 % yield. Similarly, treating 1,3,5-triethynylbenzene with 3 equiv. of paraformaldehyde and piperidine produced product **1j** (**Scheme 2**) in 90 % yield, further indicating the versatility and effectiveness of our catalytic system and its compatibility with hitherto unexplored substrates.

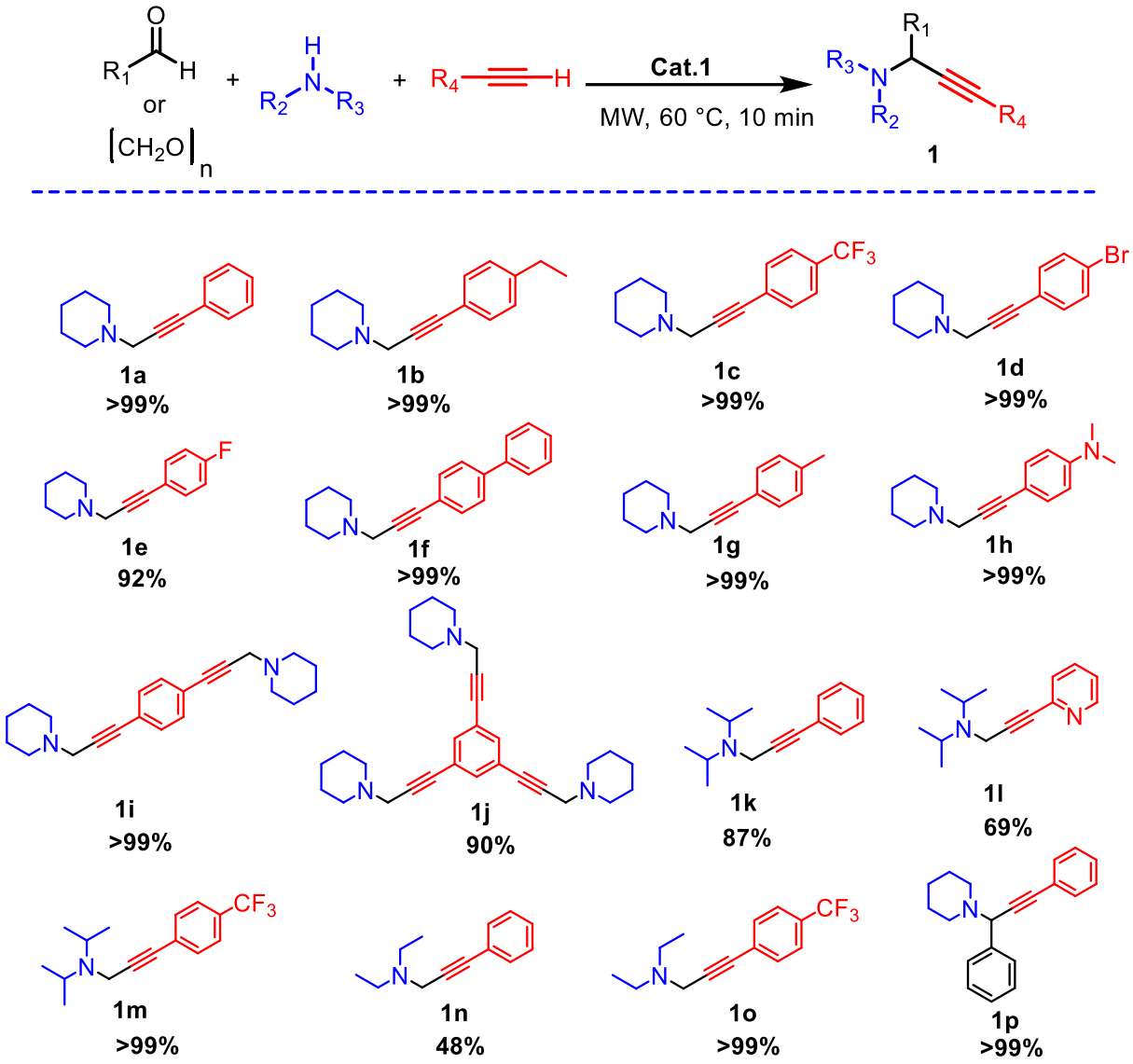

Scheme 2: Substrate Scope of A^3 Coupling reaction catalyzed by NHSi-supported Cu(I) bromide complex. All are isolated yields, calculated after column chromatography by performing a reaction on a 0.5 mmol scale.

1p: Temperature: 70°C

4.3 KA^2 Coupling reaction

Following successfully exploring the A^3 coupling reaction using our catalyst, we focused on the challenging KA^2 reaction, which has not been extensively studied with silylene-supported Cu(I) catalysts. To this end, we selected cyclohexanone, piperidine, and phenylacetylene as reactants and conducted the KA^2 coupling reaction under microwave irradiation.

4.3.1 Optimization of KA^2 coupling reaction

Our investigation began by utilizing 1 mol % of the catalyst at 100 °C for 60 minutes under microwave irradiation. After completion of the reaction, the product was isolated through column chromatography with 86 % yield. Subsequent attempts to reduce either the reaction time or temperature while maintaining the catalyst loading resulted in decreased yields. Interestingly, increasing the temperature to 150 °C for 120 minutes did not significantly impact the yield. However, lowering the catalyst loading to 0.5 mol % at 100 °C led to a decrease in yield.

Through systematic optimization, we identified the optimal conditions for the KA^2 coupling reaction, achieving the highest yield of the product with 1 mol % of catalyst at 100 °C for 60 minutes (Entry-1) (**Table 2**). These findings significantly advance the exploration of the KA^2 reaction using silylene-supported Cu(I) catalysts and pave the way for further investigations into this challenging reaction.

Table 2: Reaction optimization of KA^2 Coupling reaction catalyzed by NHSi-supported Cu(I) complex.

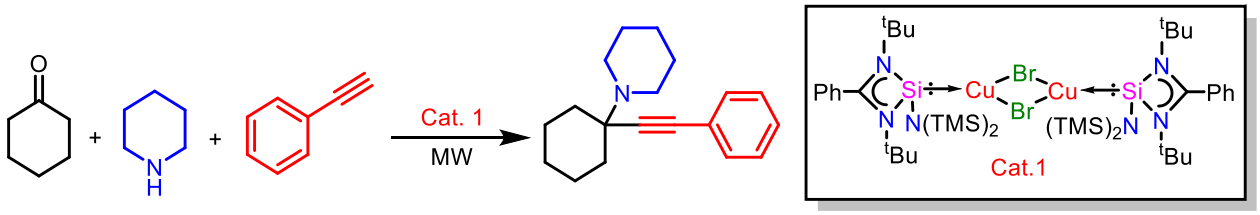

Entry	Catalyst	Mol (%)	Temp (°C)	Time (min)	Yield* (%)
1	Cat. 1	1	100	60	86
2	Cat. 1	1	100	30	78
3	Cat. 1	1	80	60	58
4	Cat. 1	1	150	120	90
5	Cat. 1	0.5	100	60	75
6	Cat. 1	1	100	120	89

*Isolated yields were calculated after column chromatography

4.3.2 Substrate Scope

Following the successful outcome of the KA^2 coupling reaction under optimized conditions, our focus transitioned to assessing the reaction's versatility through

substrate scope studies. Keeping piperidine and cyclohexanone constant, we systematically varied the alkyne substrates to explore the catalyst's ability to perform under diverse conditions. We obtained the corresponding products in moderate to good yields by utilizing a range of electron-donating and electron-withdrawing alkyne. The amine component of the reaction was also varied, and excellent product yields were observed upon using a variety of amines. Good to excellent product yields were also obtained by using morpholine, which is less nucleophilic than carbocyclic amines due to the presence of an electronegative oxygen atom. Variations in the ketone component were also explored by utilizing different ketones in the reaction. To show our system's compatibility with linear ketones, we conducted the reaction of 2-butanone with pyrrolidine and phenylacetylene, which gave positive results. Similar to our studies for the A^3 reaction, we extended our investigation to include dialkynes. Treating 1,4-diethynylbenzene with 2 equiv. of cyclohexanone and morpholine produced the desired product with a >99 % yield. These findings underscore the potential applicability of our developed methodology across various KA^2 coupling reactions with diverse substrates (**Scheme 3**)

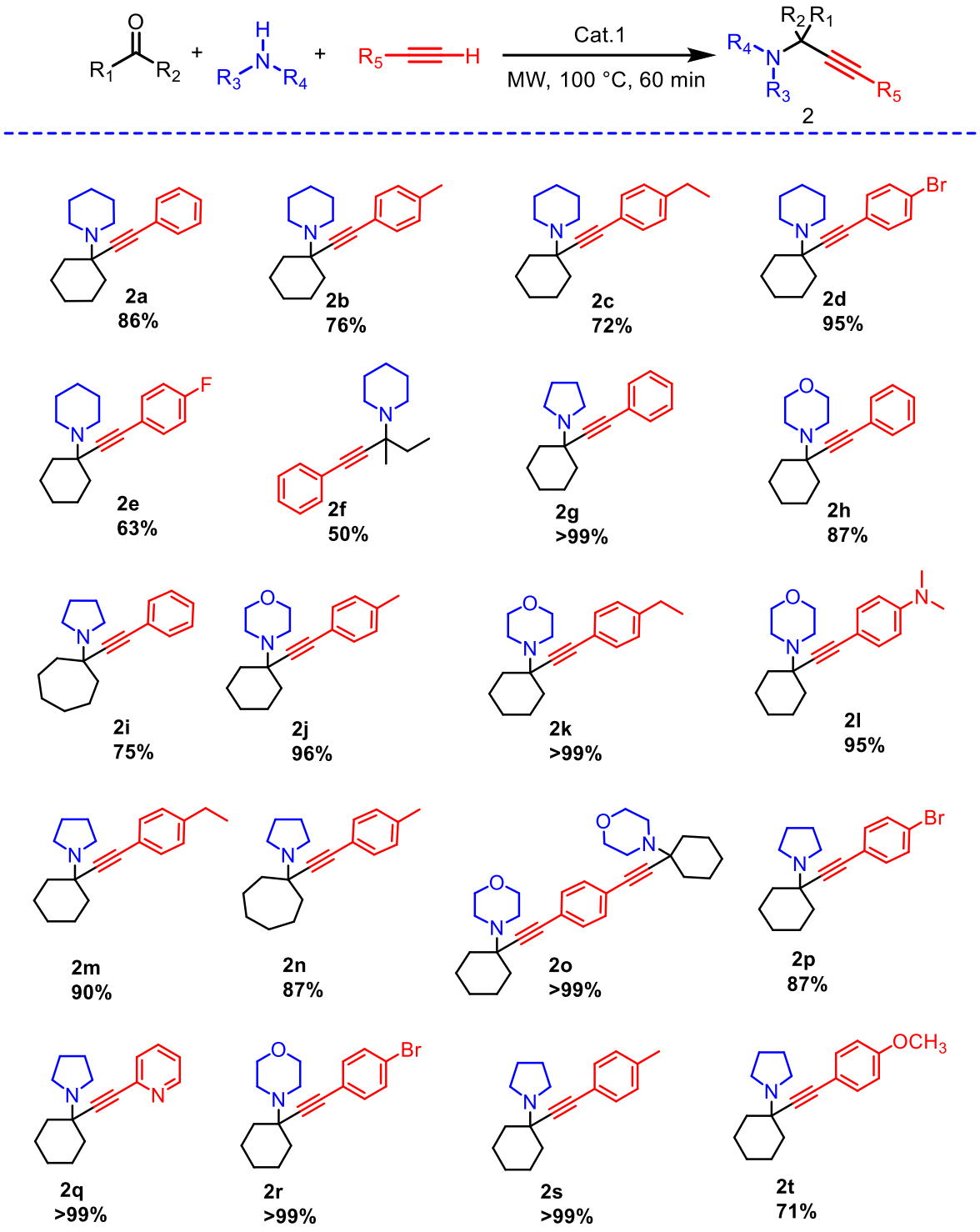

Scheme 3: Substrate scope of KA^2 coupling reaction catalyzed by NHSi-supported Cu(I) bromide complex. Isolated yields were calculated after column chromatography by performing the reaction at a 0.5 mmol scale.

4.4 Comparison of NHSi and NHGe-supported Cu(I) complexes

After successfully conducting the A^3 and KA^2 coupling reactions using NHSi-supported Cu(I) bromide complex, we extended our investigation to include NHGe-supported Cu(I) complexes. Specifically, we utilized four complexes: NHSi-supported Cu(I) bromide complex, NHSi-supported Cu(I) iodide complex, and their respective NHGe analogs (**Figure 4**).

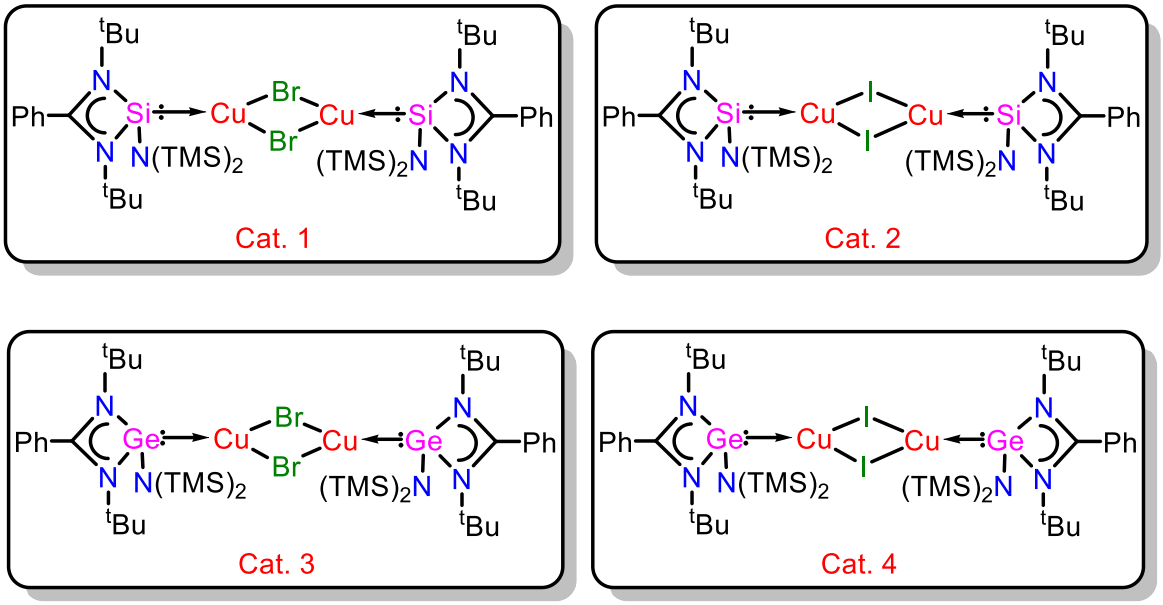

Figure 4: NHSi and NHGe supported Cu(I) halide complexes used for A^3 and KA^2 coupling reaction.

The NHGe-supported complexes were tested using them as catalysts for the A^3 reaction under the previously optimized conditions. It was observed that the NHSi-supported Cu(I) bromide and iodide complexes yielded better results than their germylene counterparts (**Table 3**). This outcome suggests that NHSi exhibits superior ligand efficiency over NHGe in catalytic applications. Interestingly, the silylene-supported Cu(I) bromide complex demonstrated higher efficiency than its iodide counterpart, possibly due to its larger size.

Table 3: A^3 coupling with NHSi and NHGe supported Cu(I) halide complexes

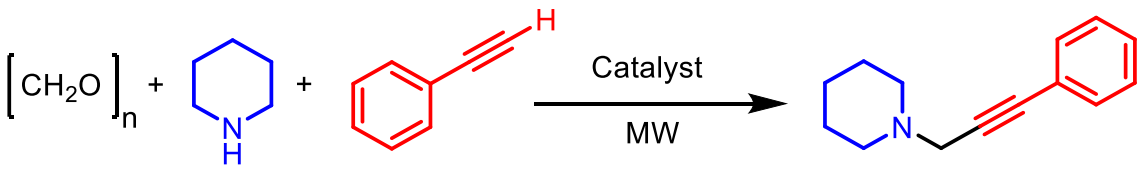

Entry	Catalyst	Mol (%)	Temp (°C)	Time (min)	Yield* (%)
1	Cat. 1	0.125	60	10	>99
2	Cat. 2	0.125	60	10	>99
3	Cat. 3	0.125	60	10	60
4	Cat. 4	0.125	60	10	40

*Isolated yields were calculated after column chromatography.

After optimizing the A^3 coupling, we moved towards the catalysis of the KA^2 coupling reaction with these four complexes. The previously optimized reaction conditions were employed, and it was observed that the NHSi-supported complexes yielded better than the germylene analogs (**Table 4**). Also, as noted previously, NHSi and NHGe-supported Cu(I) bromide complexes gave better yields than the corresponding iodide complexes.

Table 4: KA^2 coupling with NHSi and NHGe supported Cu(I) halide complexes.

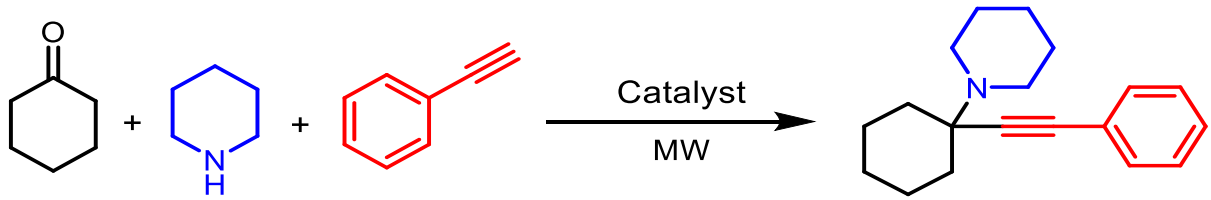

Entry	Catalyst	Mol (%)	Temp (°C)	Time (min)	Yield* (%)
1	Cat. 1	1	100	60	86
2	Cat. 2	1	100	60	77
3	Cat. 3	1	100	60	73
4	Cat. 4	1	100	60	54

*Isolated yields were calculated after column chromatography.

4.5 A plausible mechanism of A^3 and KA^2 coupling reaction

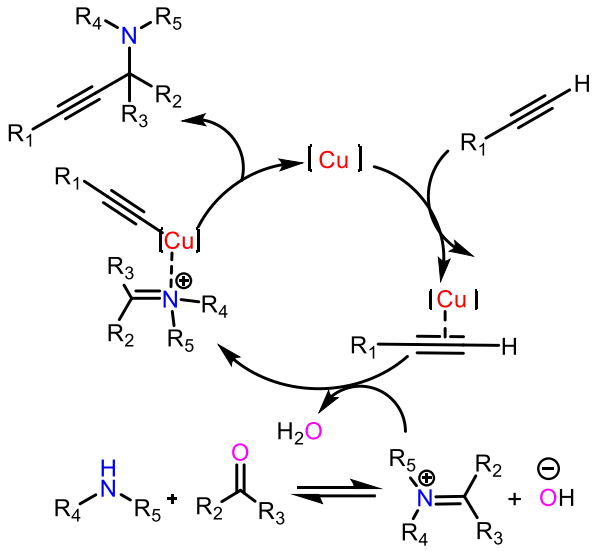

Scheme 4: Plausible mechanistic cycle for A^3 and KA^2 coupling reaction.

The A^3 and KA^2 coupling reactions is likely to be initiated by the interaction of the alkyne with the Cu-complex, leading to the formation of a Cu acetanilide complex and increasing the acidity of the neighboring hydrogen atom, rendering it susceptible to abstraction even by a weaker base. Subsequently, the generated aldimine/ ketimine, from the reaction between the aldehyde/ketone and amine, interacts with the Cu acetanilide complex, leading to the formation of the desired product, accompanied by the release of water as a byproduct (**Scheme 4**).[35,36]

4.6 Comparison of TON and TOF with the reported literature

In our recent comparative study of A^3 coupling catalysis, we evaluated the performance of our catalyst against those catalysts existing in the literature. Our findings revealed that the catalyst we developed achieved a turnover number (TON) of 792 and a turnover frequency (TOF) of 4771 h^{-1}, positioning it second only to the Ag-cationic complex previously reported by our group in 2021 (**Table 5**). Notably, our catalyst demonstrates advantages in terms of temperature (low) and higher product yield. Despite the superior activity metrics of the Ag-cationic complex, its cationic nature predisposes it to instability and a propensity for decomposition. Conversely, our catalyst exhibits enhanced stability due to its neutral nature, presenting a significant improvement over the Ag complex.

Table 5: Comparison of A^3 coupling with the previously reported literature

Entry	Catalyst	Temp. (°C)	Yield[#] (%)	Time (h)	TON*	TOF* (h^{-1})
1	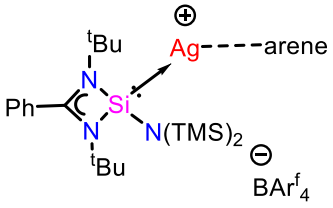 (Best report in literature)[13]	150	64	0.083	1280	15360
2	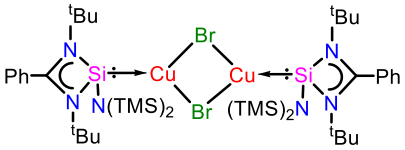 **(This Work)**	60	99	0.166	792	4771

*TON and TOF are compared by using phenylacetylene, piperidine, and paraformaldehyde as a substrate; [#]Isolated Yield

Upon comparison of the silylene complex with its previously reported lower analog, NHC, it was observed that our catalyst demonstrated superior efficiency, necessitating a significantly reduced mol % of the catalyst.(**Table-6**)

Table 6: Comparison of A^3 coupling with previously reported Cu(I) NHC Complex

Entry	Catalyst	Mol (%)	Yield[#] (%)	Time (h)	TON*	TOF* (h^{-1})
1	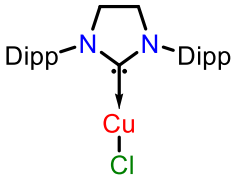 Cu(I)-NHC complex[28]	3	88	48	29.33	0.611
2	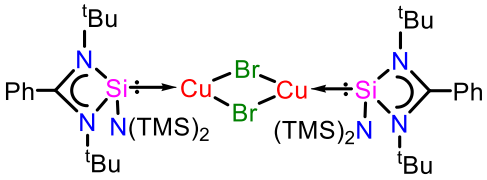 **(This Work)**	0.125	99	0.16	792	4771

*TON and TOF are compared by using phenylacetylene, piperidine, and benzaldehyde as a substrate at 70 °C; [#]Isolated Yield

Subsequent to this study, a comparative analysis was conducted on the efficiency of various homogeneous catalysts reported to date with our synthesized catalyst for the KA^2 coupling reaction. Our findings indicate that our catalyst exhibits superior performance, evidenced by a turnover number (TON) of 86 and a turnover frequency (TOF) of 86 h^{-1}, outstripping the efficiency of the previously reported NHC complex (**Table 7**), and also it shows better efficiency than all the homogenous catalyst reported so far for KA^2 coupling reaction.

Table 7: Comparison of KA^2 coupling with the previously reported literature

Entry	Catalyst	Mol (%)	Temp. (°C)	Time (h)	Yield# (%)	TON*	TOF* (h^{-1})
1	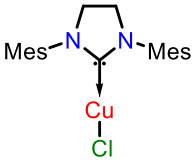 Cu(I) NHC complex[34]	4	70	4	94	23.5	5.87
2	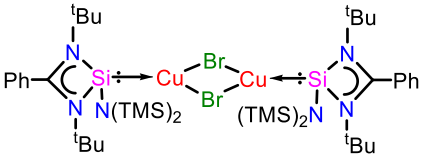 **(This Work)**	1	100	1	86	86	86

***TON** and TOF are compared by using phenylacetylene, piperidine, and cyclohexanone as a substrate; #Isolated Yield

5. Conclusion

Our exploration into NHSi-Cu(I) complexes for the A^3 and KA^2 coupling reactions marks a significant advancement in catalysis. These reactions exhibit sustainability due to low catalyst loading, rapid reaction times, and mild reaction conditions. Our catalyst demonstrates remarkable efficiency even with challenging substrates under milder conditions, showcasing its versatility and applicability in catalyzing complex reactions. Additionally, we investigated the impact of replacing NHSi with its heavier analog NHGe, observing its effect on the yield of the coupling reactions. Notably, we achieved the challenging KA^2 coupling reaction without any additives and under milder reaction conditions, highlighting the potential of our approach.

6. References

1. Arduengo, A. J.; Harlow, R. L.; Kline, M. *J. Am. Chem. Soc.* **1991**,*113*, 361-363.
2. (a) Crudden, C. M.; Allen D. P. *Coord. Chem. Rev.* **2004**, *248*, 2247-2273. (b) Sau , S. C.; Hota P. K.; Mandal S. K.; Soleilhavoup, M.; Bertrand G. *Chem. Soc. Rev.* **2020**, *49* , 1233-1252 . (c) Visbal R.; Gimeno, M. C. *Chem. Soc. Rev.* **2014**, *43*, 3551-3574. (d) Smith, C. A.; Narouz, M. R.; Lummis, P. A.; Singh I.; Nazemi, A.; Li, C. -H.; Crudden, C. M. *Chem. Rev.* **2019**, *119*, 4986-5056.
3. (a) Gaspar, P. P.; Xiao, M.; Pae, D. H.; Berger, D. J.; Haile, T.; Chen, T.; Lei, D.; Winchester, W. R.; Jiang, J. P. J. *Organomet. Chem.* **2002**, *646*, 68-79. (b) Apeloig, Y.; Pauncz, R.; Karni, M.; West, R.; Steiner, W.; Chapman, D. *Organometallics* **2003**, *22*, 3250-3256. (c) Mizuhata, Y.; Sasamori, T.; Tokitoh, N. *Chem. Rev.* **2009**, *109*, 3479-3511.
4. West, R.; Fink, M. J.; Michl, J. *Science* **1981**, *214*, 1343-1344.
5. (a) Lin, J. C.; Huang, R. T.; Lee, C.S.; Bhattacharyya, A.; Hwang, W.S.; Lin, I.J. *Chem. Rev.* **2009**, *109*, 3561-3598. (b) Mora, M.; Gimeno M. C.; Visbal R. *Chem. Soc. Rev.* **2019**, *48*, 447-462. (c) Hossain, J.; Akhtar, R.; Khan, S. *Polyhedron* **2021**, *201*, 115151-115187. (d) Jazzar, R., Soleilhavoup, M; Bertrand, G; *Chem. Rev.* **2020**, *120*, 4141-4168.
6. (a) Raoufmoghaddam, S.; Zhou, Y. -P.; Wang, Y.; Driess, M. *J. Organomet. Chem.* **2017**, *829*, 2-10. (b) Schmidt, M.; Blom, B.; Szilvási, T.; Schomäcker, R.; Driess, M. *Chem. Eur. J.* **2013**, *19*, 40-62. (c) Zhou, Y. -P.; Driess, M. *Angew. Chem. Int. Ed.* **2019**, *58*, 3715-3728.
7. Parvin, N.; Pal, S.; Echeverría, J.; Alvarez, S.; Khan, S. *Chem. Sci.* **2018**, *9*, 4333-4337.
8. Troadec, T.; Prades, A.; Rodriguez, R.; Mirgalet, R.; Baceiredo, A.; Saffon-Merceron, N.; Branchadell, V.; Kato, T. *Inorg. Chem.* **2016**, *55*, 8234-8240.
9. Paesch, A. N.; Kreyenschmidt, A. -K.; Herbst-Irmer, R.; Stalke, D. *Inorg. Chem.* **2019**, *58*, 7000-7009.
10. Parvin, N.; Hossain, J.; George, A., Parameswaran, P.; Khan, S. *Chem. Commun.* **2020**, *56*, 273-276.
11. Hossain, J.; Gopinath, J. S.; Tothadi S.; Parameswaran, P.; Khan S. *Organometallics* **2022**, *41*, 3706-3717.

12. Parvin, N.; Mishra, B.; George, A.; Neralkar, M.; Hossain, J;. Parameswaran, P.; Hotha, S.; Khan, S. *Chem. Commun.* **2020**, *56*, 7625-7628.
13. Parvin, N.; Sen, N.; Tothadi S.; Muhammed, S.; Parameswaran P.; Khan, S. *Organometallics* **2021**, *40*, 1626-1632.
14. (a)Sen, S. S.; Khan, S.; Samuel, P. P.; Roesky, H. W. *Chem. Sci.* **2012**, *3*, 659-682. (b) So, C. W.; Roesky, H. W.; Magull J.; Oswald R. B. *Angew. Chem. Int. Ed.* **2006**, *45*, 3948-3950. (c) Sen, S. S.; Roesky, H. W.; Stern D.; Henn, J.; Stalke D. *J. Am. Chem. Soc.* **2010**, *132*, 1123-1126.
15. Ghosh, M.; Tothadi S.; Khan, S. *Organometallics* **2021**, *40*, 3201-3210.
16. (a) Baranyi, M.; Porceddu, P. F.; Gölöncsér, F.; Kulcsár, S; Otrokocsi, L; Kittel, Á.; Pinna, A.; Frau, L.; Huleatt, P. B.; Khoo, M. -L; Chai, C. L. L; Dunkel, P.; Mátyus, P.; Morelli, M.; Sperlágh, B. *Mol. Neurodegener* **2016**, *11*, 6. (b) Chen, J. J.; Swope, D. M.; *Clin. J. Pharmacol.* **2005**, *45*, 878-894. (c) Weinreb, O.; Mandel, S.; Bar-Am, O.; Yogev-Falach, M.; Avramovich-Tirosh, Y.; Amit, T.; Youdim, M. B. H. *Neurotherapeutics* **2009**, *6*, 163-174.
17. (a) Bloch, R. *Chem. Rev.***1998**, *98*, 1407. (b) Ryan, C. W.; Ainsworth, C. *J. Org. Chem.* **1961**, *26*, 1547. (c) Huffman, M. A.; Yasuda, N.; DeCamp, A. E.; Grabowski, E. J. *J. Org. Chem.* **1995**, *60*, 1590.
18. (a) Díez-González. *Advances in Organometallic Chemistry* **2016**, *66*, 93-141. (b) Yamamoto, Y.; Gridnev, I. D.; Patil, N. T.; Jin, T. *Chem. Commun.* **2009**, *34*, 5075-5087. (c) Crabtree, R. H.; Lei, A. *Chem. Rev.* **2017**, *117*, 8481-8482.
19. Li, C. -J.; Wei, C. *Chem. Commun.* **2002**, *3*, 268-269.
20. Leadbeater, N. E.; Torenius, H. M.; Tye, H. *Mol. Diversity* **2003**, *7*, 135-144
21. Shi, L.; Tu, Y. Q.; Wang, M; Zhang, F. M.; Fan, C. A. *Org. Lett.* **2004**, *6*, 1001-1003.
22. Yadav, J. S.; Reddy, B. V. S.; Naveenkumar, V.; Rao, R. S.; Nagaiah, K. *New J. Chem.* **2004**, *28,* 335-337.
23. Ju, Y.; Li, C. -J.; Varma, R. S.; *QSAR Comb. Sci.* **2004**, *23*, 891-894.
24. Bariwal, J. B.; Ermolat'ev, D. S.; Van der Eycken, E. V. *Chem. Eur. J.* **2010**, *16*, 3281-3284.
25. Park, S. B.; Alper, H. *Chem. Commun.* **2005**, *10*, 1315-1317.
26. Meyet, C. E.; Pierce, C. J.; Larsen, C. H. *Org. Lett.* **2012**, *14*, 964-967.
27. Trang, T. T. T.; Ermolat'ev, D. S.; Van der Eycken, E. V.; *RSC Advances* **2015**, *5*, 28921-28924.
28. Chen, M. -T.; Navarro, O. *Synlett.* **2013**, *24*, 1190-1192.

29. Aliaga, M. J.; Ramón, D. J.; Yus, M. *Org. Biomol. Chem.* **2009**, *8*, 43-46.
30. Pereshivko, O. P.; Peshkov, V. A.; Van der Eycken, E. V. *Org. Lett.* **2010**, *12*, 2638-2641.
31. Palchak, Z. L.; Lussier D. J.; Pierce, C. J.; Larsen, C. H. *Green Chem*. **2015**, *17*,1802-1810.
32. Pierce, C. J.; Nguyen, M.; Larsen, C. H. *Angew. Chem. Int. Ed.* **2012**, *51*, 1228-12292.
33. Tang, X.; Kuang, J.; Ma, S. *Chem. Commun.* **2013**, *49*, 8976-8978.
34. Chalkidis, S. G.; Vougioukalakis, G. C. *Eur. J. Org. Chem.* **2023**, *26*, e202301095
35. (a) Bariwal, J. B.; Ermolat'v, D. S.; Van Der Eycken, E. V. *Chem. Eur. J.* **2010**, *16*, 3281-3284. (b) Ohara, M.; Hara, Y.; Ohnuki, T.; Nakamura, S. *Chem. Eur. J.* **2014**, *20*, 8848-8851. (c) Ji, J. X.; Wu, J.; Chan, A. S. C. *Proc. Natl. Acad. Sci.* **2005**, *102*, 11196-11200. (d) Dhanasekaran, S.; Kannaujiya, V. K.; Biswas, R. G.; Singh, V. K. *J. Org. Chem.* **2019**, *84*, 3275–3292. (e) Koradin, C.; Polborn, K.; Knochel, P. *Angew. Chem. Int. Ed.* **2002**, *41*, 2535–2538.
36. (a) Zorba, L. P.; Vougioukalakis, G. C. *Coord. Chem. Rev.* **2021**, *429*, 213603. (b) Tzouras, N. V.; Neofotistos, S. P.; Vougioukalakis, G. C. *ACS Omega* **2019**, *4*, 10279–10292. (c) Neofotistos, S. P.; Tzouras, N. V.; Pauze, M.; Gómez-Bengoa, E.; Vougioukalakis, G. C. *Adv. Synth. Catal*. **2020**, *362*, 3872–3885. (d) Li M.; Tian, S.; Wu, Z.; Chin. *J. Chem.* **2017**, *35*, 567–571.

7. Analytical data of propargylamines:

Substrates of A^3 Coupling

1a: ^{1}H NMR (400 MHz, $CDCl_3$, 298 K): *δ* 7.36-7.35 (m, 2H, *Ph*), 7.21-7.20 (m, 2H, *Ph*), 3.40 (s, 2H, C*H*$_2$), 2.49 (bs, 4H, *Piperidine*), 1.59-1.54 (m, 4H, *Piperidine*), 1.37 (b, 2H, *Piperidine*) ppm; ^{13}C {^{1}H} NMR ($CDCl_3$, 100.613 MHz, 298 K): *δ* 131.79 (*Ph*), 128.30 (*Ph*), 128.07 (*Ph*), 123.35 (*Ph*), 125.24 (*C*F$_3$Ph), 85.19 (*C*Ph), 85.00 (*C*CH$_2$Piperidine), 53.48 (*Piperidine*), 48.51 (C*H*$_2$Piperidine), 25.98 (*Piperidine*), 23.98 (*Piperidine*) ppm ESI-MS: Calculated for $C_{14}H_{17}N$: *m/z* 200.1439. Found *m/z* 200.1433 ($[M]^+$).

1b: ^{1}H NMR (400 MHz, $CDCl_3$, 298 K): *δ* 7.36-7.34 (m, 2H, *Ph*CH$_2$CH$_3$), 7.12-7.10 (m, 2H, *Ph*CH$_2$CH$_3$), 3.47 (s, 2H, C*H*$_2$), 2.65-2.57 (m, 6H, *Piperidine*+ PhC*H*$_2$CH$_3$), 1.65-1.62 (m, 4H, *Piperidine*), 1.44-1.42 (m, 2H, *Piperidine*), 1.23-1.19 (t, 3H, PhCH$_2$C*H*$_3$) ppm; ^{13}C{ ^{1}H} NMR ($CDCl_3$, 100.613 MHz, 298 K): *δ* 144.37 (*Ph*), 131.74 (*Ph*), 127.86(*Ph*), 120.53 (*Ph*),85.20 (*C*Ph), 84.29 (*C*CH$_2$Piperidine), 53.45 (*Piperidine*), 48.52 (C*H*$_2$Piperidine), 28.83 (C*H*$_2$CH$_3$), 26.01(*Piperidine*), 24 (*Piperidine*), 15.44 (CH$_2$C*H*$_3$) ppm. ESI-MS: Calculated for $C_{16}H_{21}N$: *m/z* 228.1708. Found *m/z* 228.1745 ($[M]^+$).

1c: ^{1}H NMR (400 MHz, $CDCl_3$, 298 K): *δ* 7.54-7.49 (m, 2H, CF$_3$*Ph*), 3.47 (s, 2H, C*H*$_2$), 2.55 (bs, 4H, *Piperidine*), 1.66-1.60 (m, 4H, *Piperidine*), 1.44-1.43 (m, 2H, *Piperidine*) ppm; ^{13}C {^{1}H} NMR ($CDCl_3$, 100.613 MHz, 298 K): *δ* 132.01 (*Ph*), 129.98 (*Ph*), 129.66(*Ph*), 127.23 (*Ph*), 125.24 (*C*F$_3$Ph), 87.99 (*C*Ph), 83.83 (*C*CH$_2$Piperidine), 53.63 (*Piperidine*), 48.50 (C*H*$_2$Piperidine), 26.01 (*Piperidine*), 23.97 (*Piperidine*) ppm. ESI-MS: Calculated for $C_{15}H_{16}F_3N$: *m/z* 268.1313. Found *m/z* 268.1312 ($[M]^+$).

1d: ^{1}H NMR (400 MHz, $CDCl_3$, 298 K): *δ* 7.35-7.33 (d, 2H, Br*Ph*), 7.22-7.20 (d, 2H, Br*Ph*), 3.37 (s, 2H, C*H*$_2$), 2.47 (bs, 4H, *Piperidine*), 1.57-1.55 (m, 4H, *Piperidine*), 1.37 (m, 2H, *Piperidine*) ppm; ^{13}C {^{1}H} NMR ($CDCl_3$, 100.613 MHz, 298 K): *δ* 133.22 (*Ph*), 131.51 (*Ph*), 122.32 (*Ph*), 122.20 (*Ph*), 86.49 (*C*Ph), 83.99 (*C*CH$_2$Piperidine), 53.58 (*Piperidine*), 48.53 (C*H*$_2$Piperidine), 25.99 (*Piperidine*), 23.97 (*Piperidine*) ppm. ESI-MS: Calculated for $C_{14}H_{16}BrN$: *m/z* 278.0544. Found *m/z* 278.0544 ($[M]^+$).

1e: ^{1}H NMR (400 MHz, $CDCl_3$, 298 K): *δ* 7.41-7.37 (m, 2H, F*Ph*), 6.99-6.94 (m, 2H, F*Ph*), 3.44 (s, 2H, C*H*$_2$), 2.55 (bs, 4H, *Piperidine*), 1.65-1.60 (m, 4H, *Piperidine*), 1.43 (m, 2H, *Piperidine*) ppm; ^{13}C { ^{1}H} NMR ($CDCl_3$, 100.613 MHz, 298 K): *δ* 163.63 (*Ph*),

133.67 (*Ph*), 119.46 (*Ph*), 115.64 (*Ph*), 84.83 (*C*Ph), 84.01 (*C*CH_2Piperidine), 53.59 (*Piperidine*), 48.50 (C*H_2*Piperidine), 26.01 (*Piperidine*), 24.00 (*Piperidine*) ppm. ESI-MS: Calculated for $C_{14}H_{16}FN$: *m/z* 218.1345. Found *m/z* 218.1339 ($[M]^+$).

1f: ^{1}H NMR (400 MHz, $CDCl_3$, 298 K): *δ* 7.59-7.58 (m, 2H, *Naphthalene*), 7.56-7.51 (m, 4H, *Naphthalene*), 7.46-7.42 (m, 2H, *Naphthalene*), 7.37-7.33 (m, 1H, *Naphthalene*), 3.52 (s, 2H, C*H_2*), 2.61 (bs, 4H, *Piperidine*), 1.69-1.66 (m, 4H, *Piperidine*), 1.47 (m, 2H, *Piperidine*) ppm; ^{13}C {^{1}H} NMR ($CDCl_3$, 100.613 MHz, 298 K): *δ* 140.79 (*Naphthalene*), 140.47 (*Naphthalene*), 132.20 (*Naphthalene*), 128.90 (*Naphthalene*), 127.62 (*Naphthalene*),127.06 (*Naphthalene*), 122.30 (*Naphthalene*), 85.85 (*C*Ph), 84.96 (*C*CH_2Piperidine), 53.55 (*Piperidine*), 48.62 (C*H_2*Piperidine), 26.04 (*Piperidine*), 24.02 (*Piperidine*) ppm. ESI-MS: Calculated for $C_{20}H_{21}N$: *m/z* 276.1752. Found *m/z* 276.1751 ($[M]^+$).

1g: ^{1}H NMR (400 MHz, $CDCl_3$, 298 K): *δ* 7.33-7.31 (d, 2H, CH_3*Ph*), 7.09-7.07 (d, 2H, CH_3*Ph*), 3.45 (s, 2H, C*H_2*), 2.56 (bs, 4H, *Piperidine*), 2.32 (s, 3H, C*H_3*), 1.64-1.62 (m, 4H, *Piperidine*), 1.43 (m, 2H, *Piperidine*) ppm; ^{13}C {^{1}H} NMR ($CDCl_3$, 100.613 MHz, 298 K): *δ* 138.02 (*Ph*), 131.64 (*Ph*), 129.01 (*Ph*), 120.30 (*Ph*), 85.10 (*C*Ph), 84.36 (*C*CH_2Piperidine), 53.51 (*Piperidine*), 48.56 (C*H_2*Piperidine), 26.02 (*Piperidine*), 24.02 (*Piperidine*), 21.47 (*C*H_3Ph) ppm. ESI-MS: Calculated for $C_{15}H_{19}N$: *m/z* 214.1595. Found *m/z* 214.1590 ($[M]^+$).

1h: ^{1}H NMR (400 MHz, $CDCl_3$, 298 K): *δ* 7.24-7.22 (d, 2H, *Ph*N$(CH_3)_2$), 6.53-6.51 (d, 2H, *Ph*N$(CH_3)_2$), 3.37 (s, 2H, C*H_2*), 2.86 (s, 3H, PhN(C*H_3*)$_2$), 2.48 (bs, 4H, *Piperidine*), 1.58-1.53 (m, 4H, *Piperidine*), 1.36 (m, 2H, *Piperidine*) ppm; ^{13}C{^{1}H} NMR ($CDCl_3$, 100.613 MHz, 298 K): *δ* 150.02 (*Ph*N$(CH_3)_2$), 132.80 (*Ph*N$(CH_3)_2$), 111.83 (*Ph*N$(CH_3)_2$), 110.33 (*Ph*N$(CH_3)_2$), 85.84 (*C*Ph), 82.40 (*C*CH_2Piperidine), 53.42 (*Piperidine*), 48.67 (C*H_2*Piperidine), 40.31 (PhN(*C*H_3)$_2$), 25.98 (*Piperidine*), 24.03 (*Piperidine*) ppm ESI-MS: Calculated for $C_{16}H_{22}N_2$: *m/z* 243.1861. Found *m/z* 243.1861 ($[M]^+$).

1i: ^{1}H NMR (400 MHz, $CDCl_3$, 298 K): *δ* 7.31 (s, 4H, *Ph*), 3.42 (s, 4H, C*H_2*), 2.51 (bs, 8H, *Piperidine*), 1.56-1.62 (m, 8H, *Piperidine*), 1.40 (m, 4H, *Piperidine*) ppm; ^{13}C{^{1}H} NMR ($CDCl_3$, 100.613 MHz, 298 K): *δ* 131.51 (*Ph*), 122.88 (*Ph*), 86.80 (*C*Ph), 84.68 (*C*CH_2Piperidine), 53.47 (*Piperidine*), 48.49 (C*H_2*Piperidine), 25.93 (*Piperidine*), 23.96

(*Piperidine*) ppm. ESI-MS: Calculated for $C_{22}H_{28}N_2$: *m/z* 321.2330. Found *m/z* 321.2324 ($[M]^+$).

1j: ^{1}H NMR (400 MHz, $CDCl_3$, 298 K): δ 7.40-7.35 (d, 3H, *Ph*), 3.40 (s, 6H, C*H*$_2$), 2.49 (bs, 12H, *Piperidine*), 1.60-1.55 (m, 12H, *Piperidine*), 1.39 (m, 6H, *Piperidine*) ppm; ^{13}C {^{1}H} NMR ($CDCl_3$, 100.613 MHz, 298 K): δ 134.16 (*Ph*), 123.73 (*Ph*), 86.20 (*C*Ph), 83.60 (*C*CH$_2$Piperidine), 53.41 (*Piperidine*), 48.37 (C*H*$_2$Piperidine), 25.94 (*Piperidine*), 23.88 (*Piperidine*) ppm. ESI-MS: Calculated for $C_{30}H_{39}N_3$: *m/z* 442.3222. Found *m/z* 442.3216 ($[M]^+$).

1k: ^{1}H NMR (400 MHz, $CDCl_3$, 298 K): *δ* 7.33-7.30 (m, 2H, *Ph*), 7.21-7.18 (m,3H, *Ph*), 3.57 (s, 2H, CH_2),3.22-3.15(m, 2H, C*H*$(CH_3)_2$), 1.08-1.07 (d,12H, CH(C*H*$_3)_2$) ppm; ^{13}C{^{1}H} NMR ($CDCl_3$, 100.613 MHz, 298 K): *δ* 131.53 (*Ph*), 128.29 (*Ph*), 89.08 (*C*Ph), 83.63 (*C*CH$_2$N(^{i}Pr)$_2$), 48.63 (*C*H(CH$_3)_2$), 24.90 (C*H*$_2$ N(iPr)$_2$), 23.88 (CH(*C*H$_3)_2$) ppm. ESI-MS: Calculated for $C_{15}H_{21}N$: *m/z* 216.1752. Found *m/z* 216.1746 ($[M]^+$).

1l: ^{1}H NMR (400 MHz, $CDCl_3$, 298 K): *δ* 8.54(s, 1H, *Py*), 7.61-7.57 (t, 1H, *Py*), 7.37-7.35(m, 1H, *Py*),7.18-7.15 (m, 1H, *Py*),3.66 (s, 2H, CH_2),3.29-3.22(m, 2H, C*H*$(CH_3)_2$), 1.14-1.13 (d,12H, CH(C*H*$_3)_2$) ppm; ^{13}C {^{1}H} NMR ($CDCl_3$, 100.613 MHz, 298 K): *δ* 149.93 (*Py*), 143.78 (*Py*), 136.09 (*Py*), 127.04 (*Py*), 122.58 (*Py*), 89.55 (*C*Py), 83.27 (*C*CH$_2$N(iPr)$_2$), 48.70 (*C*H(CH$_3)_2$), 34.81 (C*H*$_2$ N(iPr)$_2$), 20.73 (CH(*C*H$_3)_2$) ppm. ESI-MS: Calculated for $C_{14}H_{20}N_2$: *m/z* 217.1704. Found *m/z* 217.1698 ($[M]^+$).

1m: ^{1}H NMR (400 MHz, $CDCl_3$, 298 K): *δ* 7.54-7.52 (d, 2H, *Ph*CF_3), 7.49-7.47 (d,2H, *Ph* CF_3), 3.66 (s, 2H, CH_2),3.28-3.22 (m, 2H, C*H*$(CH_3)_2$), 1.16-1.14 (d,12H, CH(C*H*$_3)_2$) ppm; ^{13}C {^{1}H} NMR ($CDCl_3$, 100.613 MHz, 298 K): *δ* 131.79 (*Ph*CF_3), 129.47 (*Ph*CF_3), 127.72 (*Ph*CF_3), 125.24 (*Ph*CF_3), 122.77 (Ph*C*F_3), 92.05 (*C*Ph), 82.46 (*C*CH$_2$N(iPr)$_2$), 48.78 (*C*H(CH$_3)_2$), 34.96 (C*H*$_2$N(iPr)$_2$), 20.75 (CH(*C*H$_3)_2$) ppm. ESI-MS: Calculated for $C_{16}H_{20}F_3N$: *m/z* 244.2065. Found *m/z* 244.2054 ($[M]^+$).

1n: ^{1}H NMR (400 MHz, $CDCl_3$, 298 K): *δ* 7.44-7.41 (m, 2H, *Ph*), 7.30-7.28 (m, 3H, *Ph*), 3.66 (s, 2H, CH_2), 2.66-2.64 (m, 4H, C*H*$_2$CH$_3$), 1.15-1.11 (t, 6H, CH$_2$C*H*$_3$) ppm; ^{13}C {^{1}H} NMR ($CDCl_3$, 100.613 MHz, 298 K): *δ* 131.85 (*Ph*CF_3), 128.37 (*Ph*CF_3), 128.12 (*Ph*CF_3), 123.39 (*Ph*CF_3), 85.34 (*C*Ph), 84.12 (*C*CH$_2$N), 47.48 (*C*H$_2$CH$_3$), 41.53 (C*H*$_2$NCH$_2$CH$_3$), 12.66 (CH$_2$*C*H$_3$) ppm. ESI-MS: Calculated for $C_{13}H_{17}N$: *m/z* 187.1361. Found *m/z* 187.1206 ($[M]^+$).

1o: ^{1}H NMR (400 MHz, $CDCl_3$, 298 K): δ 7.54-7.49 (m, 4H, *Ph*CF_3), 3.64 (s, 2H, CH_2),2.63-2.61 (m, 4H, C*H*$_2$$CH_3$),1.13-1.09 (t, 6H, CH_2C*H*$_3$) ppm; ^{13}C {^{1}H} NMR ($CDCl_3$, 100.613 MHz, 298 K): δ 132.03 (*Ph*CF_3), 129.97 (*Ph*CF_3), 127.28 (*Ph*CF_3), 125.23 (Ph*C*F_3), 122.70 (*Ph*CF_3), 87.39 (*C*Ph), 83.89 (*C*CH_2N), 47.45 (*C*H_2CH_3), 41.54 (C*H*$_2$$NCH_2CH_3$),12.65 ($CH_2$*C*$H_3$) ppm. ESI-MS: Calculated for $C_{14}H_{16}F_3N$: *m/z* 256.1313. Found *m/z* 256.1304 ([M]$^+$).

1p: ^{1}H NMR (400 MHz, $CDCl_3$, 298 K): δ 7.54-7.26 (m, 4H, *Ph*), 3.66 (s, 2H, CH_2),2.66-2.64(m, 4H, C*H*$_2$$CH_3$),1.16-1.11 (t, 6H, CH_2C*H*$_3$) ppm; ^{13}C{^{1}H} NMR ($CDCl_3$, 100.613 MHz, 298 K): δ 138.74 (*Ph*), 131.91 (*Ph*), 128.61 (*Ph*), 128.37 (*Ph*), 128.14 (*Ph*), 127.54 (*Ph*), 123.45 (*Ph*), 87.95 (*C*Ph), 86.19 (*C*CH_2Piperidine), 62.49 (C*H*Piperidine), 50.80 (*Piperidine*), 26.30 (*Piperidine*), 24.55 (*C*H_3Ph) ppm. ESI-MS: Calculated for $C_{20}H_{21}N$: *m/z* 276.1752. Found *m/z* 276.1746 ([M]$^+$).

Substrates of KA^2 Coupling

2a: ^{1}H NMR (400 MHz, $CDCl_3$, 298 K): δ 7.31 (m, 2H, *Ph*), 7.16 (m, 3H, *Ph*), 2.56 (bs, 4H, *Piperidine*), 1.99-1.96 (m, 2H, *Cyclohexanone*), 1.59-1.34 (m, 14H, *Cyclohexanone* + *Piperidine*); ^{13}C{^{1}H} NMR ($CDCl_3$, 100.613 MHz, 298 K): δ 131.72 (*Ph*), 128.19 (*Ph*), 127.66 (*Ph*), 123.77 (*Ph*), 90.70 (*C*CPh), 86.22 (C*C*Ph), 59.46 (*Cyclohexanone*), 47.17 (Piperidine), 35.77 (*Cyclohexanone*), 26.58 (*Piperidine*), 25.73 (*Cyclohexanone*), 24.73 (*Piperidine*), 23.13 (*Cyclohexanone*) ppm. ESI-MS: Calculated for $C_{19}H_{25}N$: *m/z* 268.2065. Found *m/z* 268.2054 ([M]$^+$).

2b: ^{1}H NMR (400 MHz, $CDCl_3$, 298 K): δ 7.26-7.24 (m, 2H, *Ph*CH_3), 7.03-7.01 (m, 2H, *Ph*CH_3), 2.60 (bs, 4H, *Piperidine*), 2.25 (s, 3H, Ph*C*H_3), 2.03-2.00 (m, 2H, *Cyclohexanone*), 1.63-1.37 (m, 14H, *Cyclohexanone* + *Piperidine*); ^{13}C{ ^{1}H} NMR ($CDCl_3$, 100.613 MHz, 298 K): δ 137.73 (*Ph*CH_3), 131.66 (*Ph*CH_3), 129.00 (*Ph*CH_3), 120.73 (*Ph*CH_3),89.81 (*C*CPh), 86.39 (C*C*Ph), 59.63 (*Cyclohexanone*), 47.22 (Piperidine), 35.82 (*Cyclohexanone*), 26.60 (*Piperidine*), 25.80 (*Cyclohexanone*), 24.77 (*Piperidine*), 23.22 (*Cyclohexanone*), 21.48 (Ph*C*H_3) ppm. ESI-MS: Calculated for $C_{20}H_{27}N$: *m/z* 282.2177. Found *m/z* 282.2213 ([M]$^+$).

2c: ^{1}H NMR (400 MHz, $CDCl_3$, 298 K): δ 7.38-7.36 (m, 2H, *Ph*CH_2CH_3), 7.14-7.12 (m, 2H, *Ph*CH_2CH_3), 2.69-2.62 (m, 6H, *Piperidine*+ PhC*H*$_2$$CH_3$), 2.11-2.08 (m, 2H, *Cyclohexanone*), 1.71-1.46 (m, 14H, *Cyclohexanone* + *Piperidine*), 1.24-1.20 (t, 3H,

PhCH$_2$C*H*$_3$); ^{13}C{ ^{1}H} NMR ($CDCl_3$, 100.613 MHz, 298 K): *δ* 144.18 (*Ph*CH$_2$CH$_3$), 131.81 (*Ph*CH$_2$CH$_3$), 127.87 (*Ph*CH$_2$CH$_3$), 121.03 (*Ph*CH$_2$CH$_3$),89.90 (*C*CPh), 86.43 (C*C*Ph), 59.66 (*Cyclohexanone*), 47.28 (Piperidine), 35.90 (*Cyclohexanone*), 28.91 (PhC*H*$_2$CH$_3$), 26.67 (*Piperidine*), 25.84 (*Cyclohexanone*), 24.81 (*Piperidine*), 23.27 (*Cyclohexanone*), 15.63 (PhCH$_2$C*H*$_3$) ppm. ESI-MS: Calculated for $C_{21}H_{29}N$: *m/z* 296.2378. Found *m/z* 296.2370 ([M]$^+$).

2d: ^{1}H NMR (400 MHz, $CDCl_3$, 298 K): *δ* 7.35-7.33 (m, 2H, *Ph*Br), 7.23-7.21 (m, 2H, *Ph*Br), 2.59 (bs, 4H, *Piperidine*), 2.02-1.18 (m, 2H, *Cyclohexanone*), 1.67-1.63 (m, 2H, *Cyclohexanone*), 1.57-1.37 (m, 12H, *Cyclohexanone* + *Piperidine*); ^{13}C{ ^{1}H} NMR ($CDCl_3$, 100.613 MHz, 298 K): *δ* 133.27 (*Ph*Br), 131.49 (*Ph*Br), 122.64 (*Ph*Br), 121.90 (*Ph*Br), 91.81 (*C*CPh), 85.46 (C*C*Ph), 59.85 (*Cyclohexanone*), 47.28 (Piperidine), 35.61 (*Cyclohexanone*), 26.46 (*Piperidine*), 25.68 (*Cyclohexanone*), 24.67 (*Piperidine*), 23.16 (*Cyclohexanone*) ppm. ESI-MS: Calculated for $C_{19}H_{24}BrN$: *m/z* 346.1170. Found *m/z* 346.1161 ([M]$^+$).

2e: ^{1}H NMR (400 MHz, $CDCl_3$, 298 K): *δ* 7.42-7.39 (m, 2H, *Ph*F), 7.00-6.96 (m, 2H, *Ph*F), 2.68 (bs, 4H, *Piperidine*), 2.09-2.06 (m, 2H, *Cyclohexanone*), 1.74-1.71 (m, 2H, *Cyclohexanone*), 1.66-1.45 (m, 12H, *Cyclohexanone* + *Piperidine*); ^{13}C{ ^{1}H} NMR ($CDCl_3$, 100.613 MHz, 298 K): *δ* 163.53 (*Ph*F), 161.06 (*Ph*F), 133.63 (*Ph*F), 115.41 (*Ph*F), 90.16 (*C*CPh), 85.42 (C*C*Ph), 59.80 (*Cyclohexanone*), 47.29 (Piperidine), 35.71 (*Cyclohexanone*), 26.51 (*Piperidine*), 25.75 (*Cyclohexanone*), 24.72 (*Piperidine*), 23.23 (*Cyclohexanone*) ppm. ESI-MS: Calculated for $C_{19}H_{24}FN$: *m/z* 286.1926. Found *m/z* 286.1967 ([M]$^+$).

2f: ^{1}H NMR (400 MHz, $CDCl_3$, 298 K): *δ* 7.43-7.40 (m, 2H, *Ph*), 7.30-7.27 (m, 3H, *Ph*), 2.83-2.80 (m, 4H, *Piperidine*), 1.74-1.71 (m, 2H, *Butanone*), 1.42 (s, 3H, Butanone), 1.31-1.21 (m, 3H, *Piperidine*), 1.06-1.02 (m, 3H, *Piperidine*), 0.90-0.86 (t, 2H, *Butanone*); ^{13}C{ ^{1}H} NMR ($CDCl_3$, 100.613 MHz, 298 K): *δ* 131.89 (*Ph*), 128.34 (*Ph*), 126.55 (*Ph*CH$_3$), 123.64 (*Ph*), 91.00 (*C*CPh), 84.88 (C*C*Ph), 58.94 (*C*Piperidine), 48.06 (*Piperidine*), 34.09 (*C*H$_2$CH$_3$), 25.15 (*Piperidine*), 23.70 (C*C*H$_3$), 14.10 *(Piperidine*), 9.07 (CH$_2$*C*H$_3$) ppm. ESI-MS: Calculated for $C_{17}H_{23}N$: *m/z* 242.1864. Found *m/z* 242.2841 ([M]$^+$).

2g: ^{1}H NMR (400 MHz, $CDCl_3$, 298 K): *δ* 7.37-7.34 (m, 2H, *Ph*), 7.21-7.18 (m, 3H, *Ph*), 2.74 (bs, 4H, *Pyrrolidine*), 1.98-1.95 (m, 2H, *Cyclohexanone*), 1.72-1.43 (m, 12H,

Cyclohexanone + *Pyrrolidine*); $^{13}C\{^{1}H\}$ NMR ($CDCl_3$, 100.613 MHz, 298 K): *δ* 131.84 (*Ph*), 128.29 (*Ph*), 127.79 (*Ph*CH_3), 123.75 (*Ph*), 90.39 (*C*CPh), 86.29 (C*C*Ph), 59.57 (*Cyclohexanone*), 47.19 (*Pyrrolidine*), 37.94 (*Cyclohexanone*), 25.78 (*Cyclohexanone*), 23.62 (*Pyrrolidine*), 23.18 (*Cyclohexanone*) ppm. ESI-MS: Calculated for $C_{18}H_{23}N$: *m/z* 254.1908. Found *m/z* 254.1901 ($[M]^+$).

2h: ^{1}H NMR (400 MHz, $CDCl_3$, 298 K): *δ* 7.45-7.43 (m, 2H, *Ph*), 7.32-7.26 (m, 3H, *Ph*), 2.74-2.72 (t, 4H, *Morpholine*), 2.05-2.02 (m, 4H, *Morpholine*), 1.72-1.67 (m, 2H, *Cyclohexanone*), 1.58-1.53(m, 3H, *Cyclohexanone*), 1.31-1.22(m, 1H, *Cyclohexanone*); $^{13}C\{^{1}H\}$ NMR ($CDCl_3$, 100.613 MHz, 298 K): *δ* 131.82 (*Ph*), 128.31 (*Ph*), 127.93 (*Ph*), 89.84 (*C*CPh), 86.64 (C*C*Ph), 67.56 (*Morpholine*), 59.07 (*Cyclohexanone*), 46.74 (*Morpholine*), 35.52 (*Cyclohexanone*), 25.78 (*Cyclohexanone*), 22.86 (*Cyclohexanone*) ppm. ESI-MS: Calculated for $C_{18}H_{23}NO$: *m/z* 270.1858. Found *m/z* 270.1855 ($[M]^+$).

2i: ^{1}H NMR (400 MHz, $CDCl_3$, 298 K): *δ* 7.34 (m, 2H, *Ph*), 7.20 (m, 3H, *Ph*), 2.73 (b, 4H, *Pyrrolidine*), 1.94-1.54 (m, 16H, *Cycloheptanone* + *Pyrrolidine*); $^{13}C\{^{1}H\}$ NMR ($CDCl_3$, 100.613 MHz, 298 K): *δ* 131.84 (*Ph*), 128.29 (*Ph*), 127.75 (*Ph*), 123.80 (*Ph*), 91.98 (*C*CPh), 84.88 (C*C*Ph), 62.69 (*Cycloheptanone*), 47.94 (*Pyrrolidine*), 40.11 (*Cycloheptanone*), 28.23 (*Cycloheptanone*), 23.86 (*Pyrrolidine*), 22.25 (*Cycloheptanone*) ppm. ESI-MS: Calculated for $C_{19}H_{25}N$: *m/z* 268.2065. Found *m/z* 268.2059 ($[M]^+$).

2j: ^{1}H NMR (400 MHz, $CDCl_3$, 298 K): *δ* 7.33-7.32 (m, 2H, *Ph*CH_3), 7.10-7.08 (m, 2H, *Ph*CH_3), 3.76 (bs, 4H, *Morpholine*), 2.72 (bs, 4H, *Morpholine*), 2.33(s, 3H, PhC*H*$_3$), 2.03-2.01 (m, 2H, *Cyclohexanone*), 1.70-1.46 (m, 7H, *Cyclohexanone*), 1.27-1.25 (m, 1H, *Cyclohexanone*); $^{13}C\{^{1}H\}$ NMR ($CDCl_3$, 100.613 MHz, 298 K): *δ* 137.91 (*Ph*CH_3), 131.68 (*Ph*CH_3), 129.03 (*Ph*CH_3), 120.43 (*Ph*CH_3),89.00 (*C*CPh), 86.67 (C*C*Ph), 67.56 (*Morpholine*), 59.07 (*Cyclohexanone*), 46.73 (*Morpholine*), 35.55 (*Cyclohexanone*), 25.79 (*Cyclohexanone*), 22.86 (*Cyclohexanone*), 21.50 (Ph*C*H_3) ppm. ESI-MS: Calculated for $C_{19}H_{25}NO$: *m/z* 284.2014. Found *m/z* 284.2014 ($[M]^+$).

2k: ^{1}H NMR (400 MHz, $CDCl_3$, 298 K): *δ* 7.31-7.29 (m, 2H, *Ph*CH_2CH_3), 7.09-7.06 (m, 2H, *Ph*CH_2CH_3), 3.72-3.70 (t, 4H, *Morpholine*), 2.68-2.66 (m, 4H, *Morpholine*), 2.60-2.55 (q, 2H, PhC*H*$_2$$CH_3$),1.99-1.96 (m, 2H, *Cyclohexanone*), 1.69-1.40 (m, 8H, *Cyclohexanone*), 1.18-1.14 (t, 3H, $PhCH_2$C*H*$_3$); $^{13}C\{^{1}H\}$ NMR ($CDCl_3$, 100.613 MHz,

298 K): δ 144.27 (*Ph*CH_2CH_3), 131.77 (*Ph*CH_2CH_3), 127.84 (*Ph*CH_2CH_3), 120.68 (*Ph*CH_2CH_3), 89.04 (*C*CPh), 86.68 (C*C*Ph), 67.56 (*Morpholine*), 59.02 (*Cyclohexanone*), 46.72 (*Morpholine*), 35.55 (*Cyclohexanone*), 28.86 (Ph*C*H_2CH_3), 25.79 (*Cyclohexanone*), 22.85 (*Cyclohexanone*), 15.55 (PhCH_2*C*H_3) ppm. Calculated for $C_{20}H_{27}NO$: *m/z* 298.2126. Found *m/z* 298.1797[$(M]^+$).

2l: ^{1}H NMR (400 MHz, $CDCl_3$, 298 K): δ 7.32-7.29 (m, 2H, *Ph*$N(CH_3)_2$), 6.62-6.60 (m, 2H, *Ph*$N(CH_3)_2$), 3.76 (bs, 4H, *Morpholine*), 2.95 (s, 6H, PhN(C*H*$_3)_2$), 2.73 (bs, 4H, *Morpholine*), 2.03-2.01 (m, 2H, *Cyclohexanone*), 1.79-1.59 (m, 6H, *Cyclohexanone*), 1.50-1.45 (m, 2H, *Cyclohexanone*); ^{13}C{ ^{1}H} NMR ($CDCl_3$, 100.613 MHz, 298 K): δ 149.94 (*Ph*$N(CH_3)_2$), 132.73 (*Ph*$N(CH_3)_2$), 111.91 (*Ph*$N(CH_3)_2$), 110.48 (*Ph*$N(CH_3)_2$),87.32 (*C*CPh), 86.87 (C*C*Ph), 67.45 (*Morpholine*), 59.28 (*Cyclohexanone*), 46.64 (*Morpholine*), 40.34 (N(*C*$H_3)_2$), 35.55 (*Cyclohexanone*), 25.78 (*Cyclohexanone*), 22.88 (*Cyclohexanone*) ppm. Calculated for $C_{20}H_{28}N_2O$: *m/z* 313.2235. Found *m/z* 313.2271[$(M]^+$).

2m: ^{1}H NMR (400 MHz, $CDCl_3$, 298 K): δ 7.36-7.34 (m, 2H, *Ph*CH_2CH_3), 7.13-7.11 (m, 2H, *Ph*CH_2CH_3), 2.81 (bs, 4H, *Pyrrolidine*), 2.66-2.60 (q, 2H, PhC*H*$_2CH_3$), 2.05-2.02 (m, 2H, *Cyclohexanone*), 1.79 (bs, 4H, *Pyrrolidine*), 1.69-1.61 (m, 6H, *Cyclohexanone*), 1.57-1.50 (m, 2H, *Cyclohexanone),* 1.24-120 (t, 3H, PhCH_2C*H*$_3$); ^{13}C{ ^{1}H} NMR ($CDCl_3$, 100.613 MHz, 298 K): δ 144.26 (*Ph*CH_2CH_3), 131.83 (*Ph*CH_2CH_3), 127.88 (*Ph*CH_2CH_3), 120.87 (*Ph*CH_2CH_3), 89.37 (*C*CPh), 86.45 (C*C*Ph), 59.76 (*Cyclohexanone*), 47.23 (*Pyrrolidine*), 37.92 (*Cyclohexanone*), 28.89 (Ph*C*H_2CH_3), 25.77 (*Pyrrolidine*), 23.63 (*Cyclohexanone*), 23.21 (*Cyclohexanone*), 15.61 (PhCH_2*C*H_3) ppm. ESI-MS: Calculated for $C_{20}H_{27}N$: *m/z* 282.2221. Found *m/z* 282.2219 ($[M]^+$).

2n: ^{1}H NMR (400 MHz, $CDCl_3$, 298 K): δ 7.24-7.23 (m, 2H, *Ph*CH_3), 7.03-7.01 (m, 3H, *Ph*CH_3), 2.74 (bs, 4H, *Pyrrolidine*), 2.26 (s, 3H, PhC*H*$_3$) 1.99-1.94 (m, 2H, *Cycloheptanone*), 1.82-1.71 (m, 6H, *Cycloheptanone* + *Pyrrolidine*), 1.60-1.54 (m,8H, *Cycloheptanone*); ^{13}C{ ^{1}H} NMR ($CDCl_3$, 100.613 MHz, 298 K): δ 137.99 (*Ph*CH_3), 131.71 (*Ph*CH_3), 129.06 (*Ph*CH_3), 120.39 (*Ph*CH_3), 90.24 (*C*CPh), 85.42 (C*C*Ph), 48.16 (*Cycloheptanone*), 39.87 (*Pyrrolidine*), 28.05 (*Cycloheptanone*), 23.90 (*Pyrrolidine*), 22.61 (*Cycloheptanone*), 21.51 (Ph*C*H_3). ESI-MS: Calculated for $C_{20}H_{27}N$: *m/z* 282.2177. Found *m/z* 282.1833 ($[M]^+$).

2o: ^{1}H NMR (400 MHz, $CDCl_3$, 298 K): *δ* 7.28 (s, 4H, *Ph*), 3.69 (bs, 8H, *Morpholine*), 2.64 (bs, 8H, *Morpholine*), 1.97-1.94 (m, 4H, *Cyclohexanone*), 1.65-1.41 (m, 14H, *Cyclohexanone*), 1.21-1.18 (m, 2H, *Cyclohexanone*); ^{13}C {^{1}H} NMR ($CDCl_3$, 100.613 MHz, 298 K): *δ* 131.52 (*Ph*), 122.82 (*Ph*CH_3), 91.42 (*C*CPh), 86.25 (C*C*Ph), 67.50 (*Morpholine*), 59.02 (*Cyclohexanone*), 46.63 (*Morpholine*), 35.34 (*Cyclohexanone*), 25.64 (*Cyclohexanone*), 22.70 (*Cyclohexanone*) ppm. ESI-MS: Calculated for $C_{30}H_{40}N_2O_2$: *m/z* 461.3168. Found *m/z* 461.3176 ($[M]^+$).

2p: ^{1}H NMR (400 MHz, $CDCl_3$, 298 K): *δ* 7.35-7.33 (m, 2H, *Ph*Br), 7.22-7.20 (m, 2H, *Ph*Br), 2.73 (bs, 4H, *Pyrrolidine*), 1.96-1.93 (m, 2H, *Cyclohexanone*), 1.72 (bs, 4H, *Pyrrolidine*), 1.64-1.45 (m, 8H, *Cyclohexanone*); ^{13}C { ^{1}H} NMR ($CDCl_3$, 100.613 MHz, 298 K): *δ* 133.37 (*Ph*Br), 131.59 (*Ph*Br), 122.60 (*Ph*Br), 122.04 (*Ph*Br), 91.53 (*C*CPh), 85.49 (C*C*Ph), 59.91 (*Cyclohexanone*), 47.35 (*Pyrrolidine*), 37.74 (*Cyclohexanone*), 25.72 (*Pyrrolidine*), 23.69 (*Cyclohexanone*), 23.20 (*Cyclohexanone*) ppm. ESI-MS: Calculated for $C_{18}H_{22}BrN$: *m/z* 332.0936. Found *m/z* 355.2843 ($[M+Na]^+$).

2q: ^{1}H NMR (400 MHz, $CDCl_3$, 298 K): *δ* 8.53-8.52 (d, 1H, *Py*), 7.59-7.55 (m, 1H, *Py*), 7.38-7.36 (d, 1H, *Py*), 7.16-7.13 (m, 1H, *Py*), 2.77 (bs, 4H, *Pyrrolidine*), 2.05-2.02 (m, 2H, *Cyclohexanone*), 1.88-1.85 (t, 1H, *Cyclohexanone*), 1.76-1.73 (m, 4H, *Pyrrolidine*), 1.68-1.50 (m, 7H, Cyclohexanone); ^{13}C{ ^{1}H} NMR ($CDCl_3$, 100.613 MHz, 298 K): *δ* 150.26 (*Py*), 142.37 (*Py*), 136.39 (*Py*), 127.72 (*Py*),123.54 (*Py*), 88.05 (*C*CPh), 86.02 (C*C*Ph), 48.41 (*Cyclohexanone*), 36.11 (*Pyrrolidine*), 31.06 (*Cyclohexanone*), 24.78 (*Cyclohexanone*), 23.72 (*Pyrrolidine*), 23.16 (*Cyclohexanone*) ppm. ESI-MS: Calculated for $C_{17}H_{22}N_2$: *m/z* 255.1861. Found *m/z* 255.1854 ($[M]^+$).

2r: ^{1}H NMR (400 MHz, $CDCl_3$, 298 K): *δ* 7.42-7.40 (m, 2H, *Ph*Br), 7.29-7.27 (m, 2H, *Ph*Br), 3.76-3.75 (m, 4H, *Morpholine*), 2.72-2.03 (bs, 4H, *Morpholine*), 2.03-1.99 (m, 2H, *Cyclohexanone*), 1.72-1.48 (m, 6H, *Cyclohexanone*), 1.32-1.24 (m, 2H, *Cyclohexanone*) ; ^{13}C{ ^{1}H} NMR ($CDCl_3$, 100.613 MHz, 298 K): *δ* 133.27 (*Ph*Br), 131.53 (*Ph*Br), 122.31 (*Ph*Br), 122.10 (*Ph*Br), 90.87 (*C*CPh), 85.78 (C*C*Ph), 67.34 (*Morpholine*), 59.40 (*Cyclohexanone*), 46.70 (*Morpholine*), 35.28 (*Cyclohexanone*), 25.64 (*Cyclohexanone*), 22.81 (*Cyclohexanone*) ppm. ESI-MS: Calculated for $C_{18}H_{22}BrNO$: *m/z* 348.0963. Found *m/z* 348.0965 ($[M]^+$).

2s: ^{1}H NMR (400 MHz, $CDCl_3$, 298 K): *δ* 7.33-7.31 (m, 2H, *Ph*CH_3), 7.11-7.09 (m, 2H, *Ph*CH_3), 2.82 (bs, 4H, *Pyrrolidine*), 2.34 (s, 3H, Ph*C*H_3), 2.04-2.01 (m, 2H, *Cyclohexanone*), 1.80 (bs, 4H, *Pyrrolidine*), 1.69-1.51 (m, 8H, *Cyclohexanone*); ^{13}C{ ^{1}H} NMR ($CDCl_3$, 100.613 MHz, 298 K): *δ* 138.18 (*Ph*CH_3), 131.77 (*Ph*CH_3), 129.12 (*Ph*CH_3), 120.27 (*Ph*CH_3), 88.46 (*C*CPh), 86.99 (C*C*Ph), 60.56 (*Cyclohexanone*), 47.50 (*Pyrrolidine*), 37.56 (*Cyclohexanone*), 25.58 (*Cyclohexanone*), 23.70 (*Pyrrolidine*), 23.22 *(Cyclohexanone*), 15.61 (Ph*C*H_3) ppm. ESI-MS: Calculated for $C_{19}H_{25}N$: *m/z* 268.2021. Found *m/z* 268.2625 ($[M]^+$).

2t: ^{1}H NMR (400 MHz, $CDCl_3$, 298 K): *δ* 7.35-7.33 (m, 2H, *Ph*OCH_3), 6.81-6.79 (m, 2H, *Ph*CH_3), 3.78 (s, 3H, O*C*H_3), 2.82-2.80 (m, 4H, *Pyrrolidine*), 2.02-1.99 (m, 2H, *Cyclohexanone*), 1.80-1.76 (m, 4H, *Pyrrolidine*), 1.67-1.50 (m, 8H, *Cyclohexanone*); ^{13}C{ ^{1}H} NMR ($CDCl_3$, 100.613 MHz, 298 K): *δ* 159.30 (*Ph*OCH_3), 133.15 (*Ph*OCH_3), 115.69 (*Ph*OCH_3), 113.87 (*Ph*OCH_3), 88.91 (*C*CPh), 86.22 (C*C*Ph), 59.89 (*Cyclohexanone*), 55.33 (O*C*H_3), 47.19 (*Pyrrolidine*), 37.71 (*Cyclohexanone*), 25.67 (*Pyrrolidine*), 23.59 (*Cyclohexanone*), 23.15 (*Cyclohexanone*) ppm. ESI-MS: Calculated for $C_{19}H_{25}NO$: *m/z* 284.2014. Found *m/z* 284.2010 ($[M]^+$).

8. Spectroscopic Data

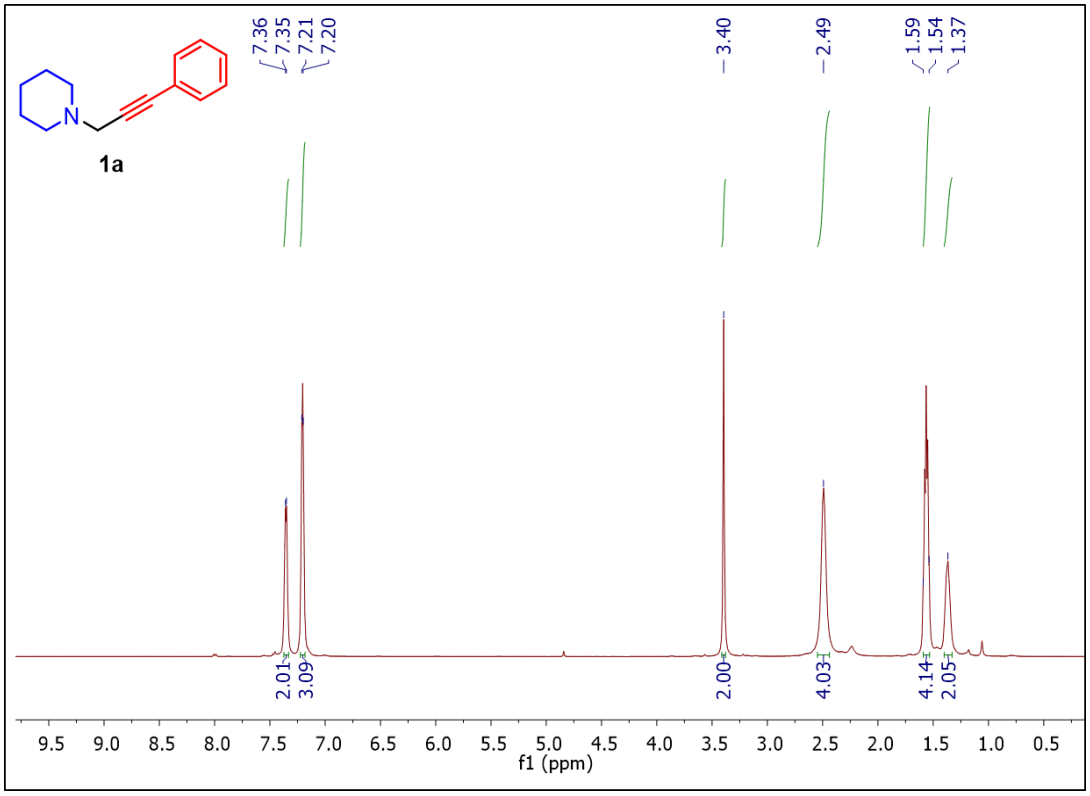

Figure 5: ^{1}H NMR spectrum of **1a** in $CDCl_3$.

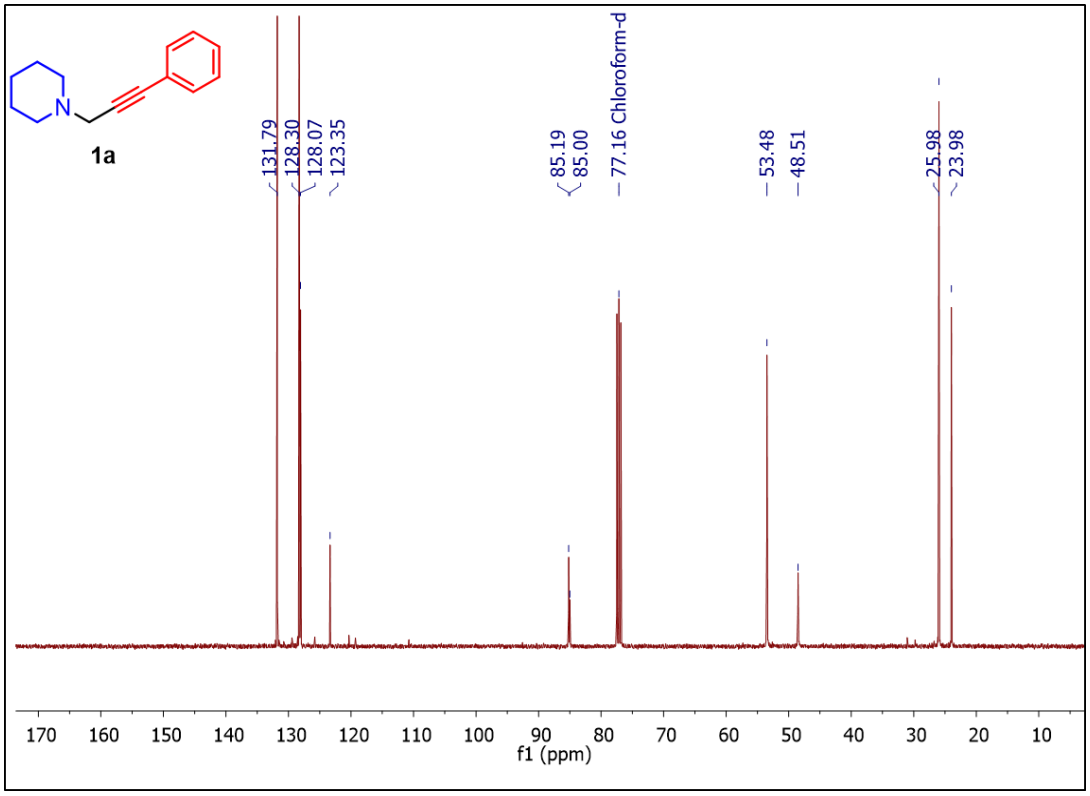

Figure 6: $^{13}C\{^{1}H\}$ NMR spectrum of **1a** in $CDCl_3$.

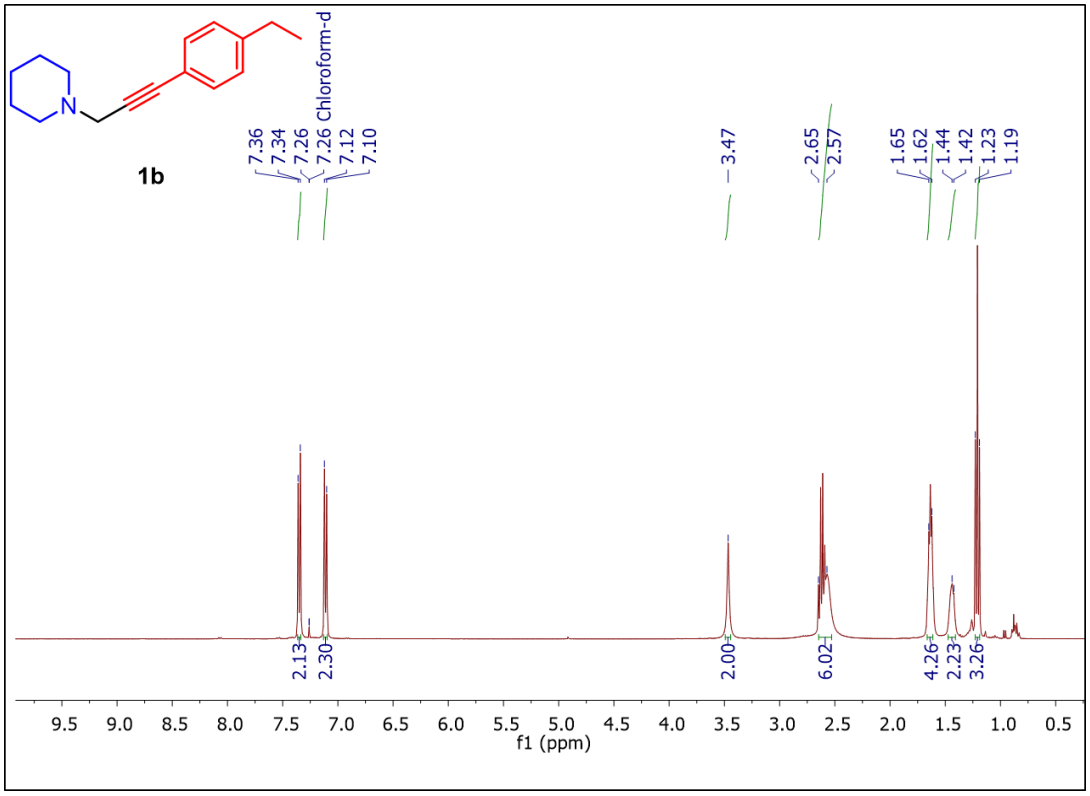

Figure 7: ^{1}H NMR spectrum of **1b** in $CDCl_3$.

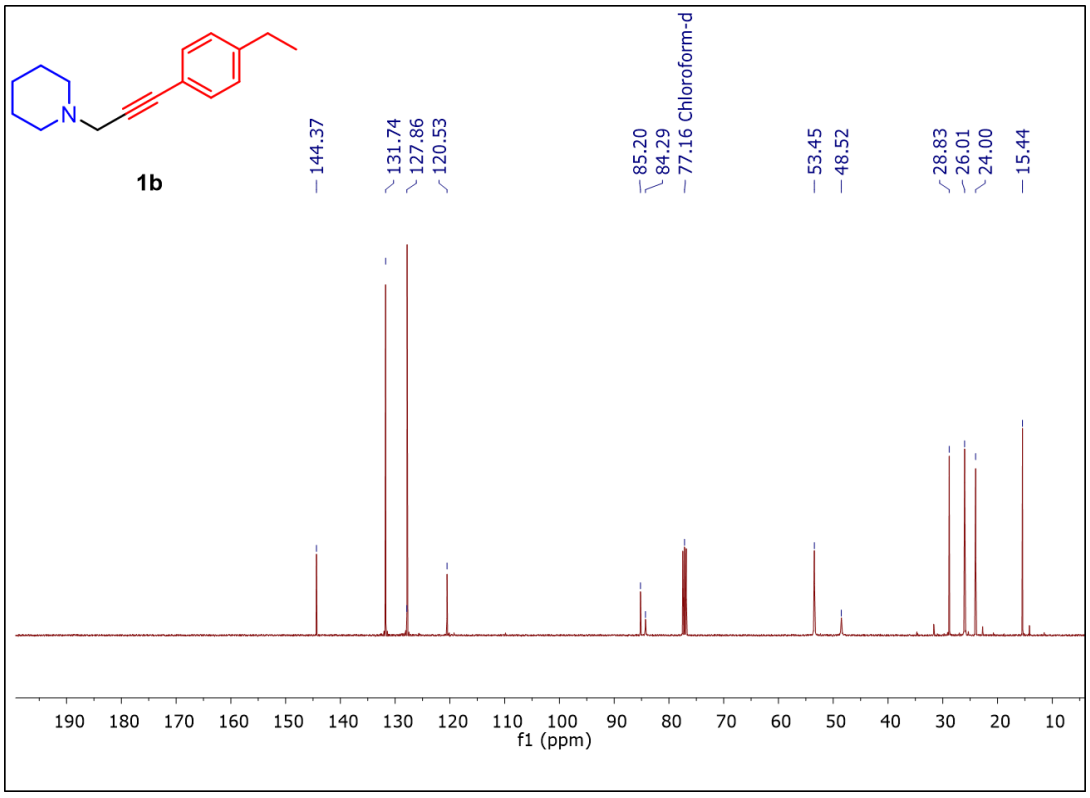

Figure 8: $^{13}C\{^{1}H\}$ NMR spectrum of **1b** in $CDCl_3$.

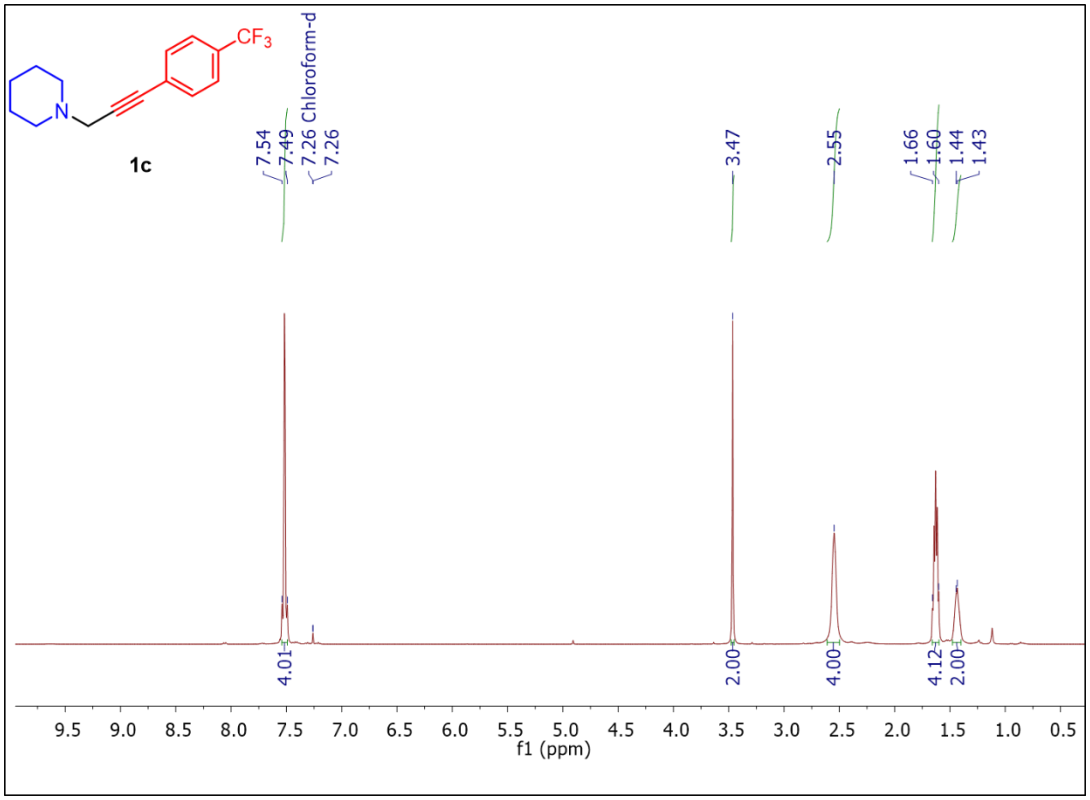

Figure 9: ^{1}H NMR spectrum of **1c** in $CDCl_3$.

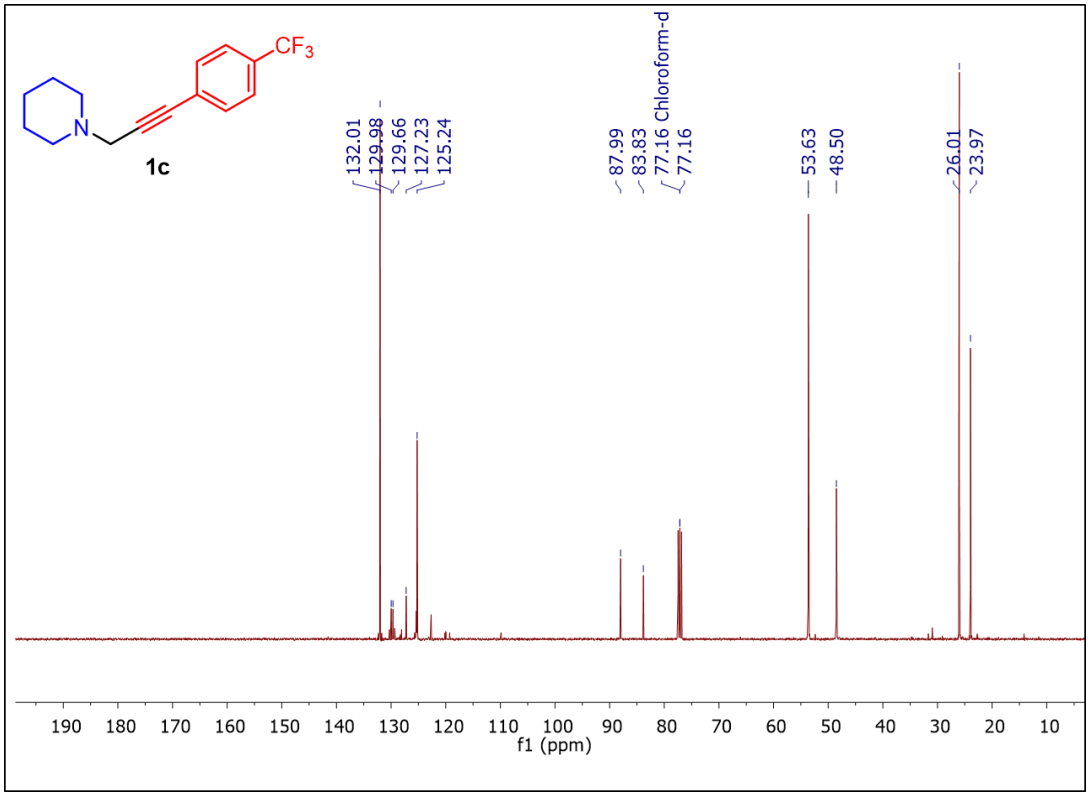

Figure 10: $^{13}C\{^{1}H\}$ NMR spectrum of **1c** in $CDCl_3$.

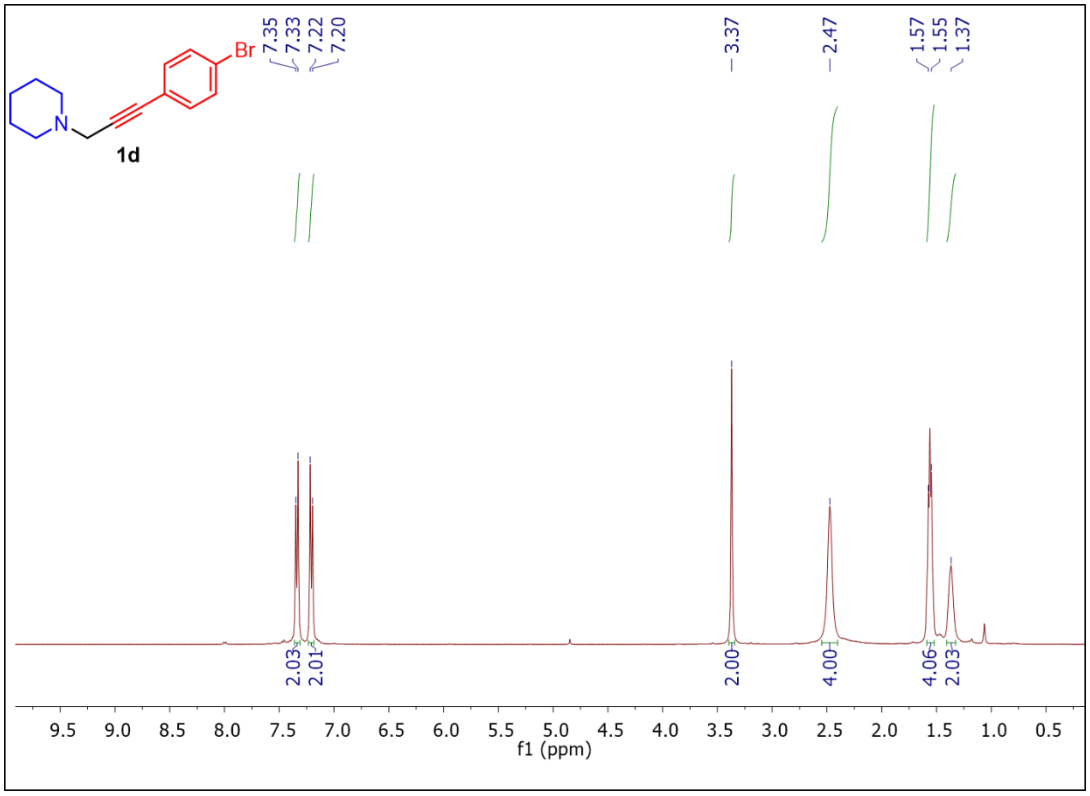

Figure 11: ^{1}H NMR spectrum of **1d** in $CDCl_3$.

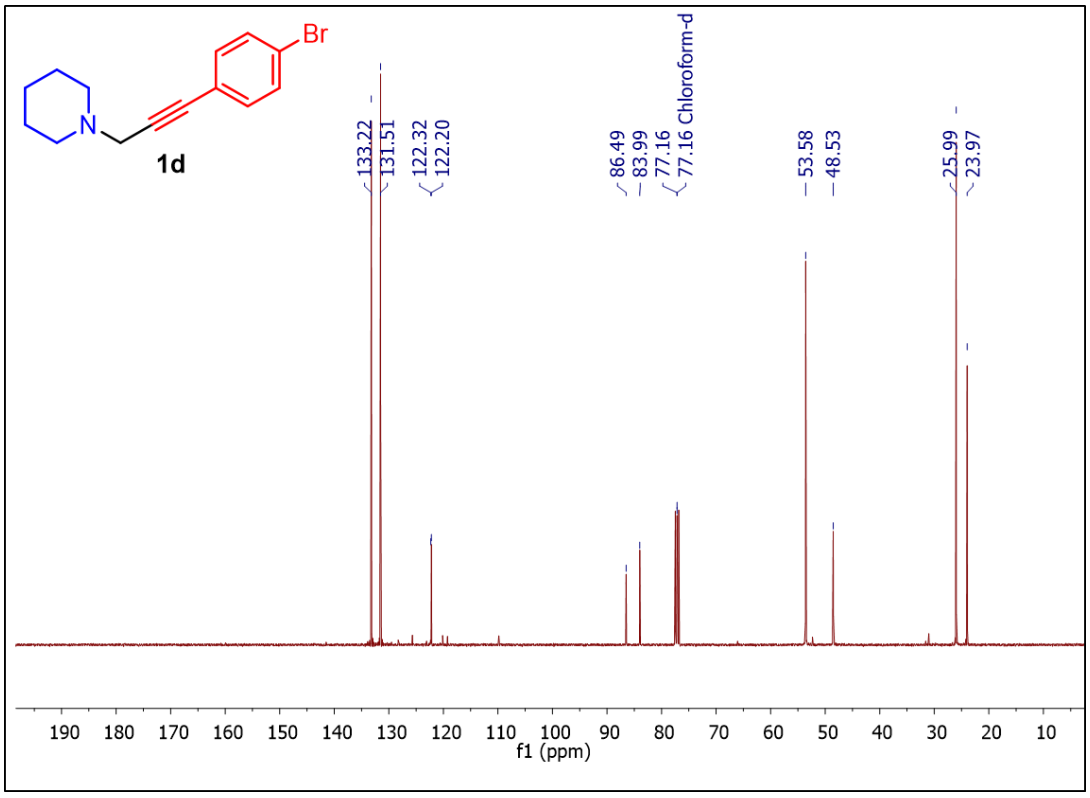

Figure 12: $^{13}C\{^{1}H\}$ NMR spectrum of **1d** in $CDCl_3$.

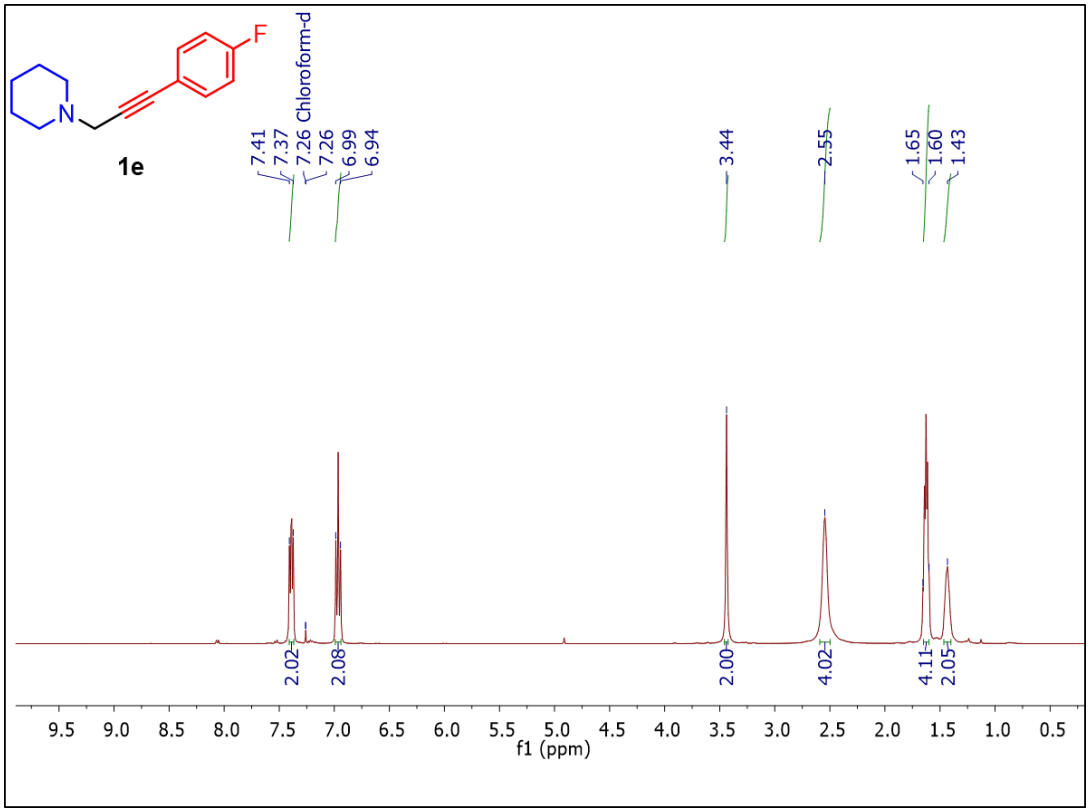

Figure 13: ^{1}H NMR spectrum of **1e** in $CDCl_3$.

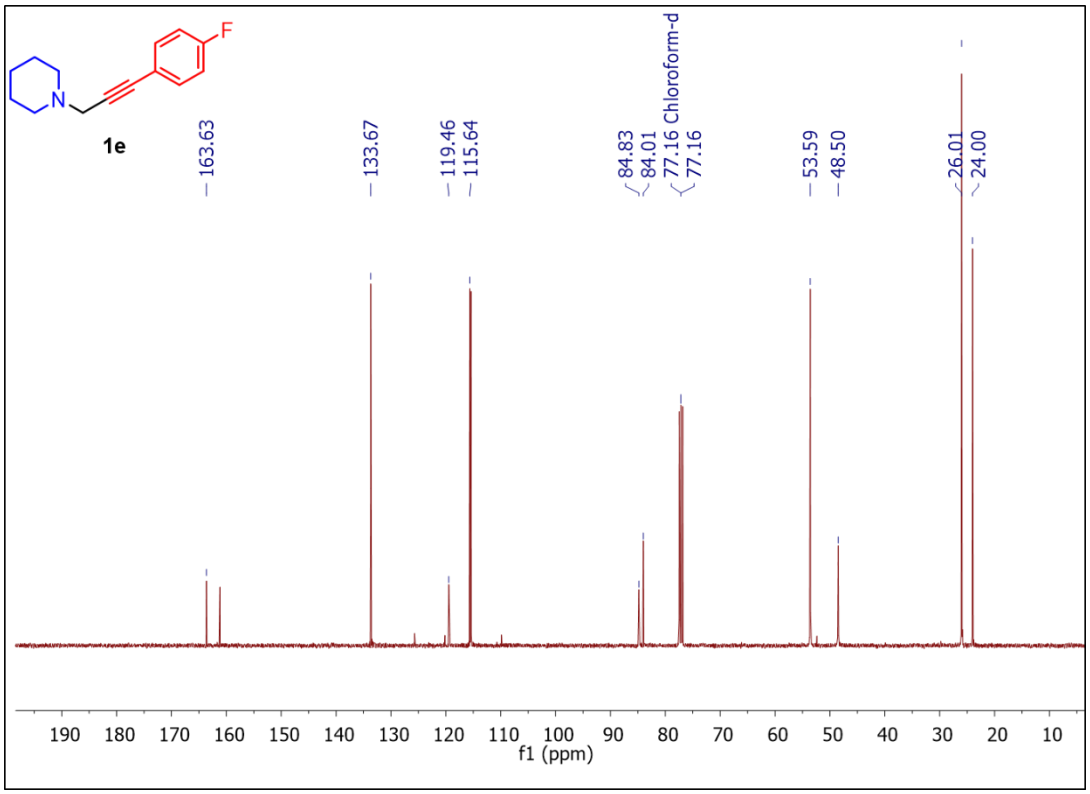

Figure 14: $^{13}C\{^{1}H\}$ NMR spectrum of **1e** in $CDCl_3$.

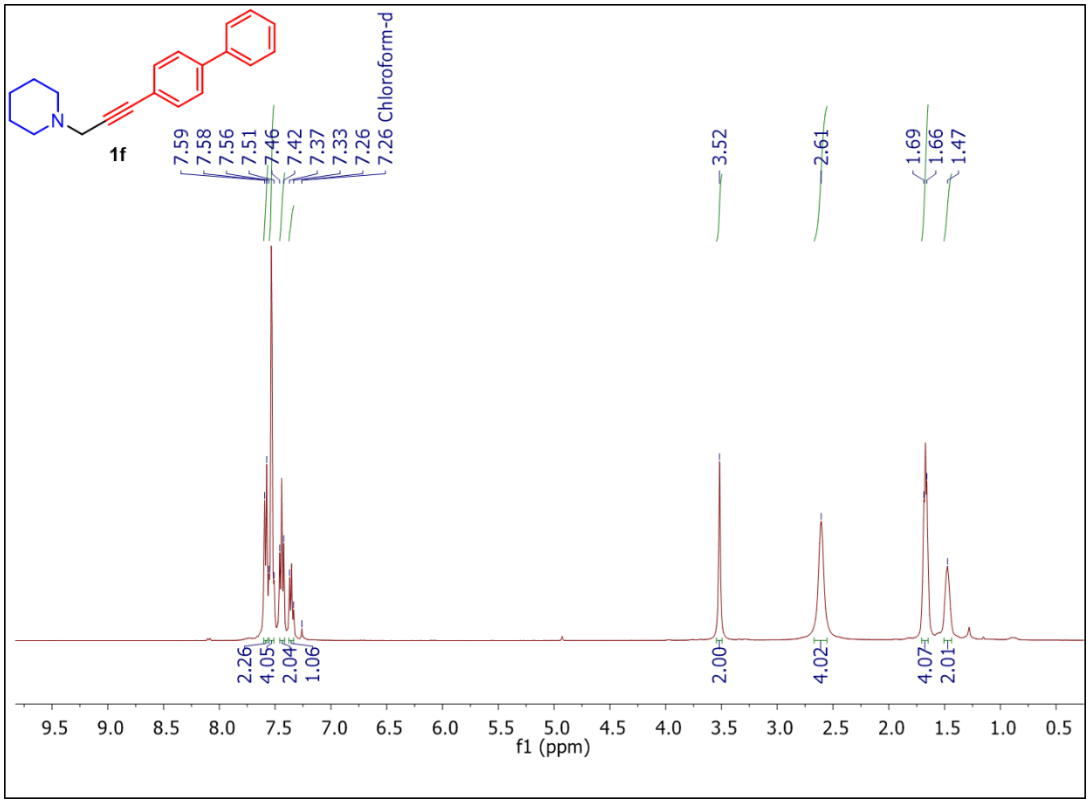

Figure 15: ^{1}H NMR spectrum of **1f** in $CDCl_3$.

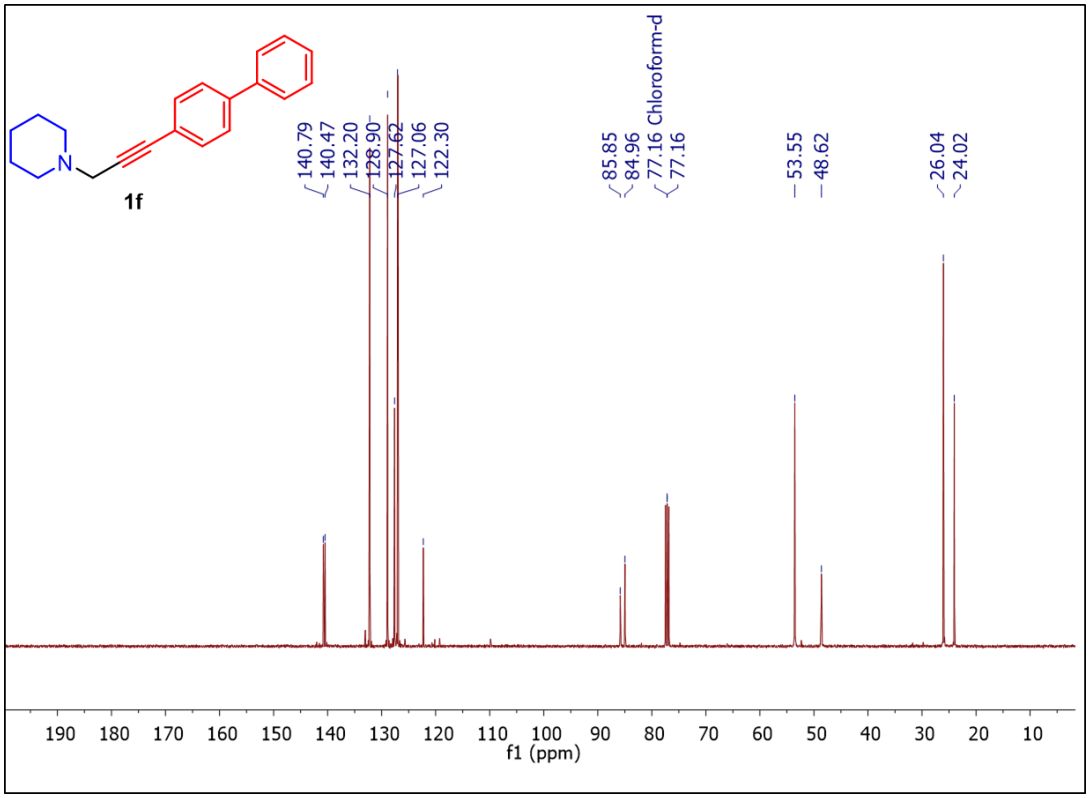

Figure 16: $^{13}C\{^{1}H\}$ NMR spectrum of **1f** in $CDCl_3$.

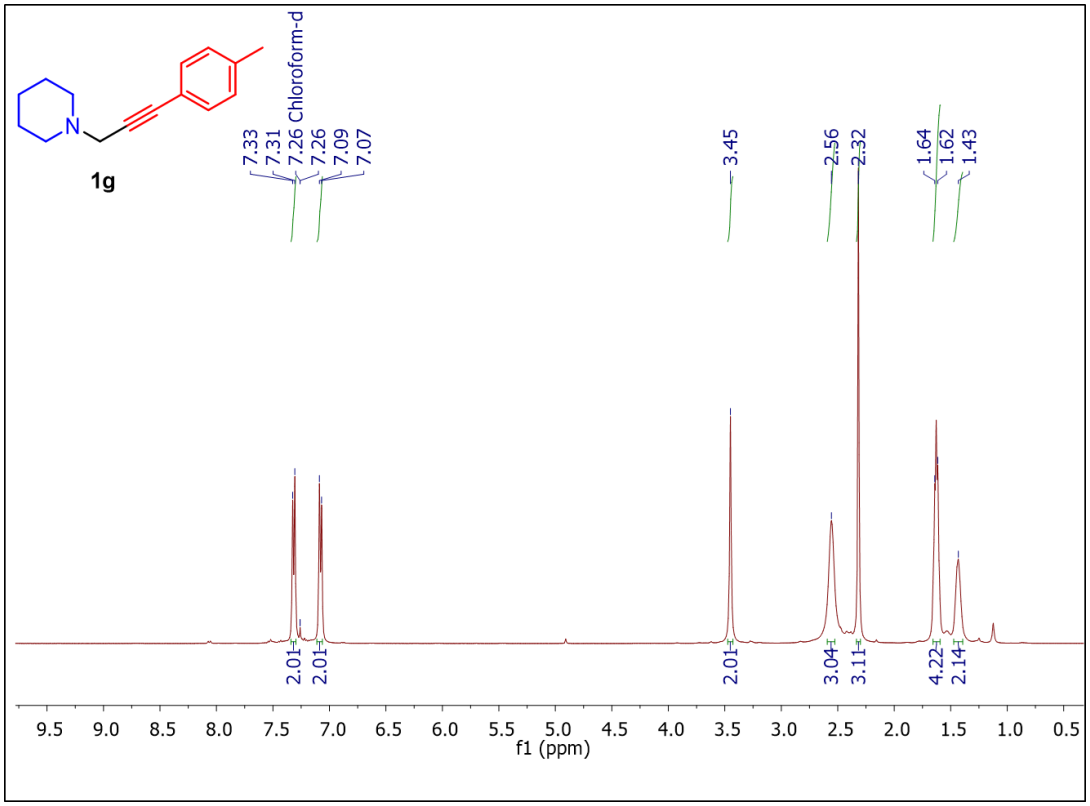

Figure 17: ^{1}H NMR spectrum of **1g** in $CDCl_3$.

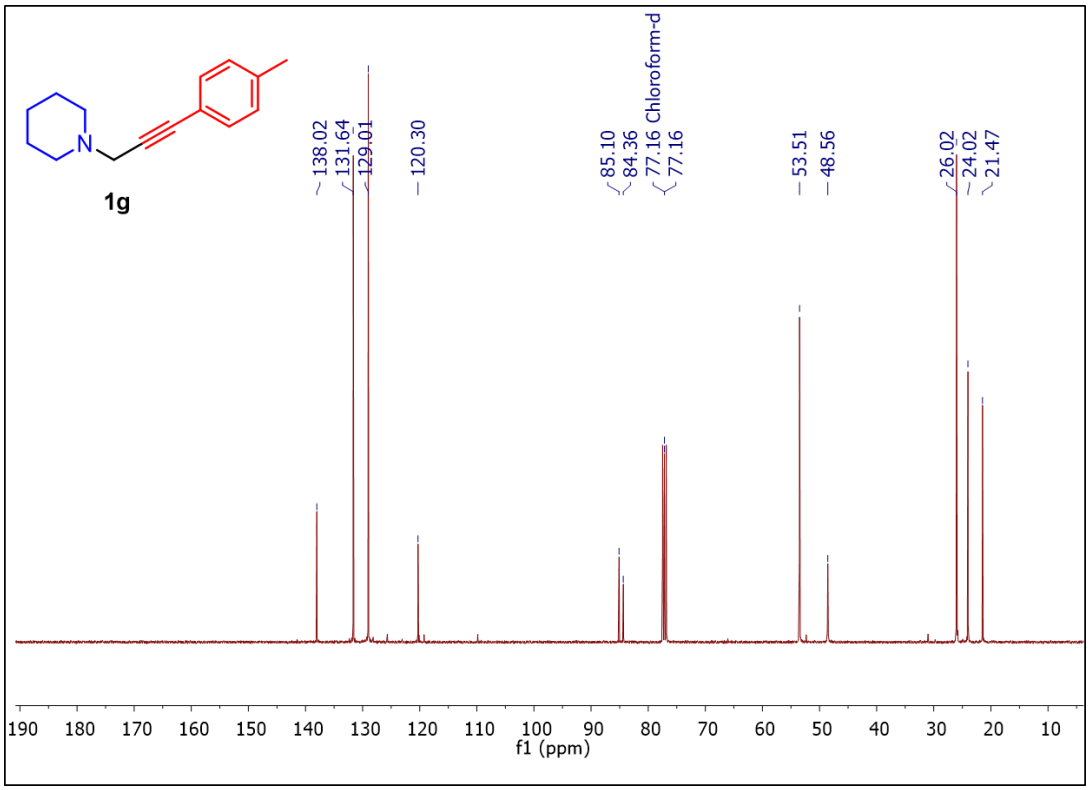

Figure 18: $^{13}C\{^{1}H\}$ NMR spectrum of **1g** in $CDCl_3$.

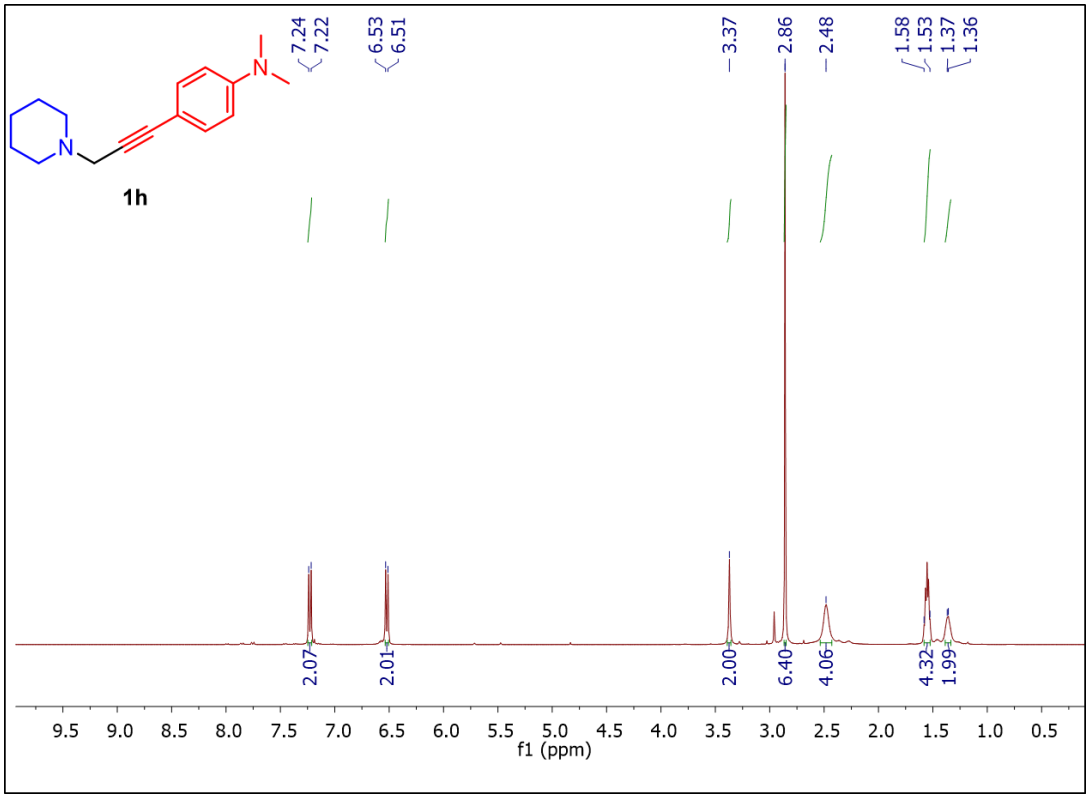

Figure 19: ^{1}H NMR spectrum of **1h** in $CDCl_3$.

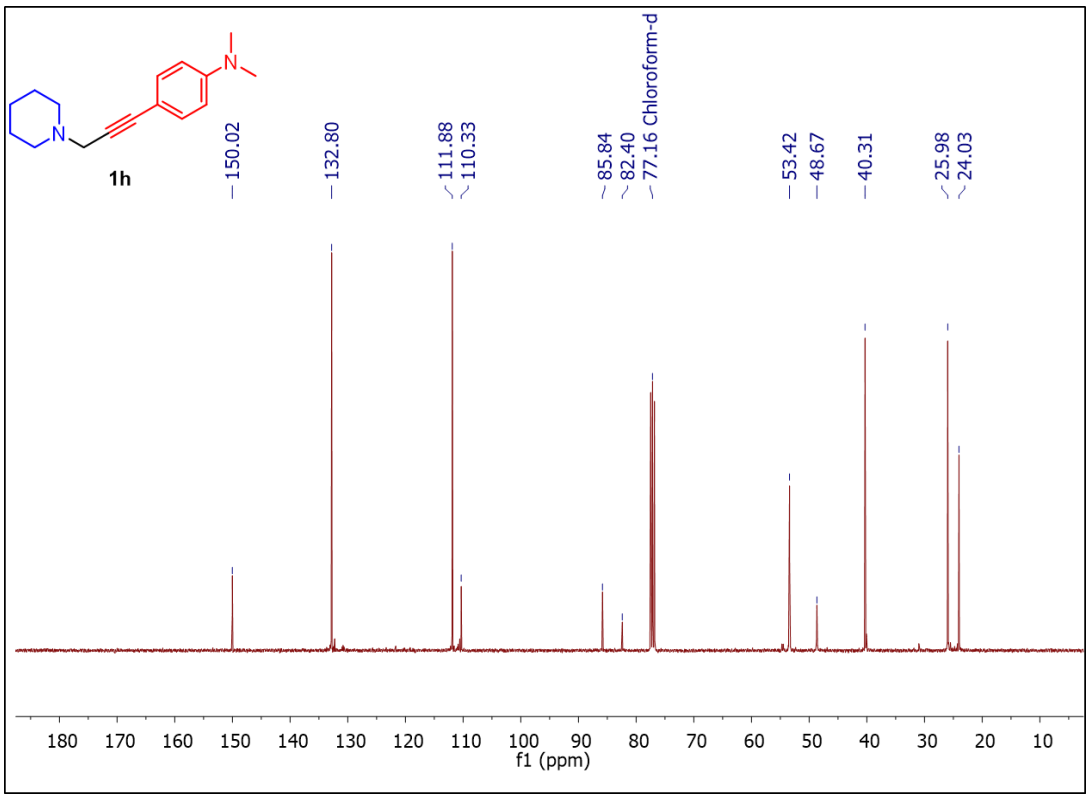

Figure 20: $^{13}C\{^{1}H\}$ NMR spectrum of **1h** in $CDCl_3$.

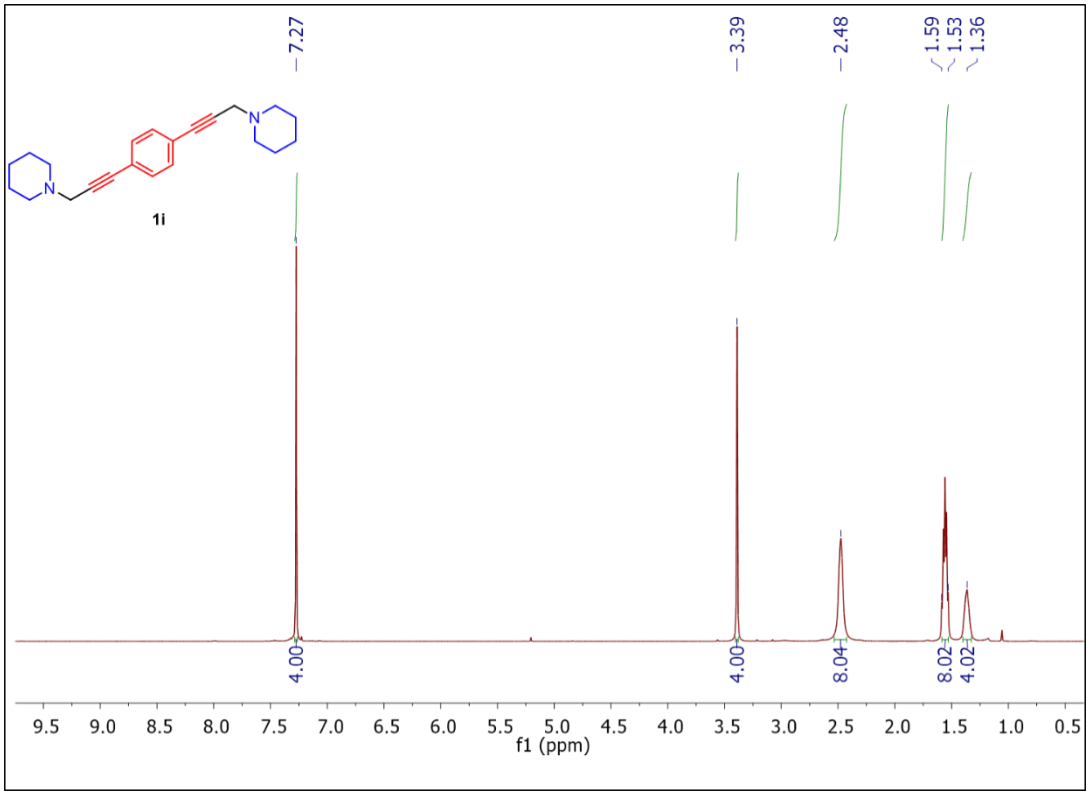

Figure 21: ^{1}H NMR spectrum of **1i** in $CDCl_3$.

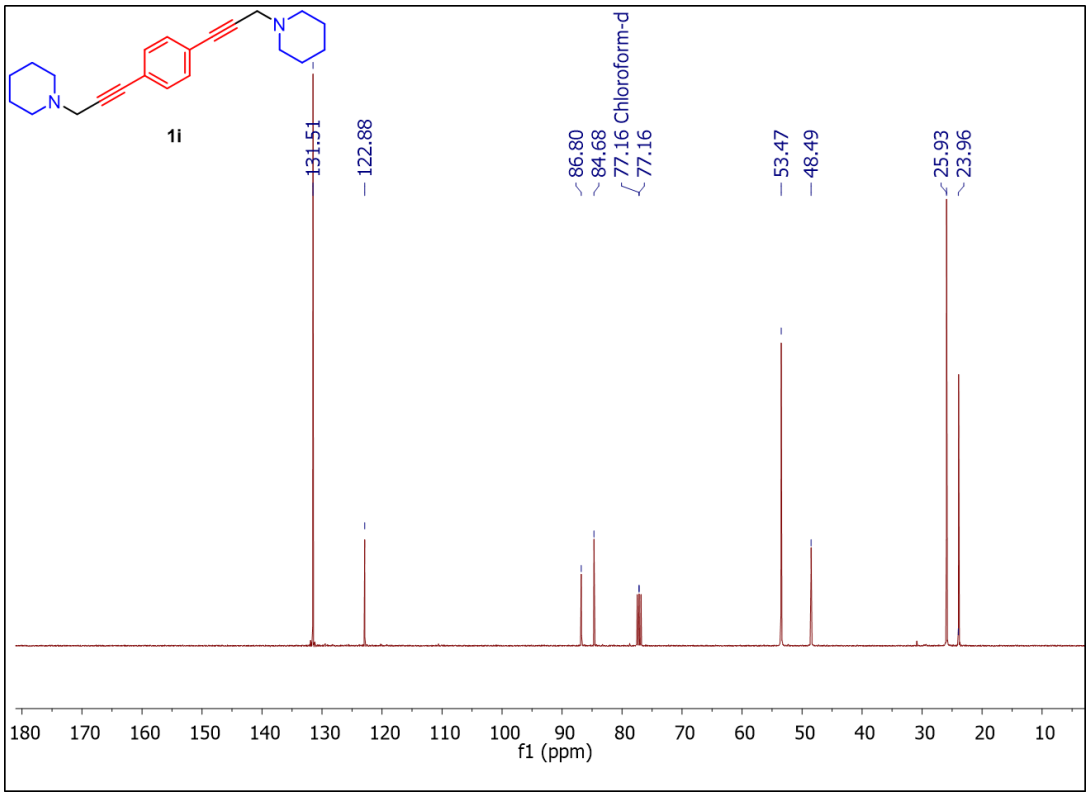

Figure 22: $^{13}C\{^{1}H\}$ NMR spectrum of **1i** in $CDCl_3$.

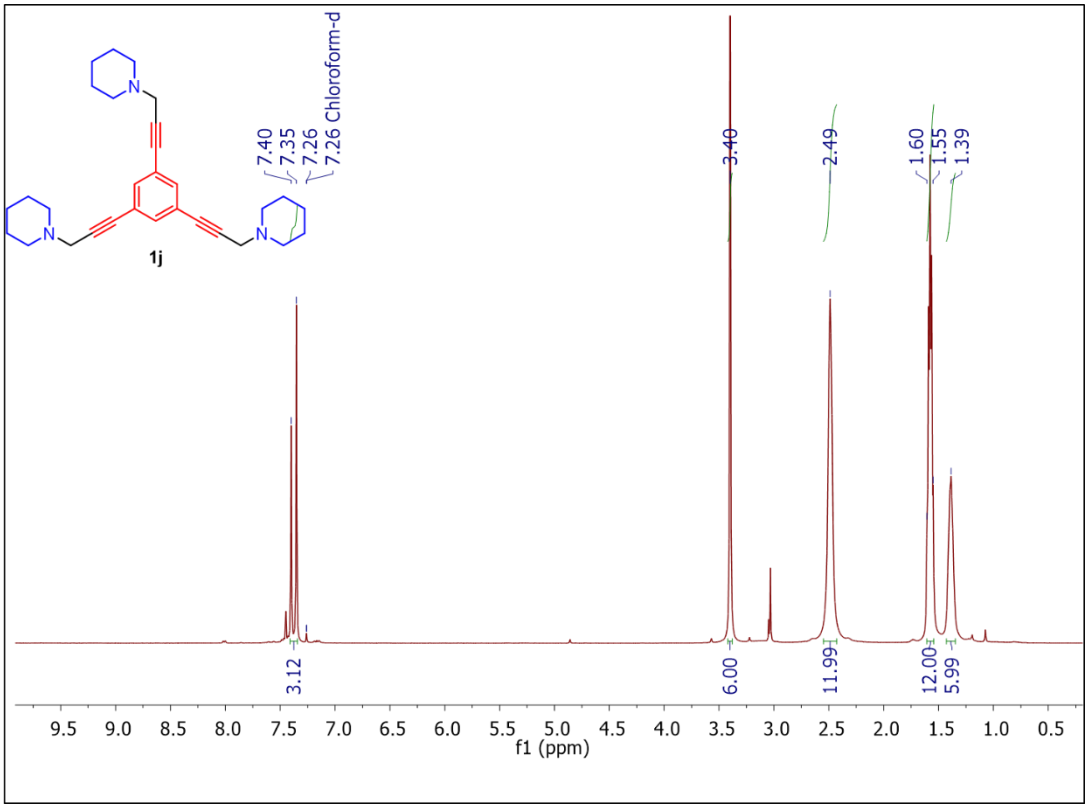

Figure 23: ^{1}H NMR spectrum of **1j** in $CDCl_3$.

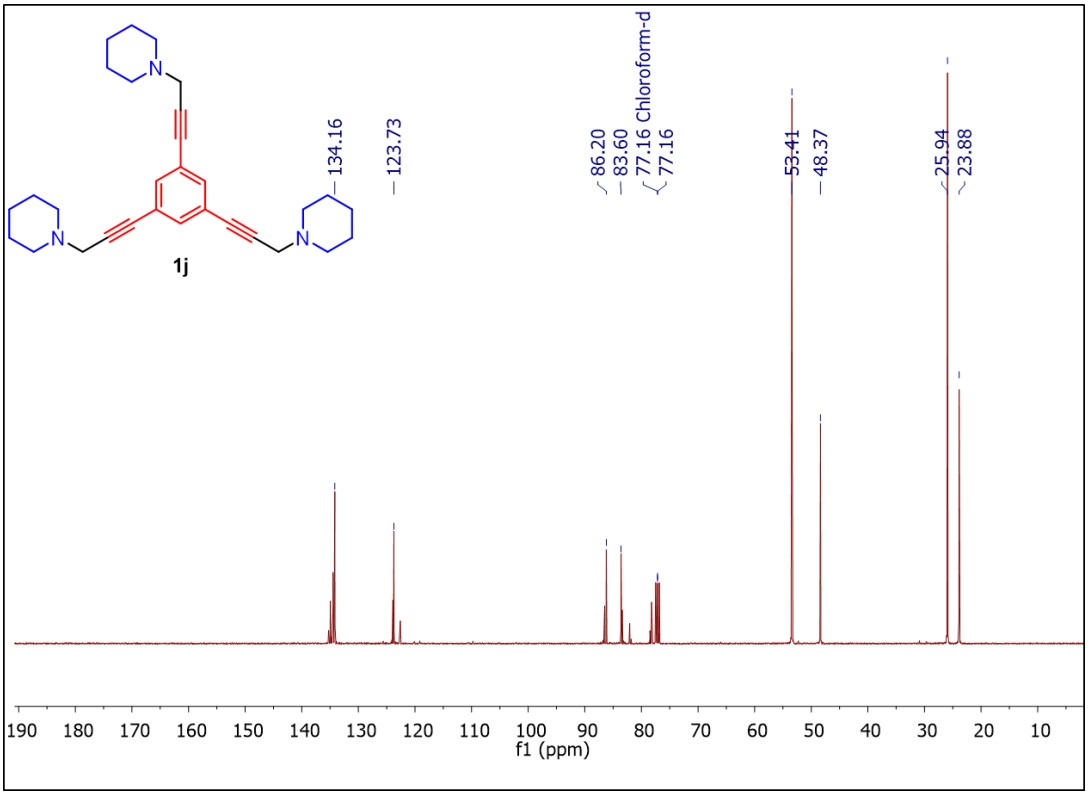

Figure 24: $^{13}C\{^{1}H\}$ NMR spectrum of **1j** in $CDCl_3$.

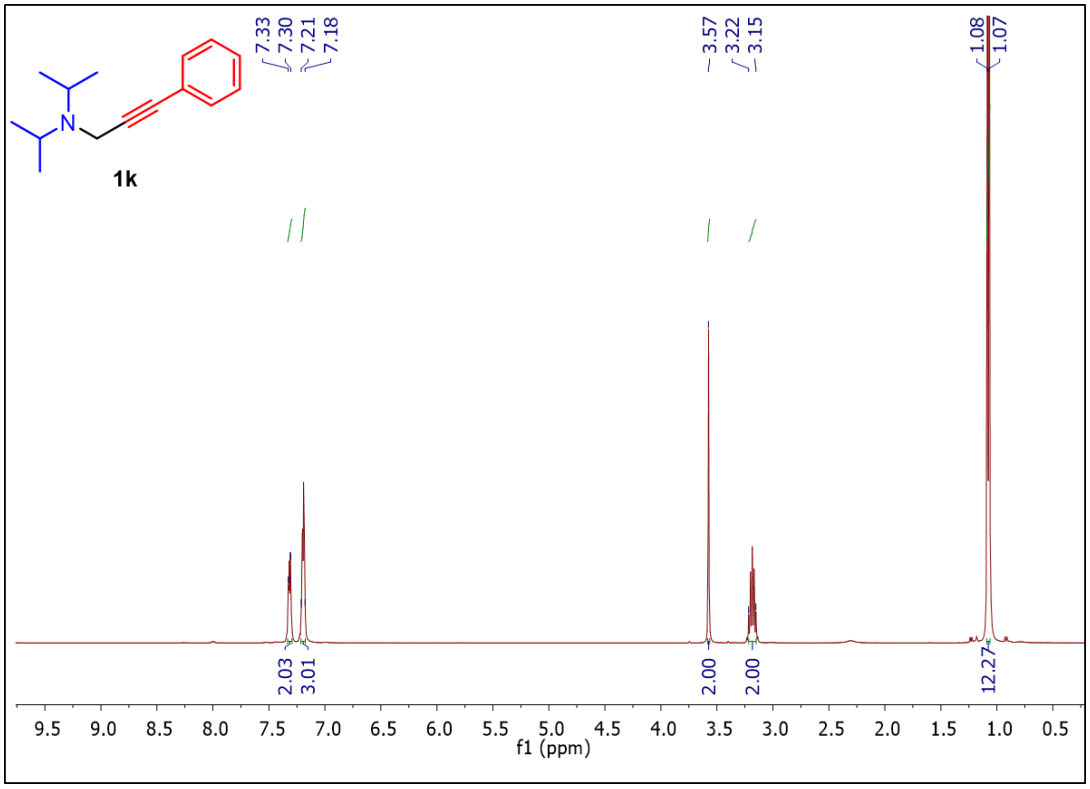

Figure 25: ^{1}H NMR spectrum of **1k** in $CDCl_3$.

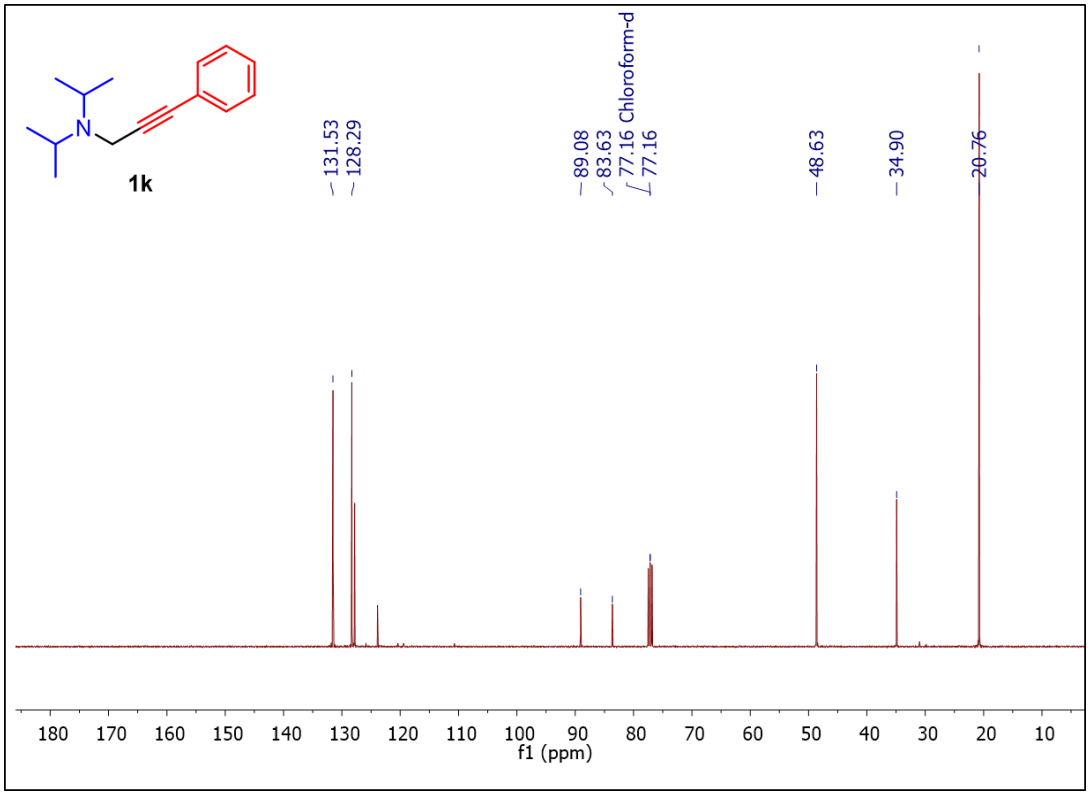

Figure 26: $^{13}C\{^{1}H\}$ NMR spectrum of **1k** in $CDCl_3$.

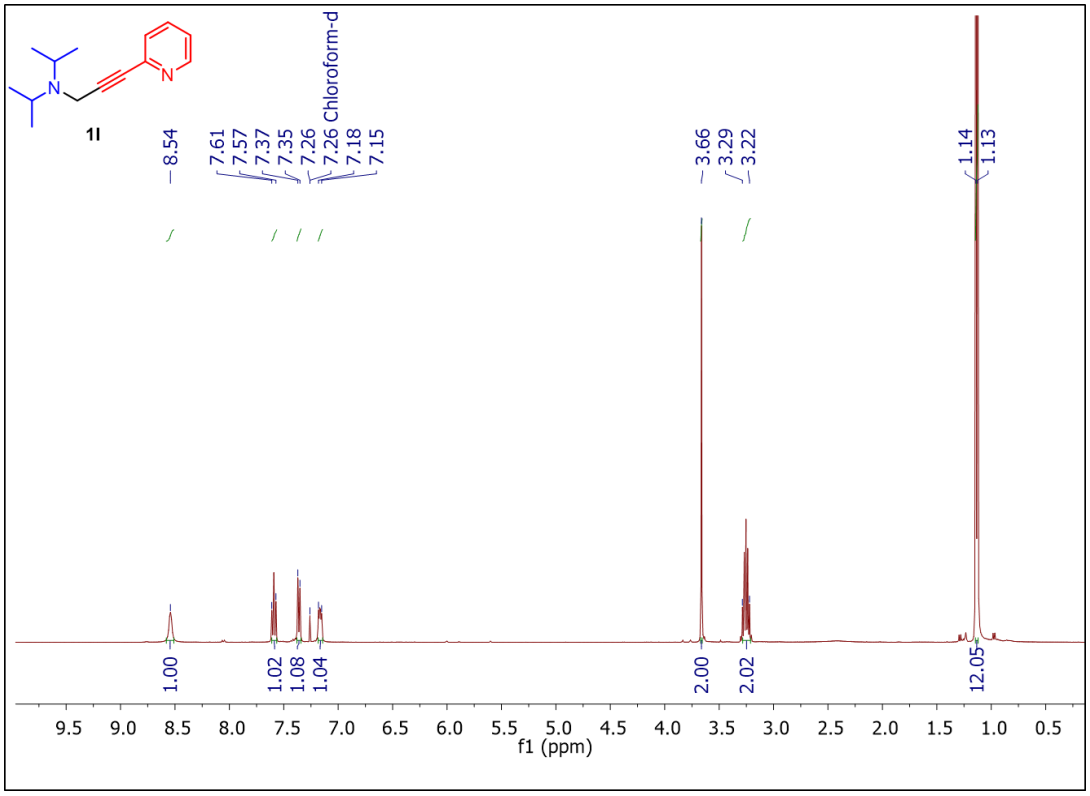

Figure 27: ^{1}H NMR spectrum of **1l** in $CDCl_3$.

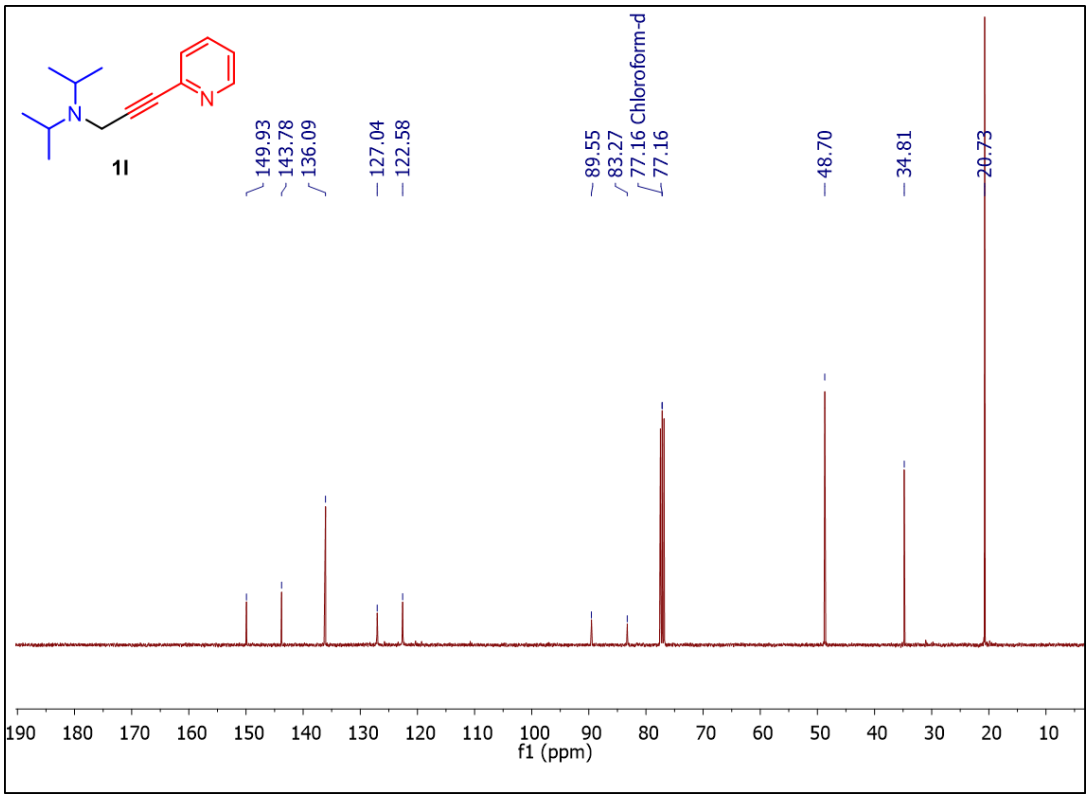

Figure 28: $^{13}C\{^{1}H\}$ NMR spectrum of **1l** in $CDCl_3$.

9. Appendix

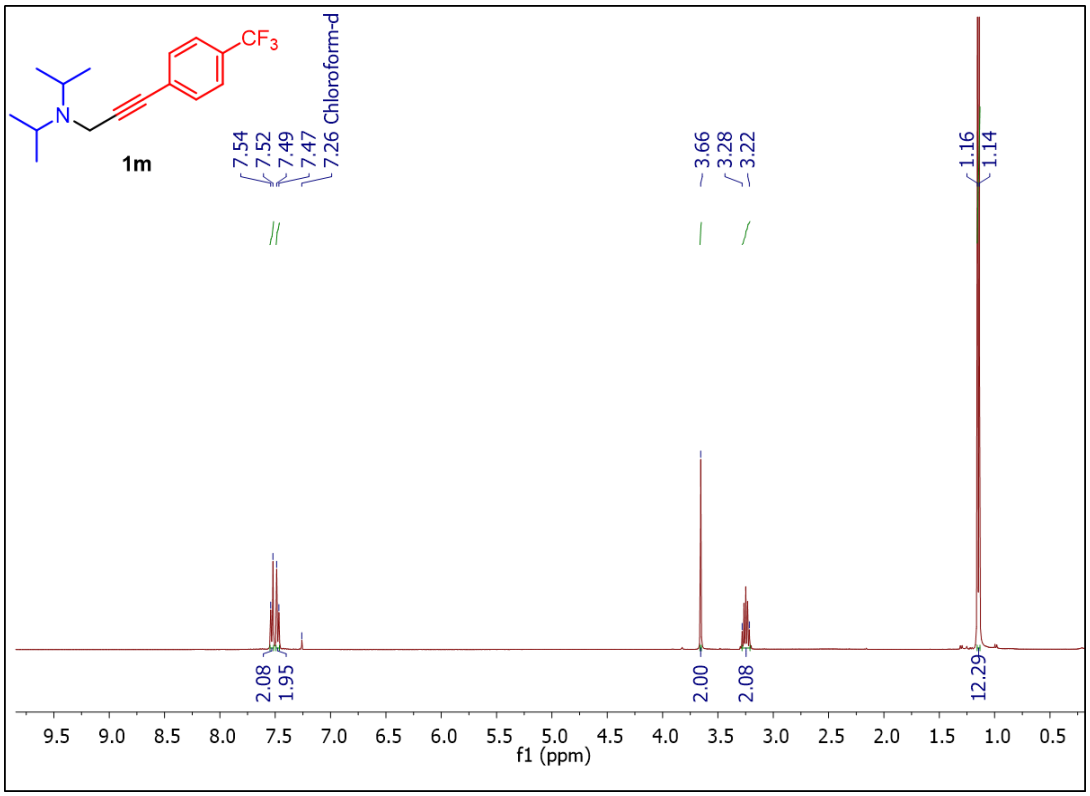

Figure 29: ^{1}H NMR spectrum of **1m** in $CDCl_3$.

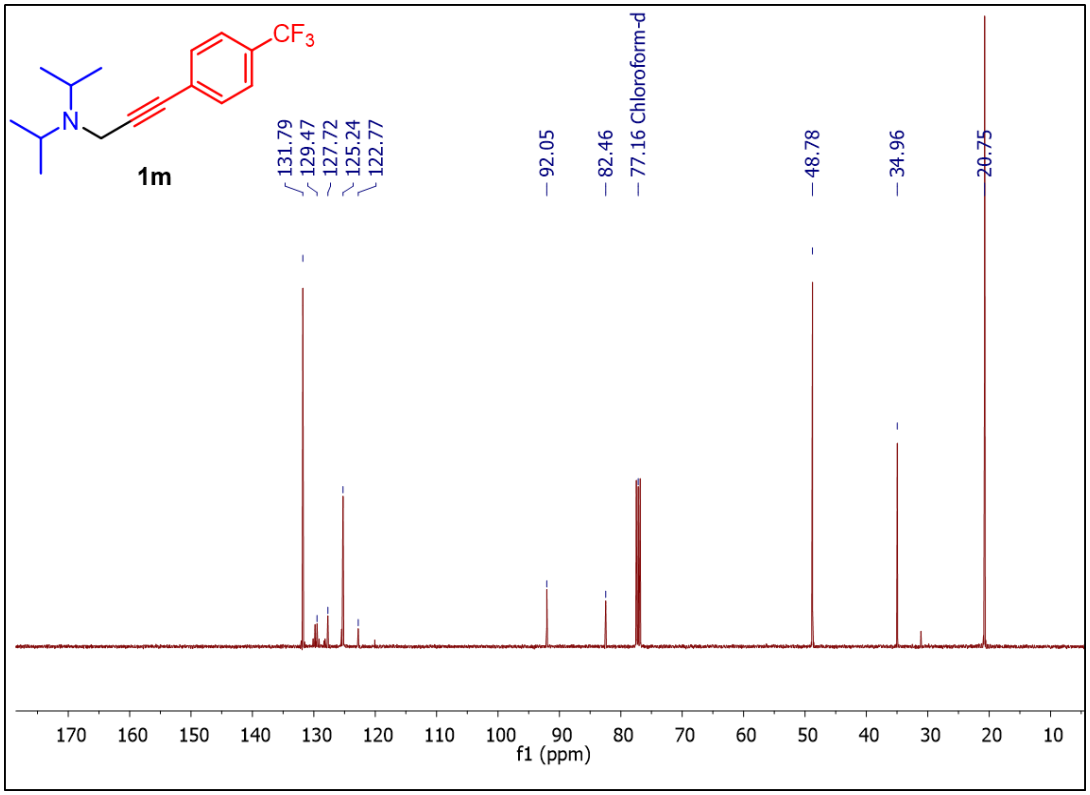

Figure 30: $^{13}C\{^{1}H\}$ NMR spectrum of **1m** in $CDCl_3$.

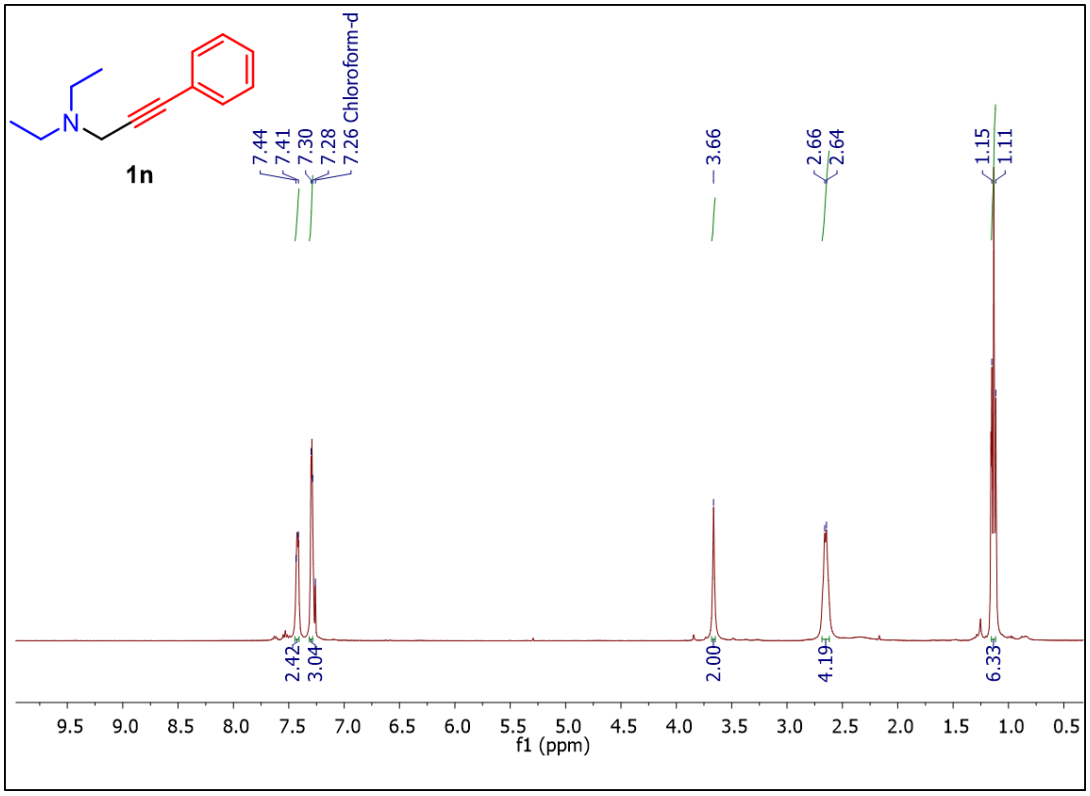

Figure 31: ^{1}H NMR spectrum of **1n** in $CDCl_3$.

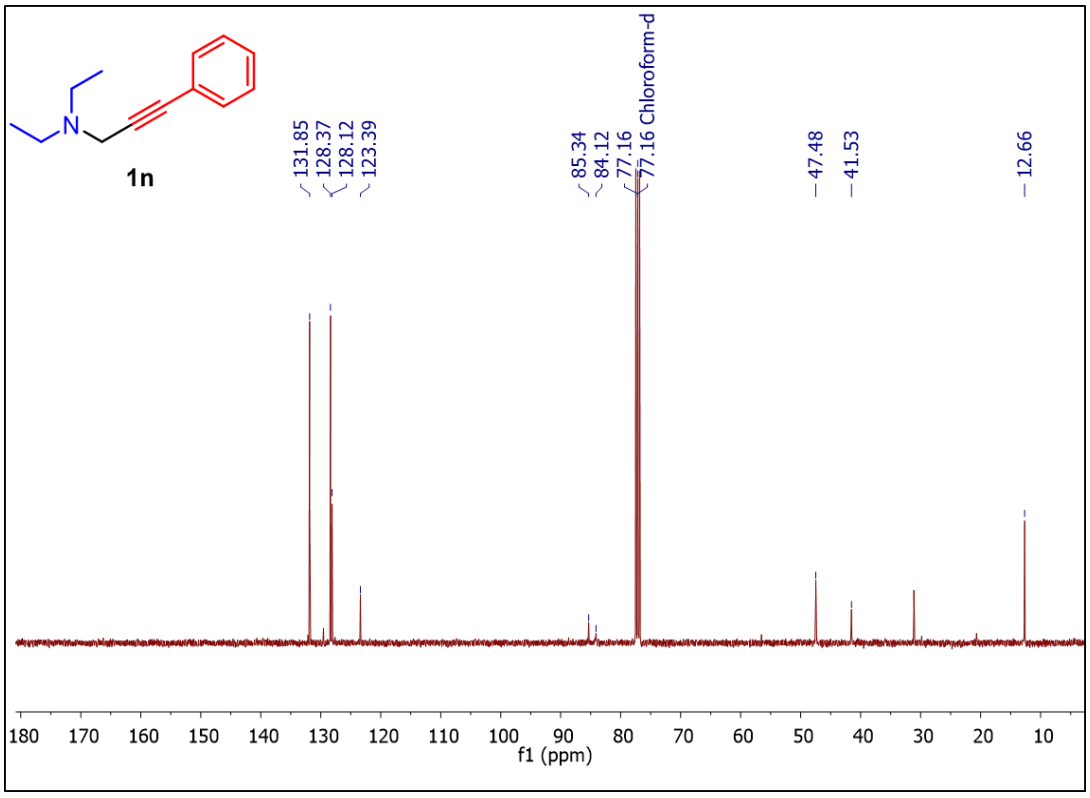

Figure 32: $^{13}C\{^{1}H\}$ NMR spectrum of **1n** in $CDCl_3$.

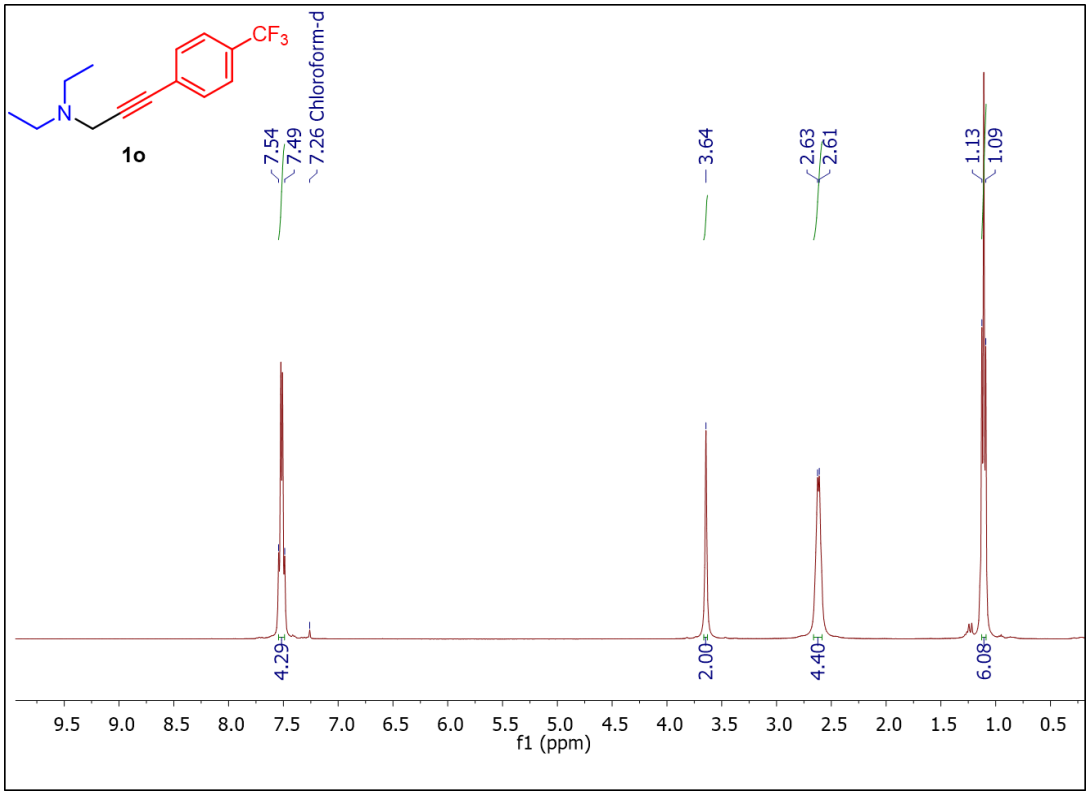

Figure 33: ^{1}H NMR spectrum of **1o** in $CDCl_3$.

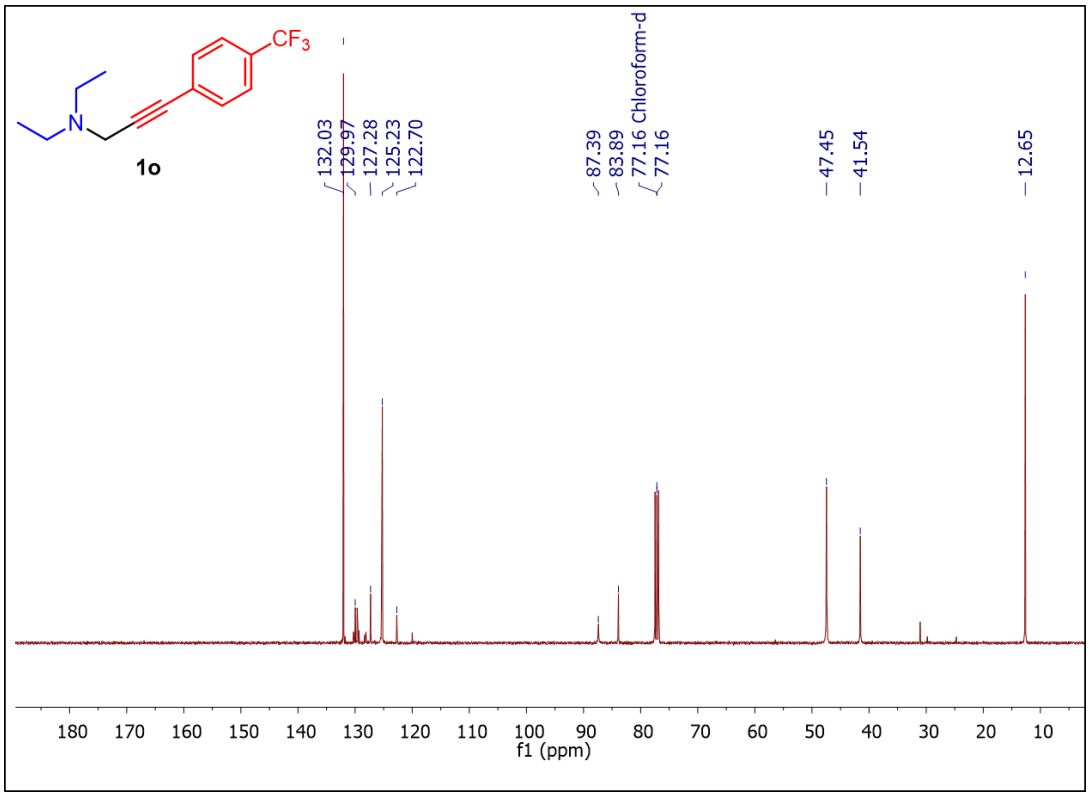

Figure 34: $^{13}C\{^{1}H\}$ NMR spectrum of **1o** in $CDCl_3$.

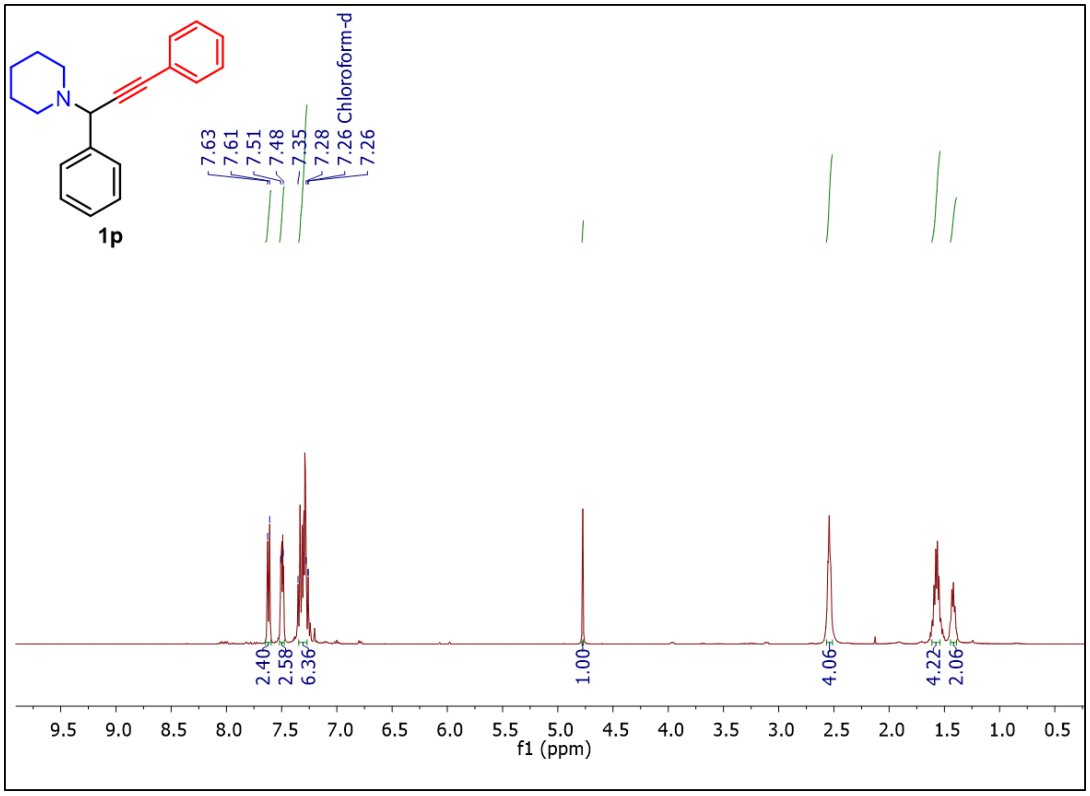

Figure 33: ^{1}H NMR spectrum of **1p** in $CDCl_3$.

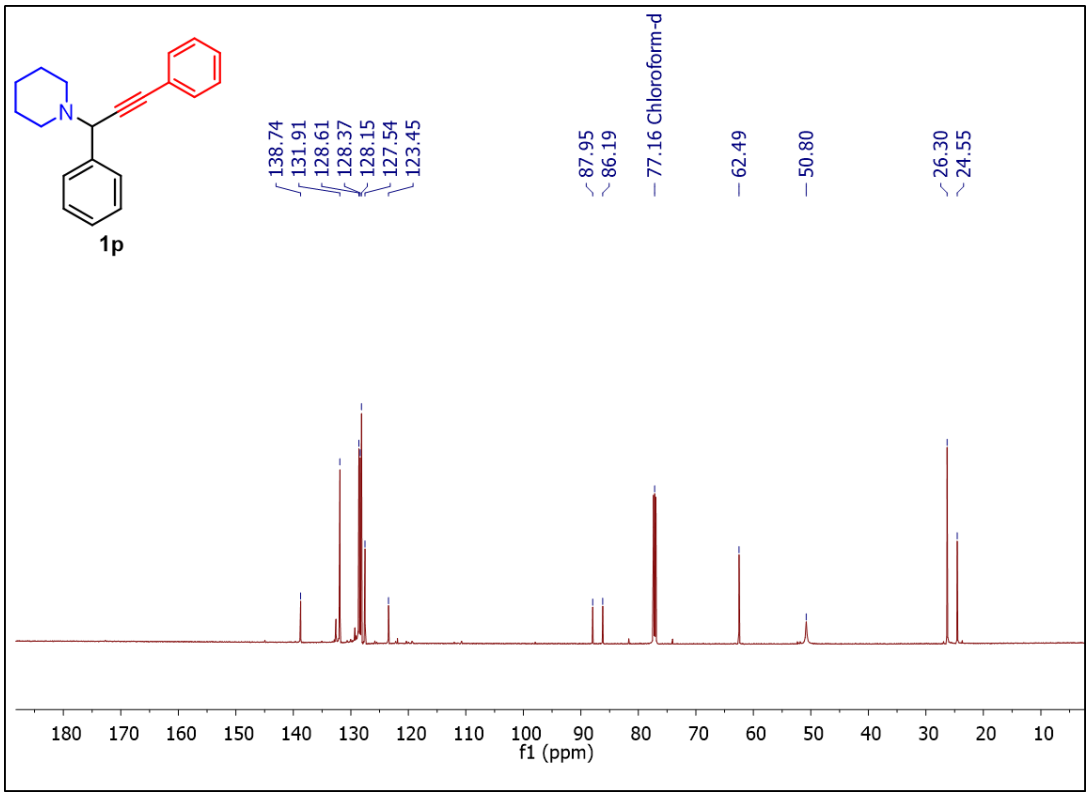

Figure 36: $^{13}C\{^{1}H\}$ NMR spectrum of **1p** in $CDCl_3$.

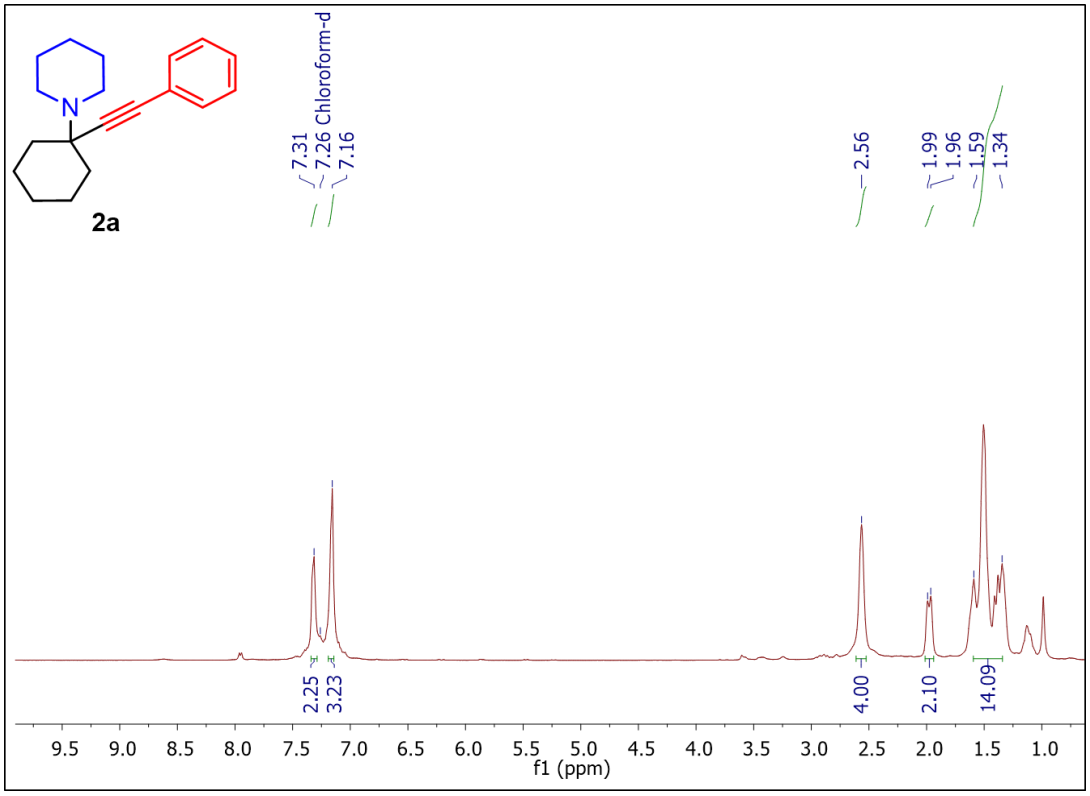

Figure 37: ^{1}H NMR spectrum of **2a** in $CDCl_3$.

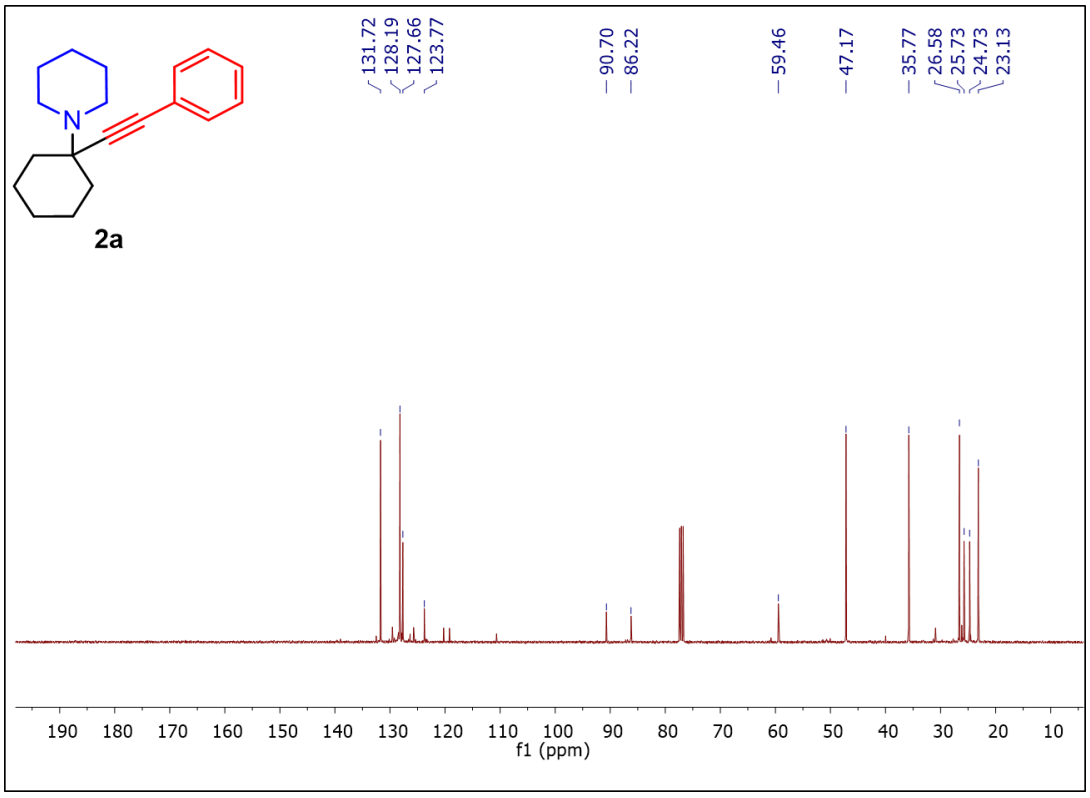

Figure 38: $^{13}C\{^{1}H\}$ NMR spectrum of **2a** in $CDCl_3$.

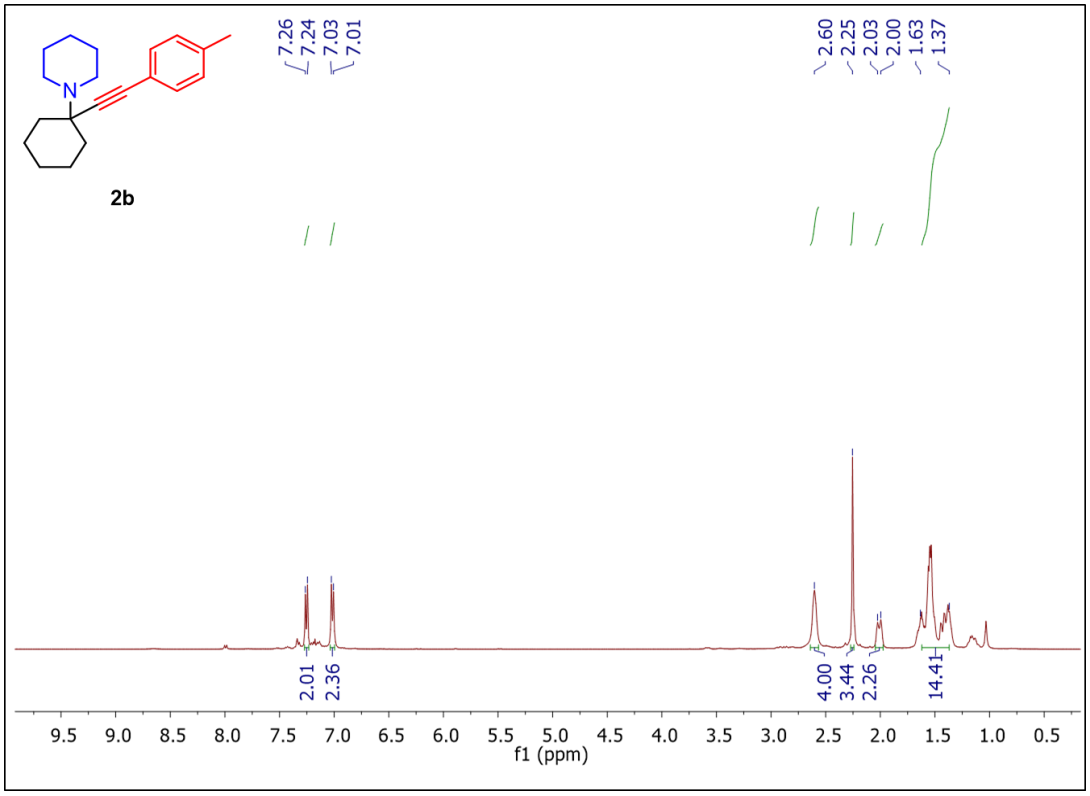

Figure 39: ^{1}H NMR spectrum of **2b** in $CDCl_3$.

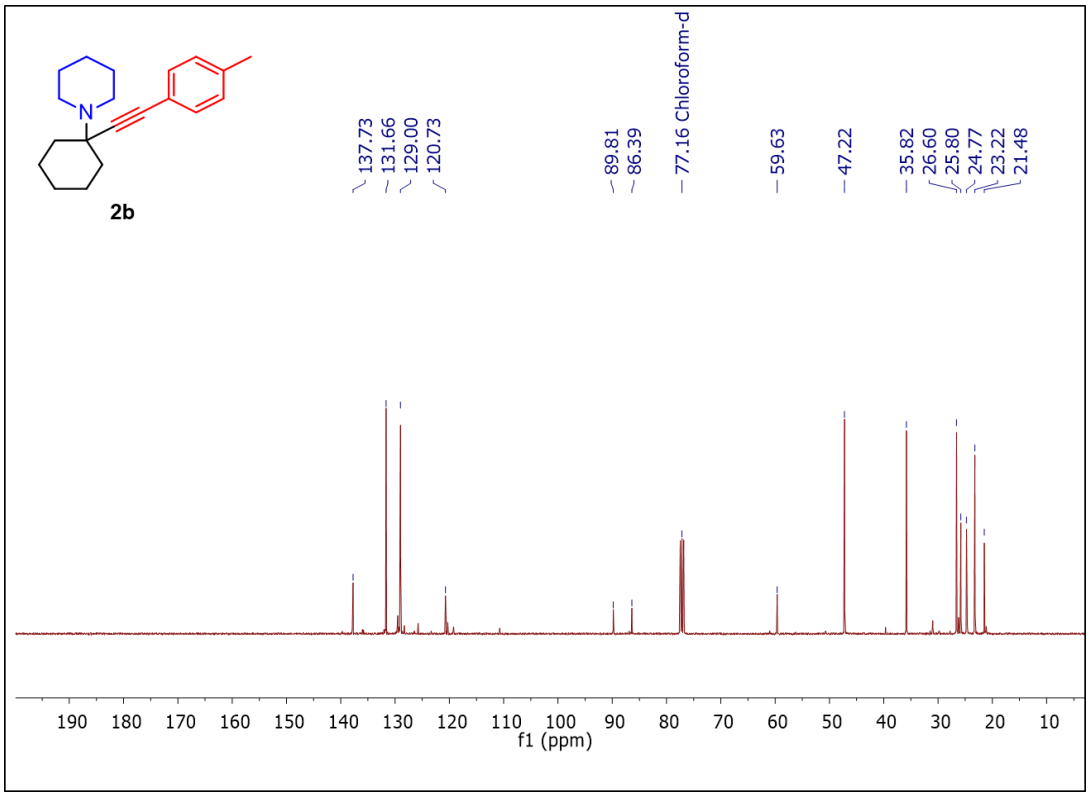

Figure 40: $^{13}C\{^{1}H\}$ NMR spectrum of **2b** in $CDCl_3$.

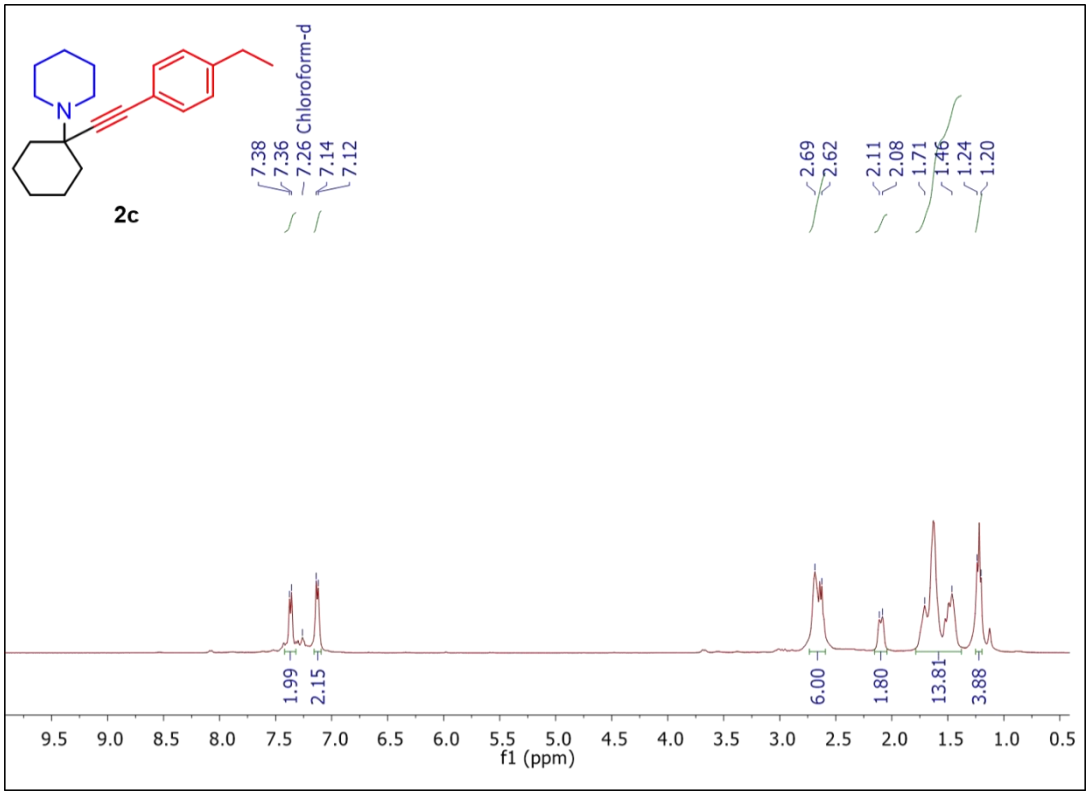

Figure 41: ^{1}H NMR spectrum of **2c** in $CDCl_3$.

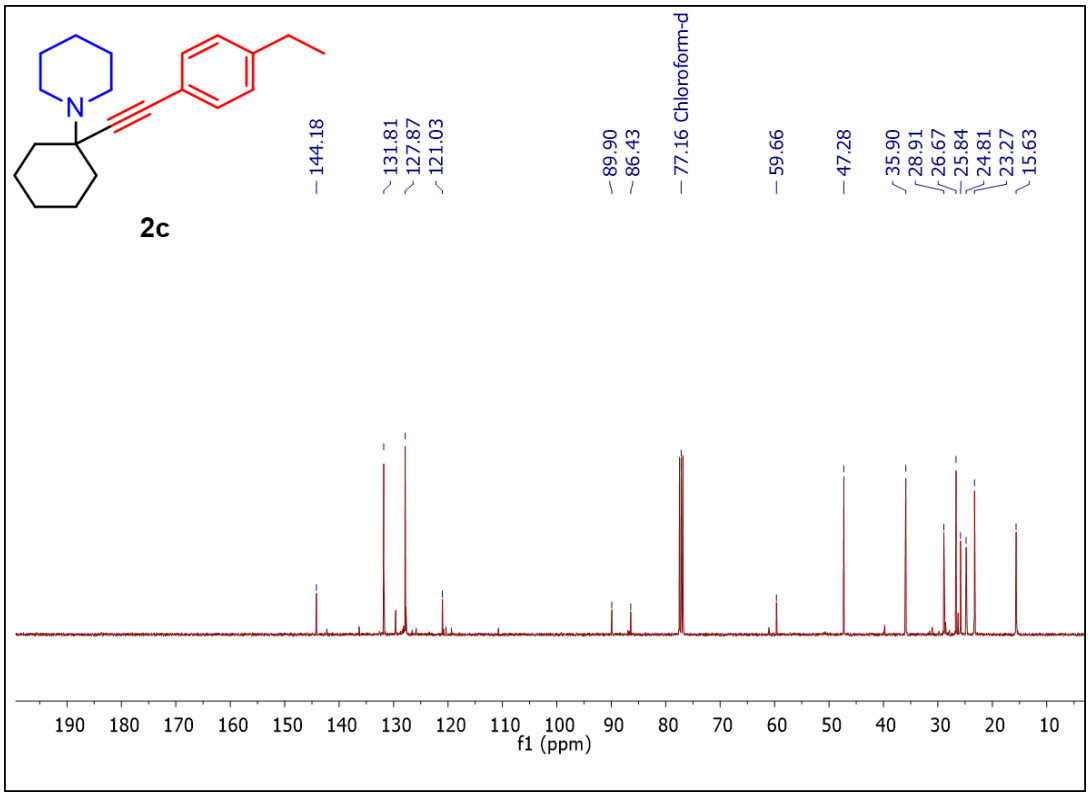

Figure 42: $^{13}C\{^{1}H\}$ NMR spectrum of **2c** in $CDCl_3$.

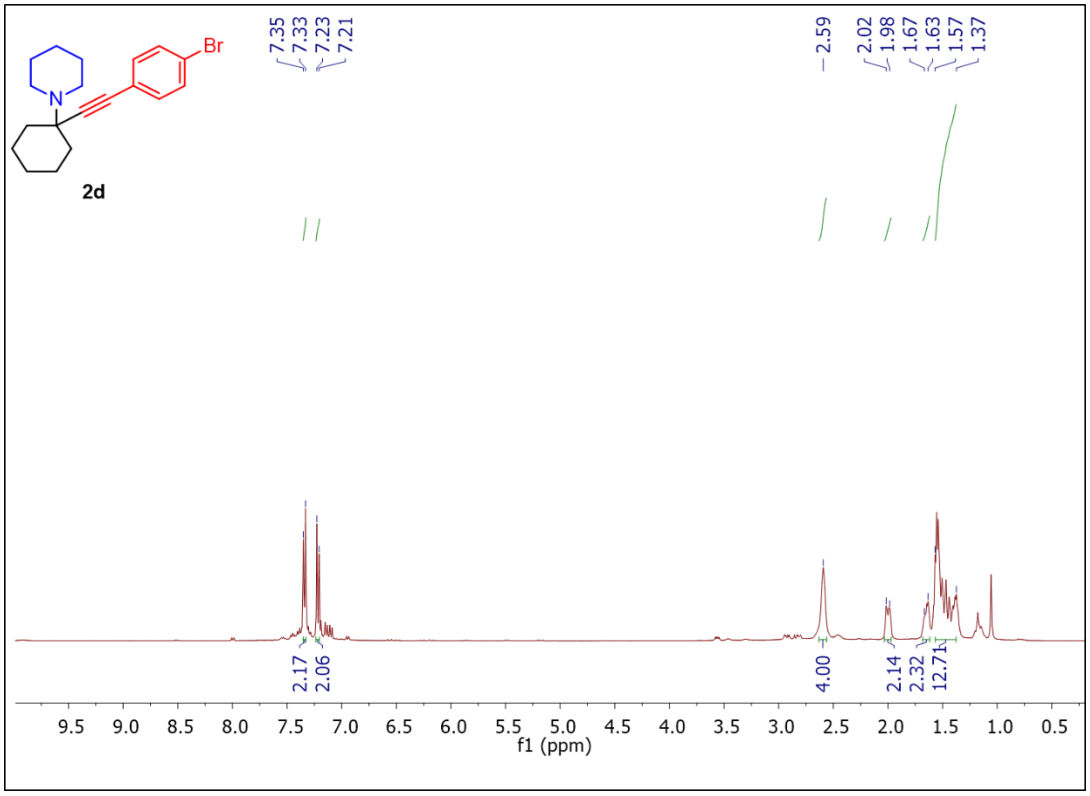

Figure 43: ^{1}H NMR spectrum of **2d** in $CDCl_3$.

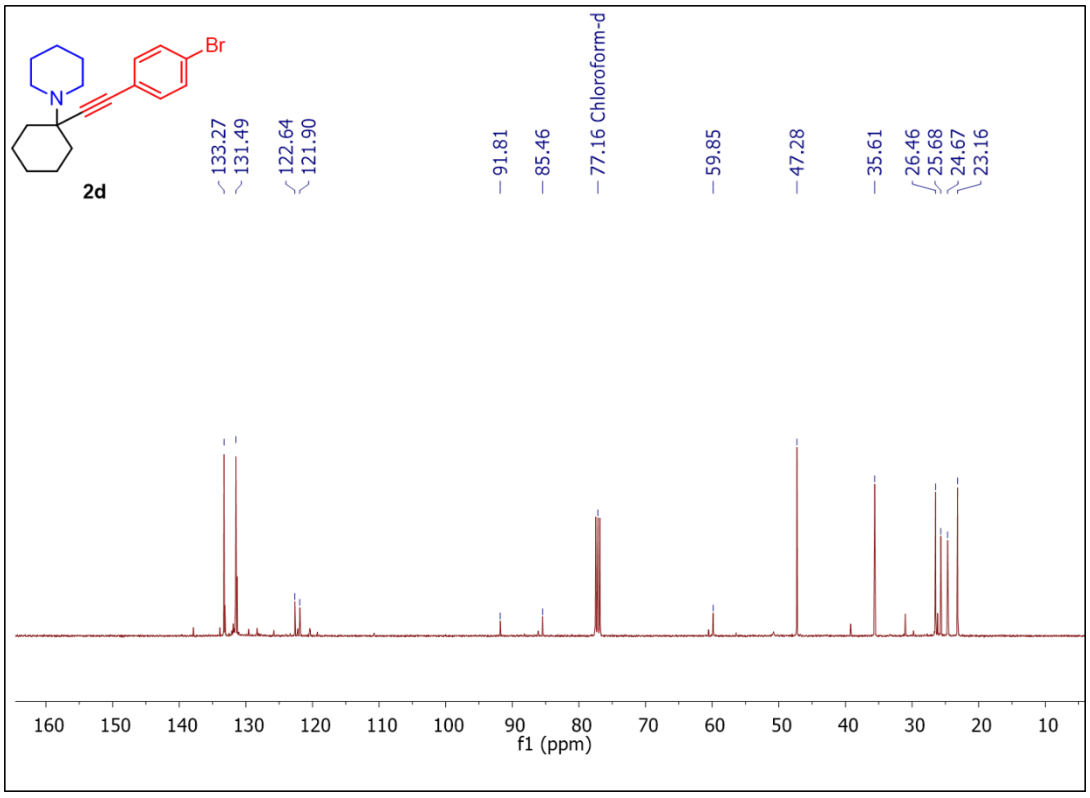

Figure 44: $^{13}C\{^{1}H\}$ NMR spectrum of **2d** in $CDCl_3$.

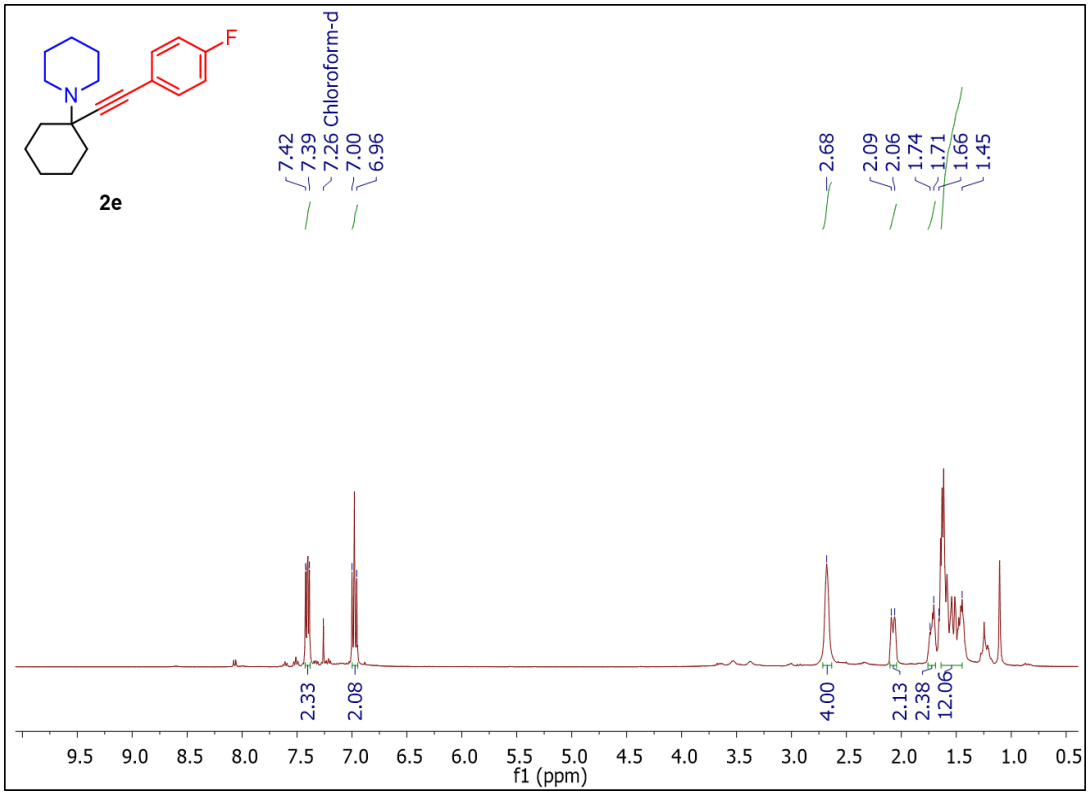

Figure 45: ^{1}H NMR spectrum of **2e** in $CDCl_3$.

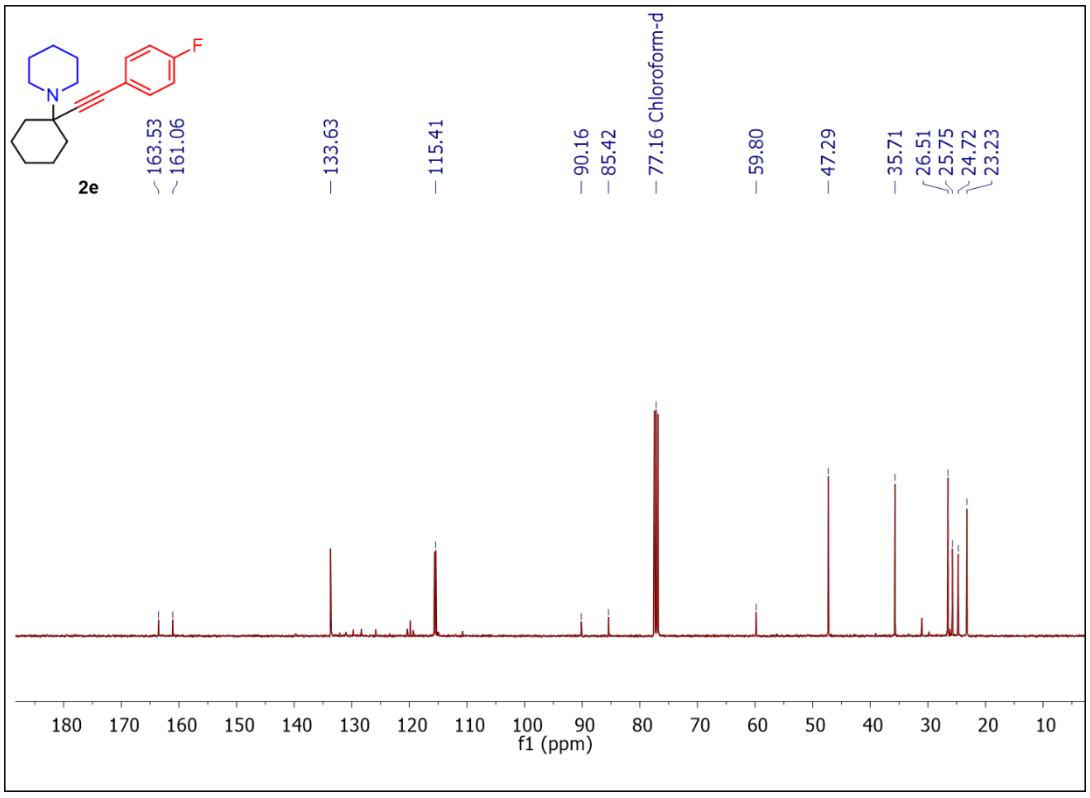

Figure 46: $^{13}C\{^{1}H\}$ NMR spectrum of **2e** in $CDCl_3$.

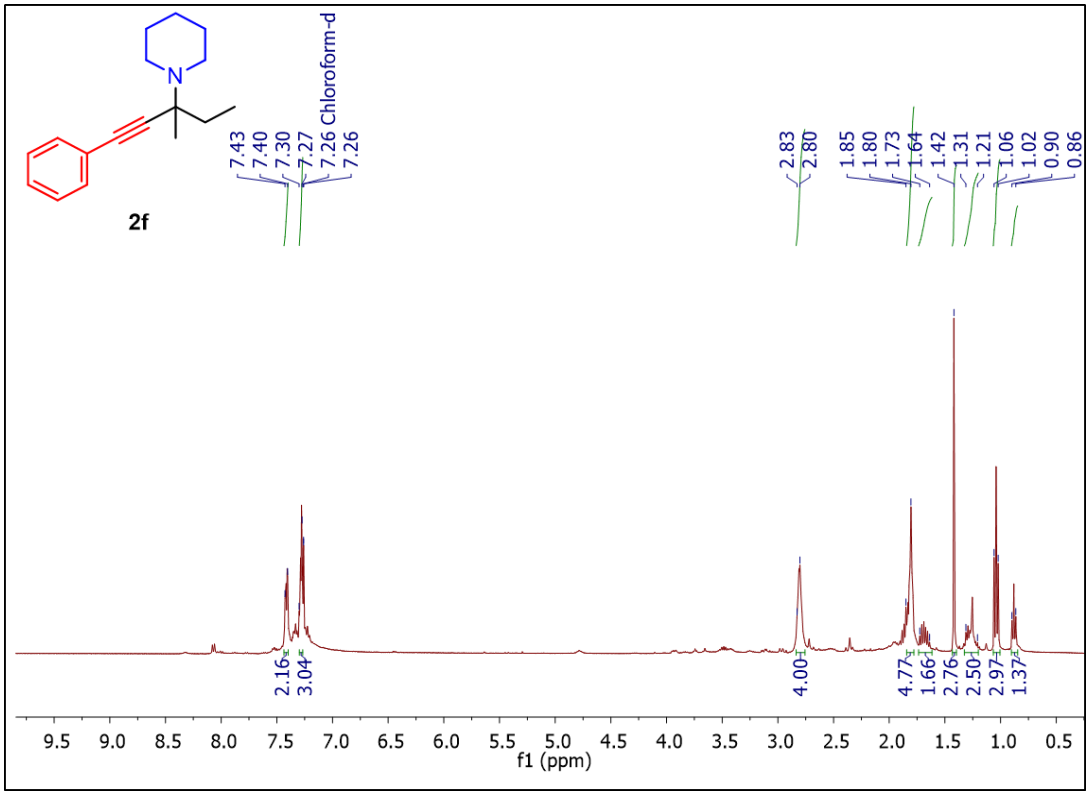

Figure 47: ^{1}H NMR spectrum of **2f** in $CDCl_3$.

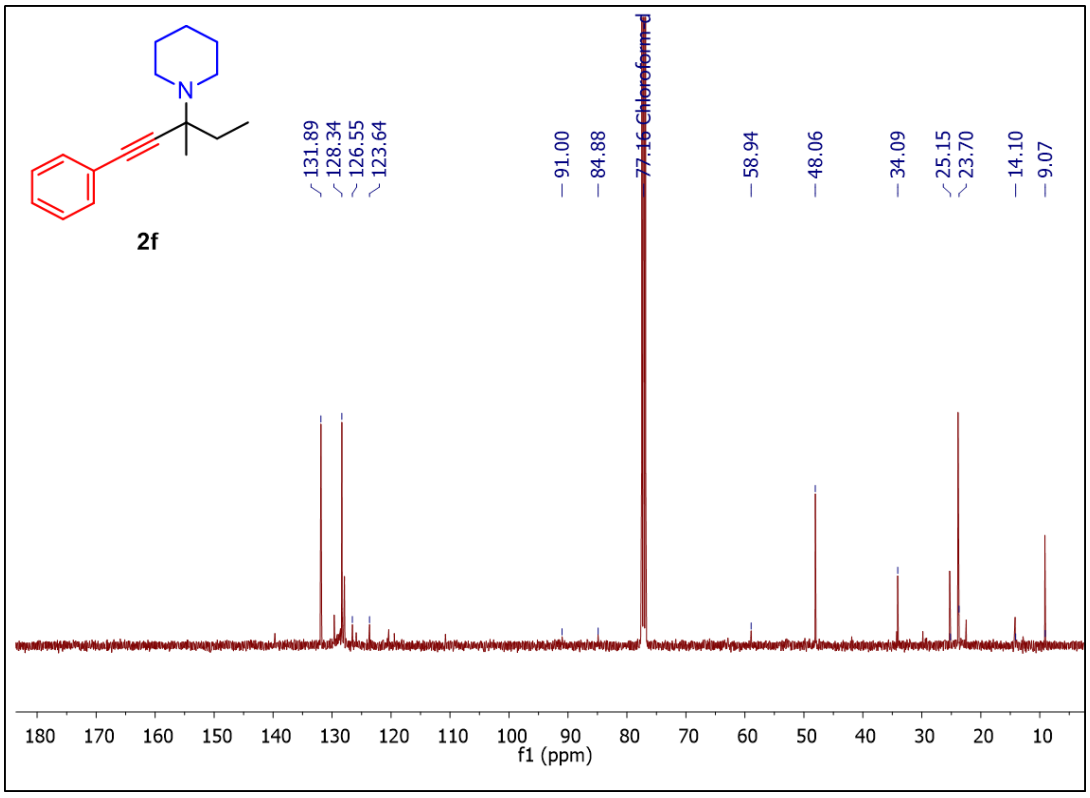

Figure 48: $^{13}C\{^{1}H\}$ NMR spectrum of **2f** in $CDCl_3$.

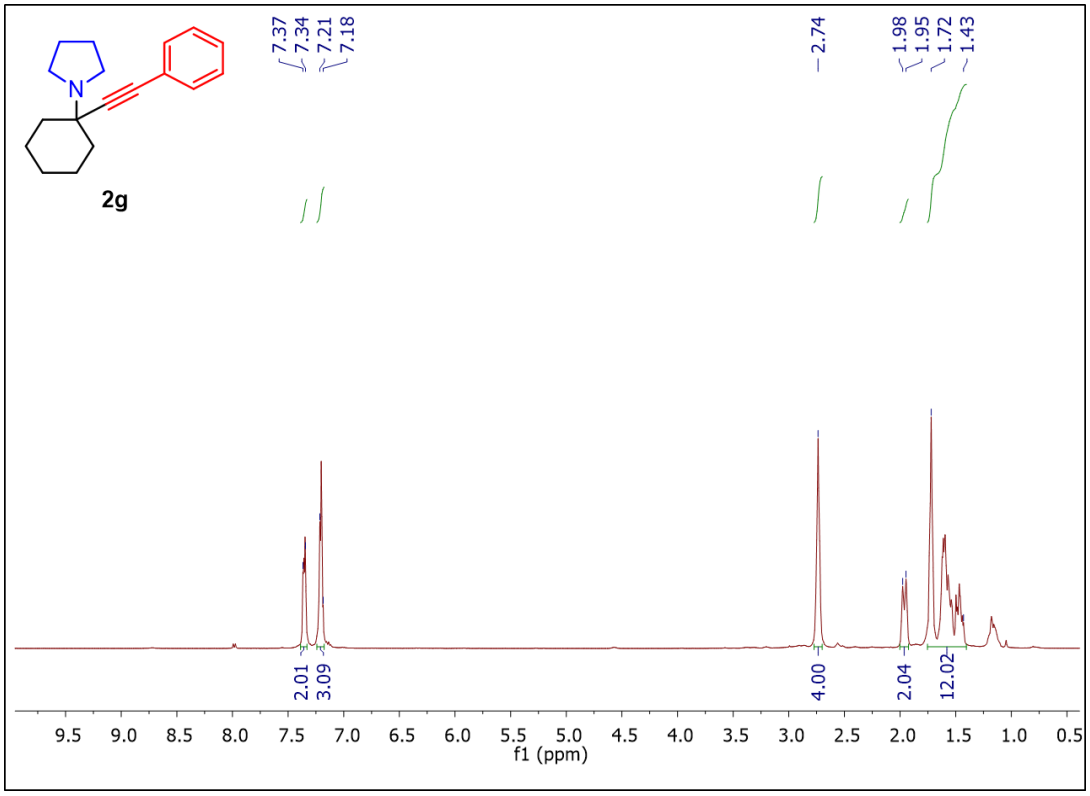

Figure 49: ^{1}H NMR spectrum of **2g** in $CDCl_3$.

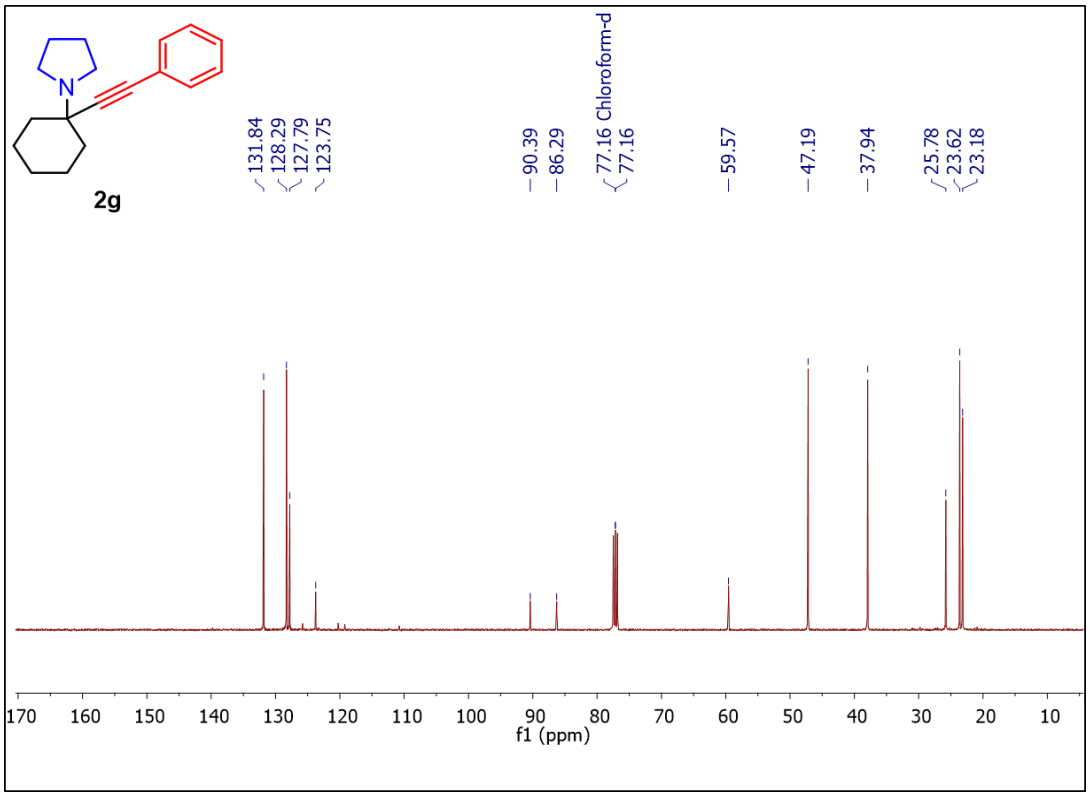

Figure 50: $^{13}C\{^{1}H\}$ NMR spectrum of **2g** in $CDCl_3$.

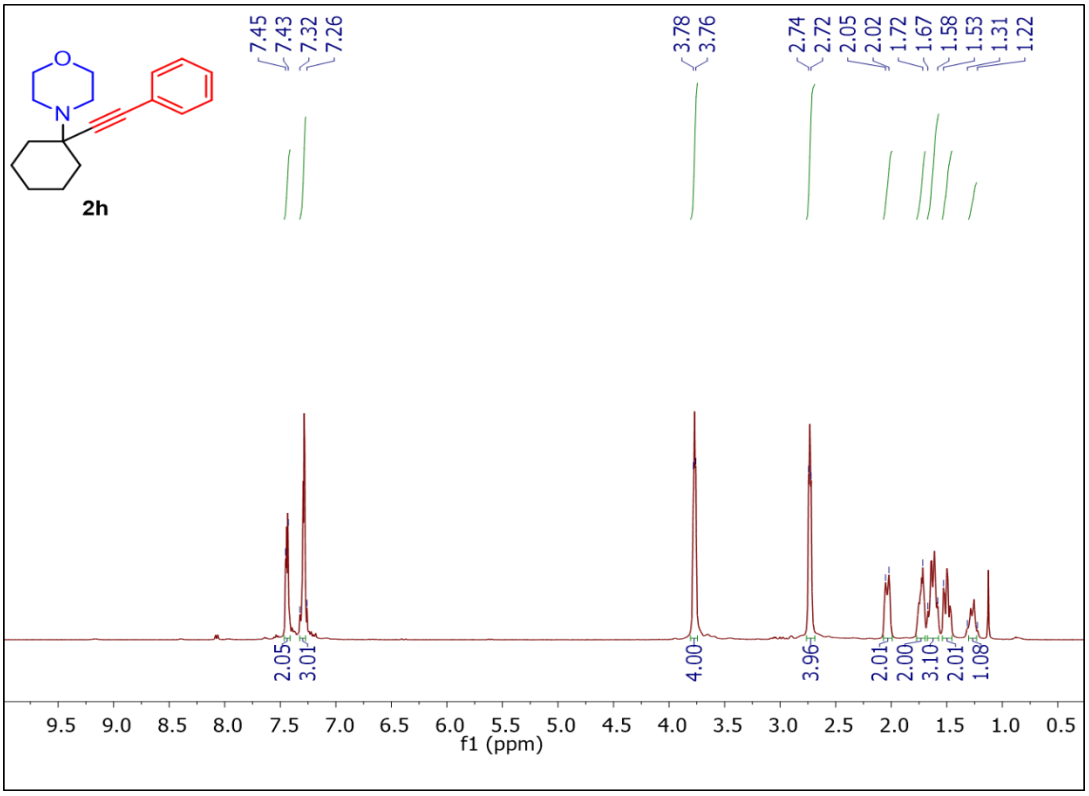

Figure 51: ^{1}H NMR spectrum of **2h** in $CDCl_3$.

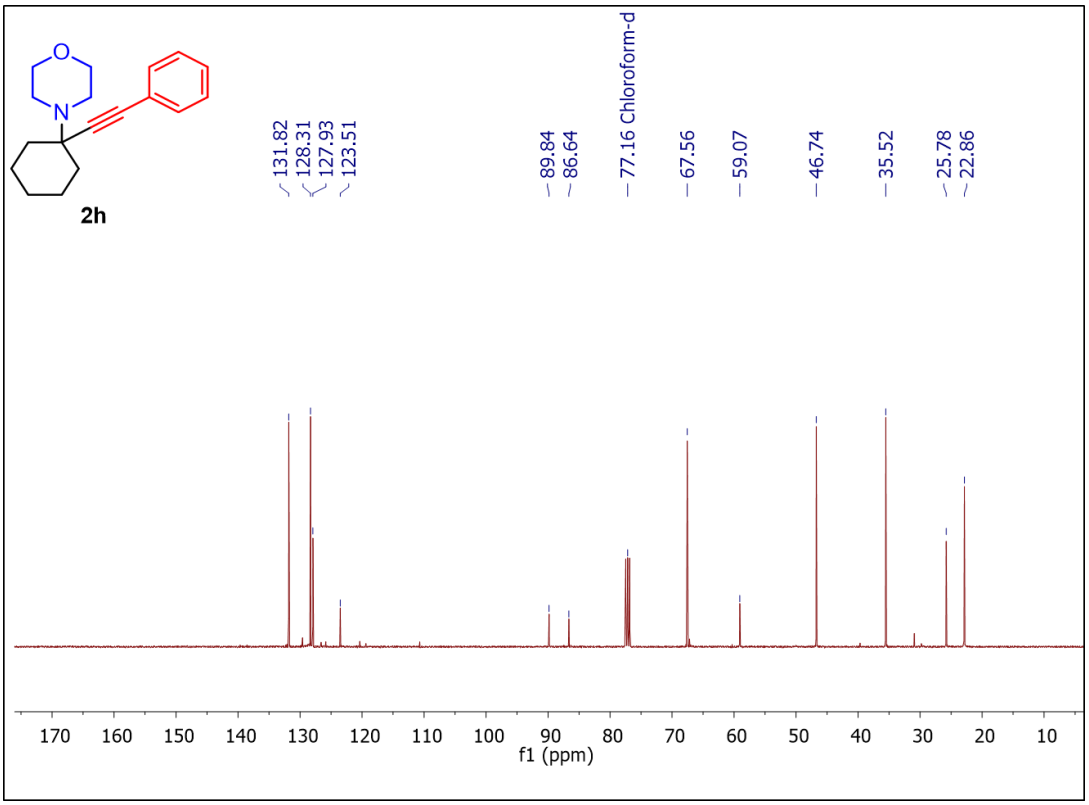

Figure 52: $^{13}C\{^{1}H\}$ NMR spectrum of **2h** in $CDCl_3$.

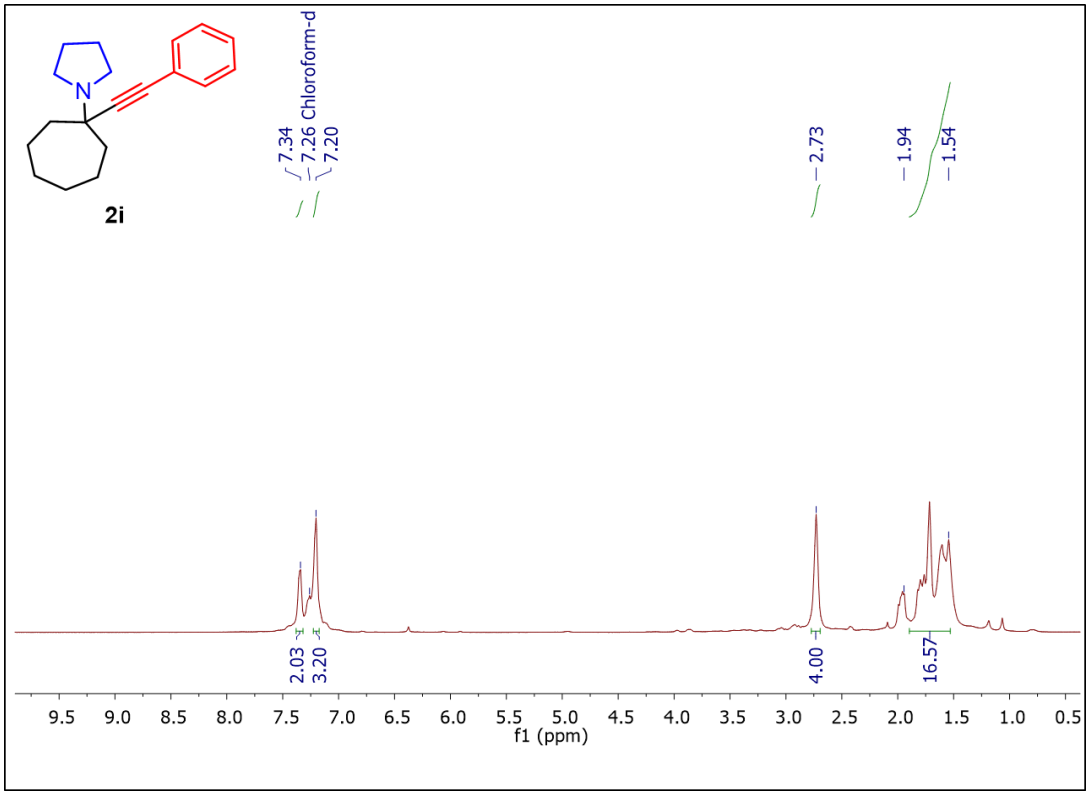

Figure 53: ^{1}H NMR spectrum of **2i** in $CDCl_3$.

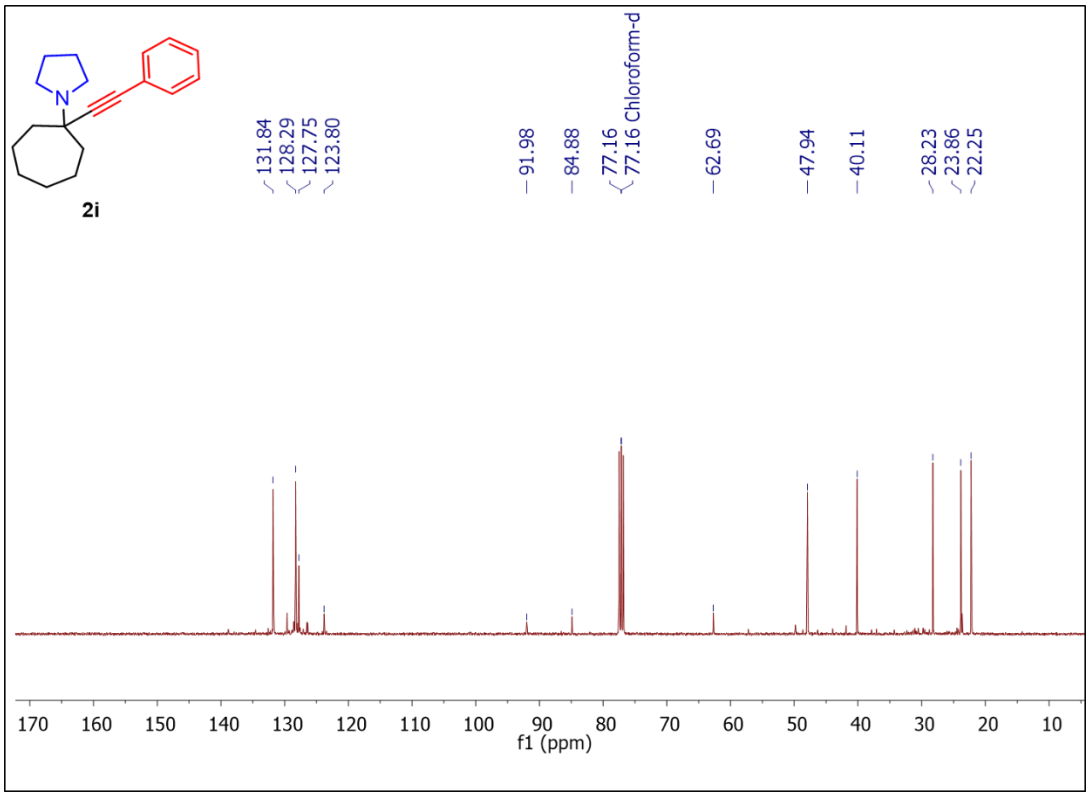

Figure 54: $^{13}C\{^{1}H\}$ NMR spectrum of **2i** in $CDCl_3$.

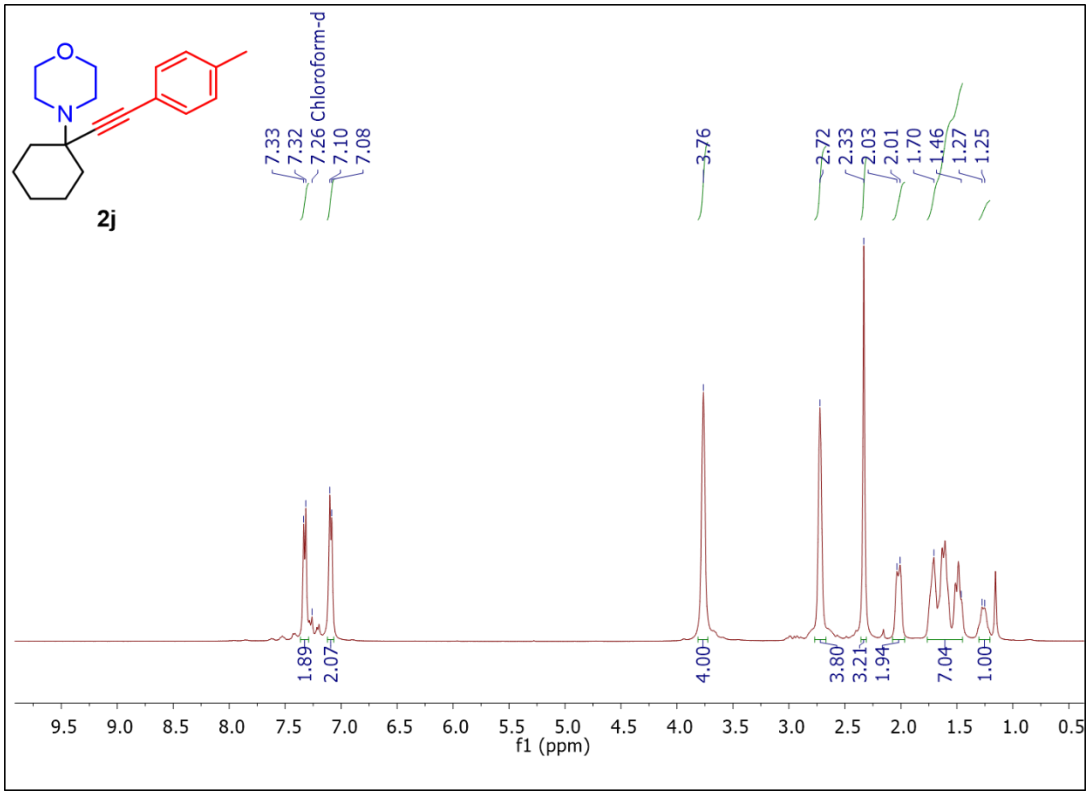

Figure 55: ^{1}H NMR spectrum of **2j** in $CDCl_3$.

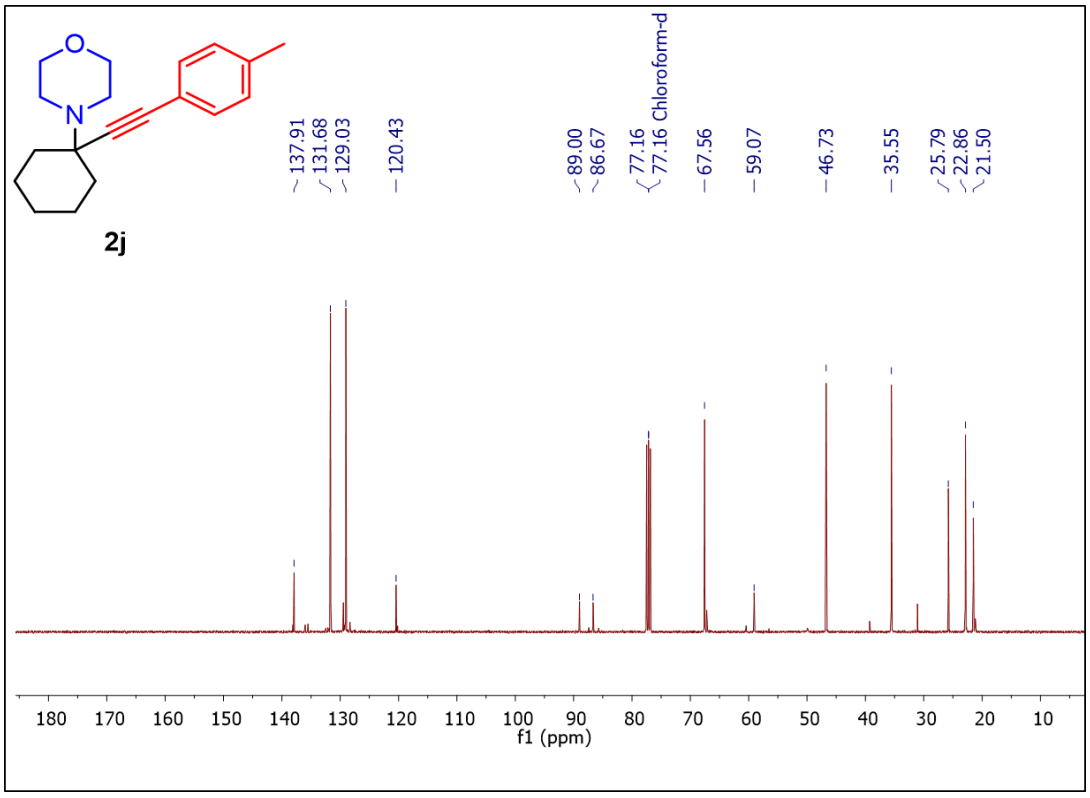

Figure 56: $^{13}C\{^{1}H\}$ NMR spectrum of **2j** in $CDCl_3$.

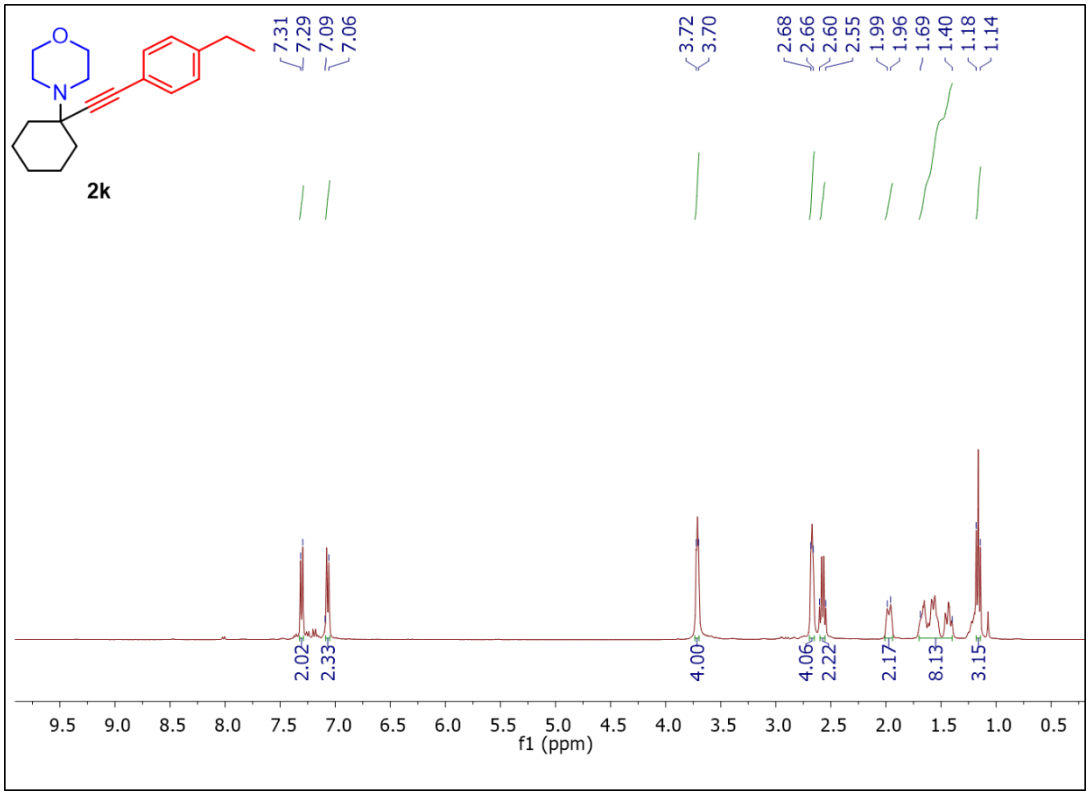

Figure 57: ^{1}H NMR spectrum of **2k** in $CDCl_3$.

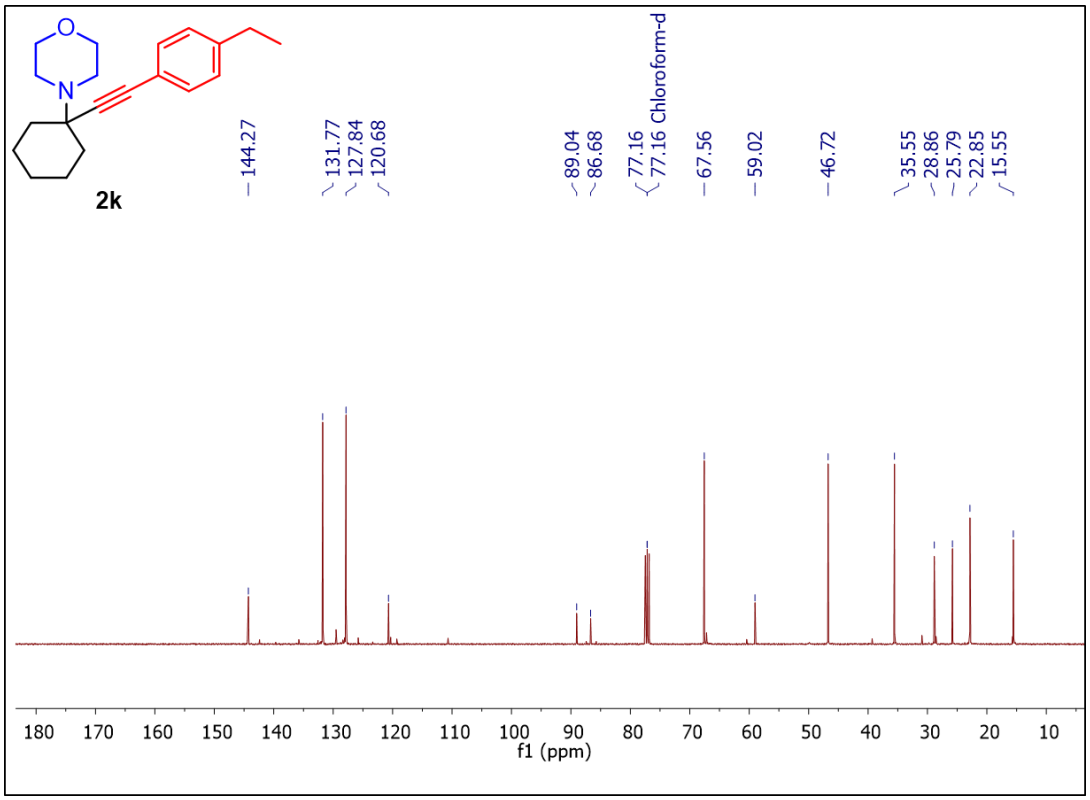

Figure 58: $^{13}C\{^{1}H\}$ NMR spectrum of **2k** in $CDCl_3$.

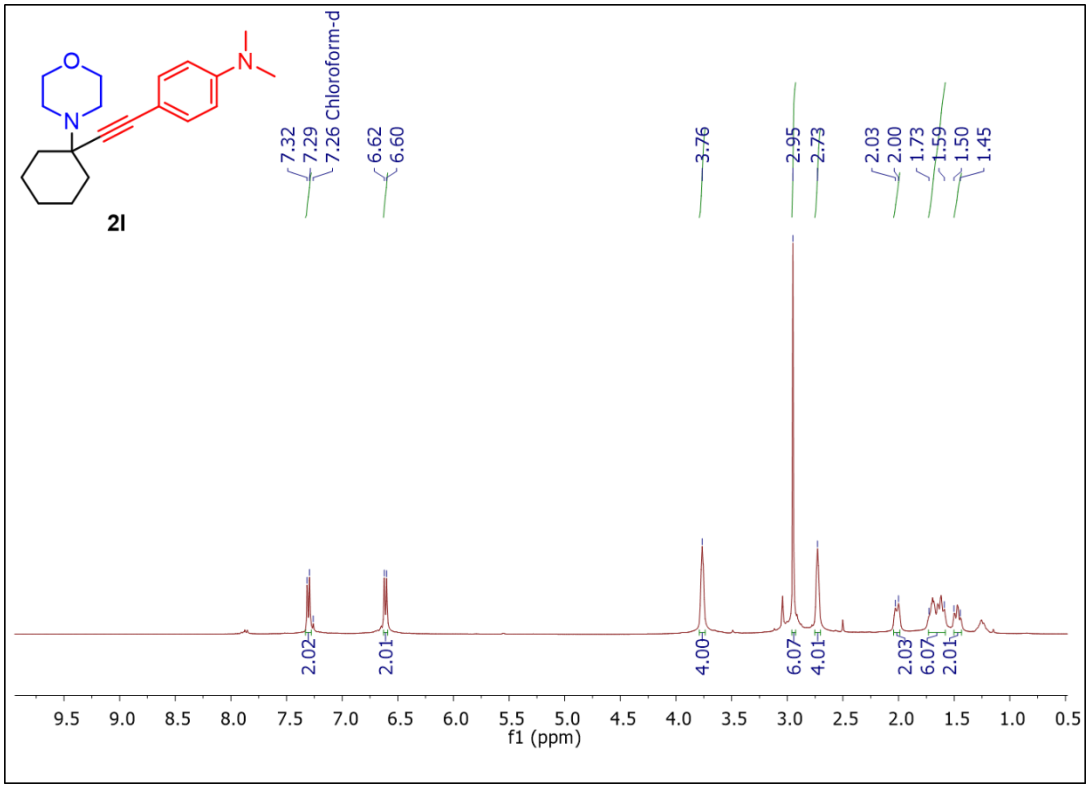

Figure 59: ^{1}H NMR spectrum of **2l** in $CDCl_3$.

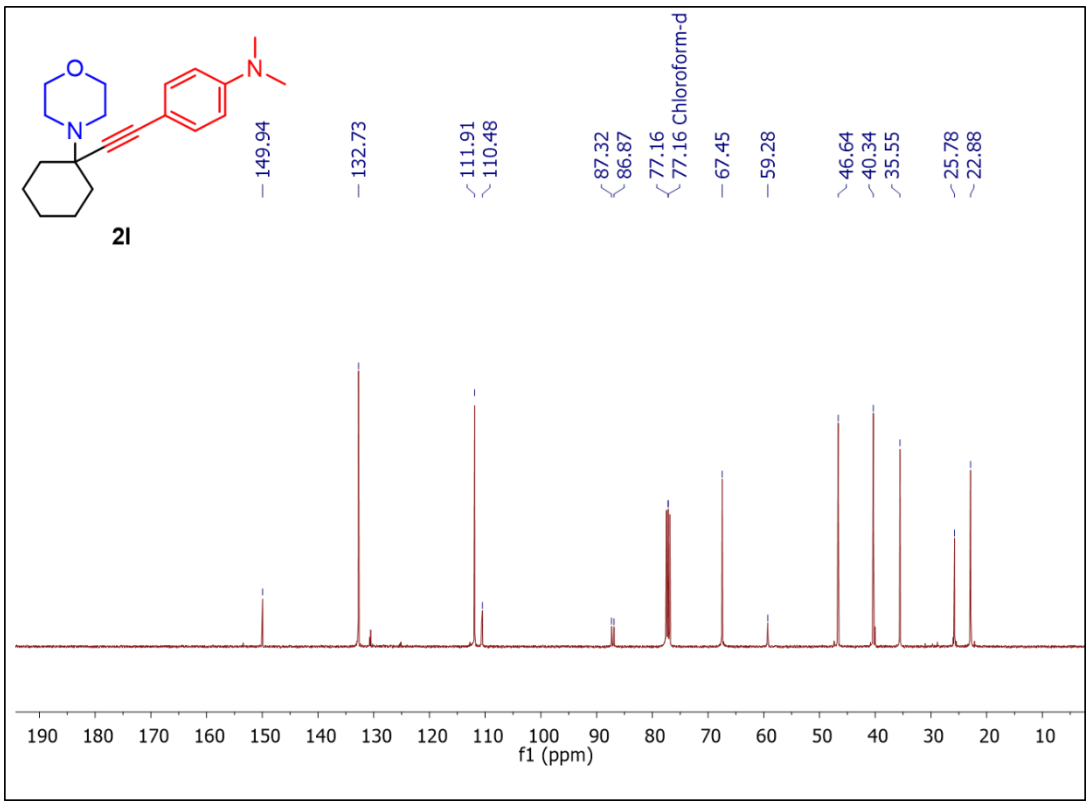

Figure 60: $^{13}C\{^{1}H\}$ NMR spectrum of **2l** in $CDCl_3$.

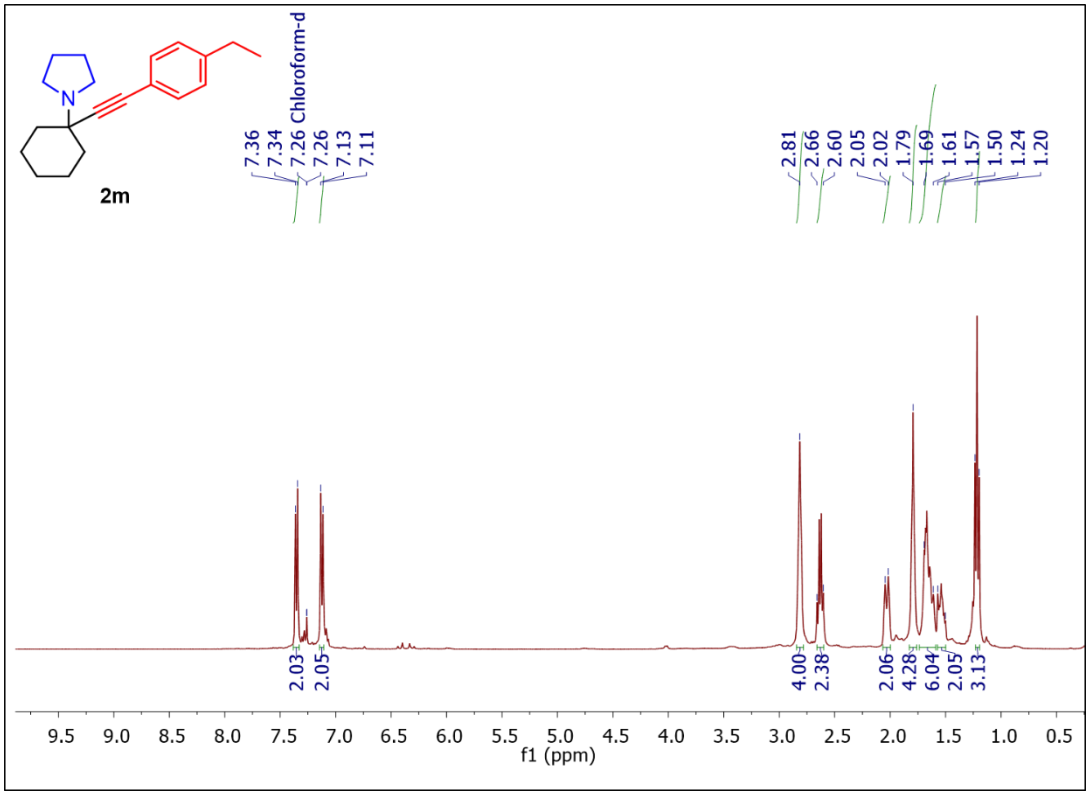

Figure 61: ^{1}H NMR spectrum of **2m** in $CDCl_3$.

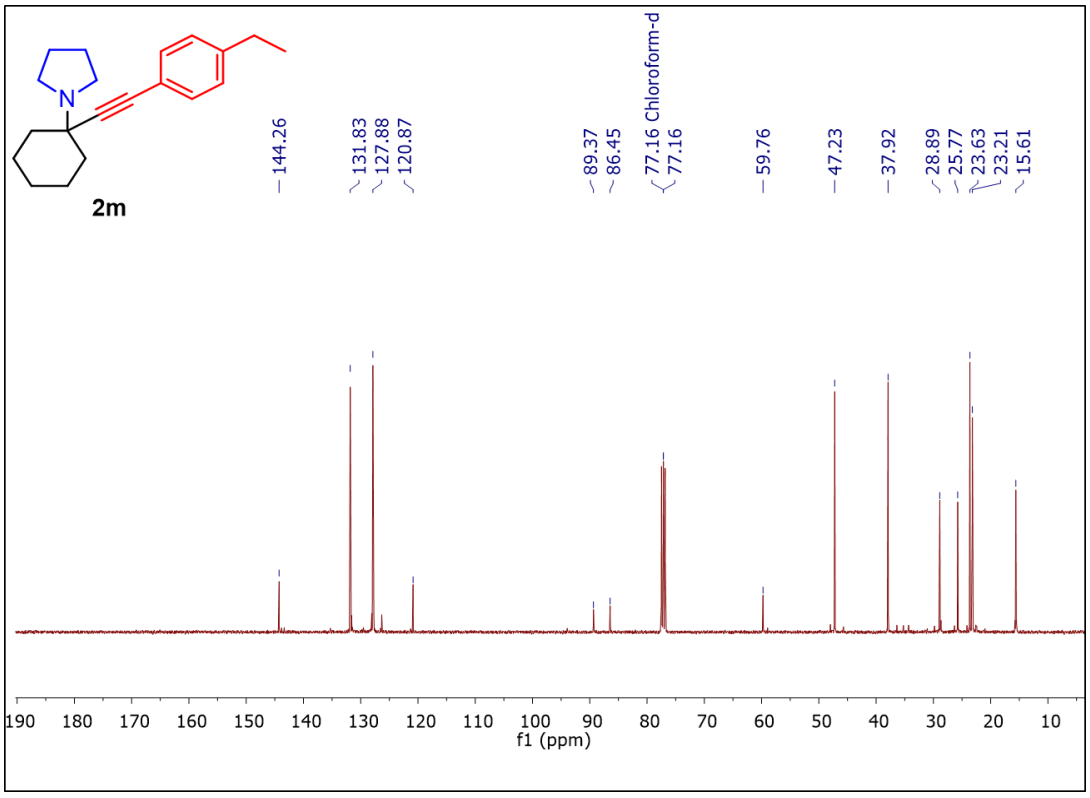

Figure 62: $^{13}C\{^{1}H\}$ NMR spectrum of **2m** in $CDCl_3$.

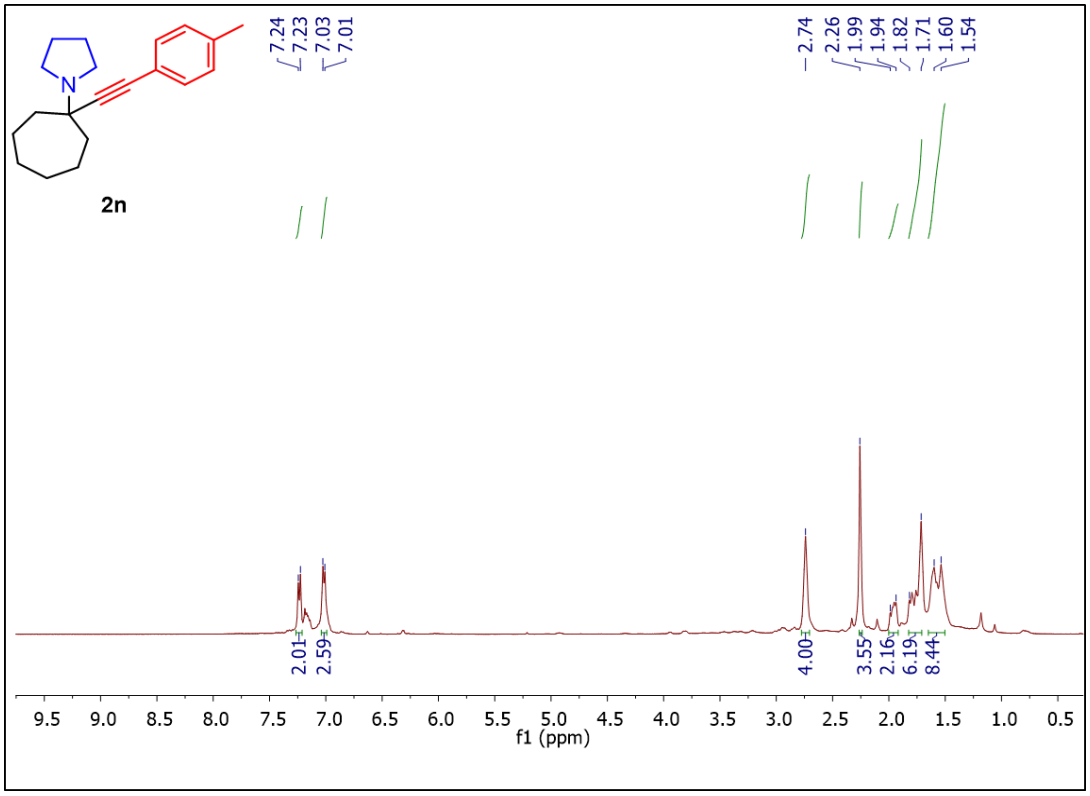

Figure 63: ^{1}H NMR spectrum of **2n** in $CDCl_3$.

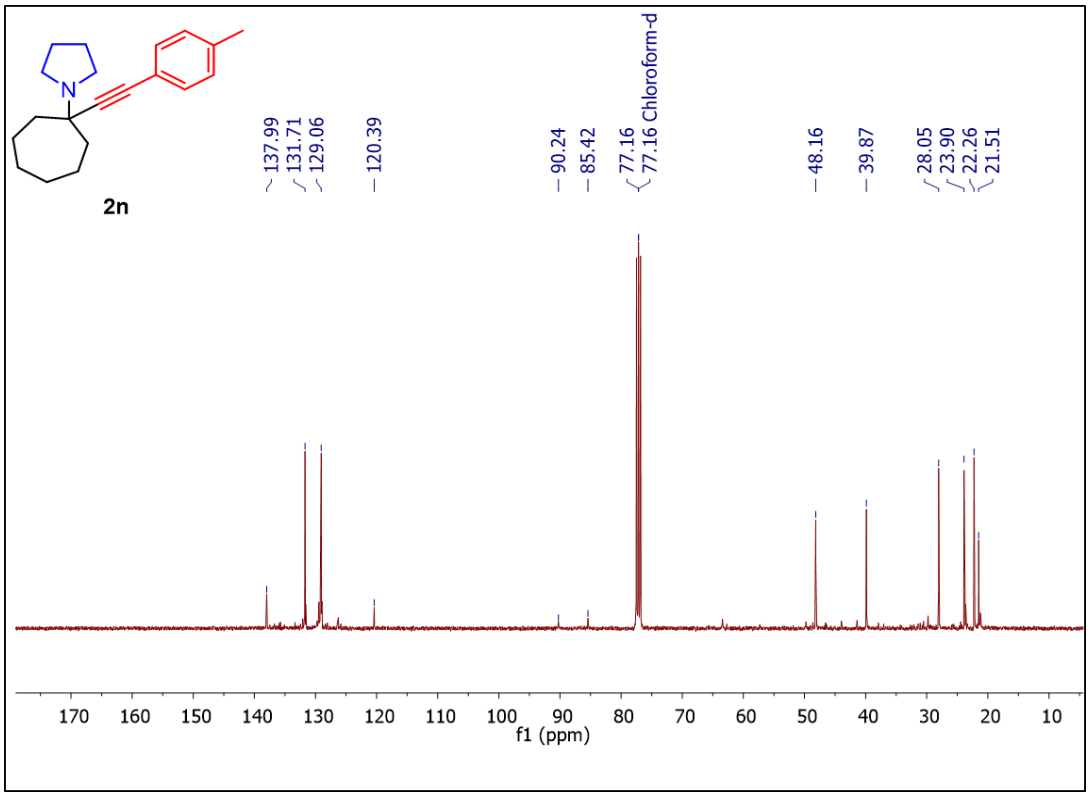

Figure 64: $^{13}C\{^{1}H\}$ NMR spectrum of **2n** in $CDCl_3$.

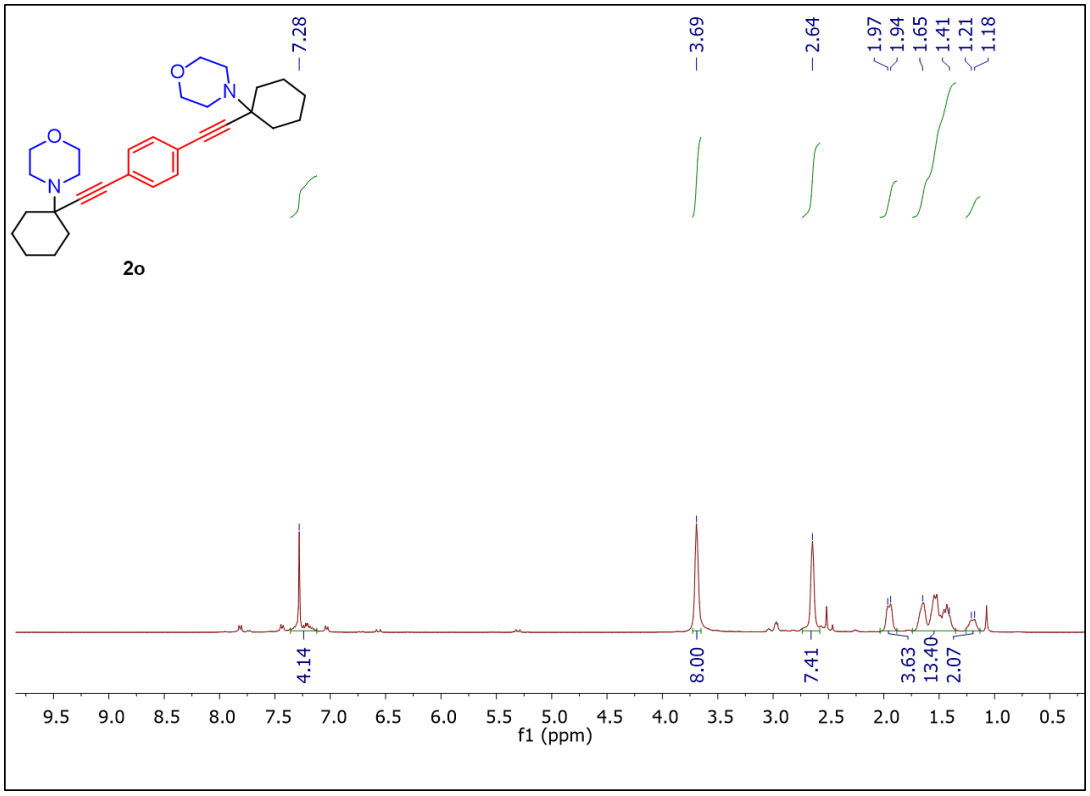

Figure 65: ^{1}H NMR spectrum of **2o** in $CDCl_3$.

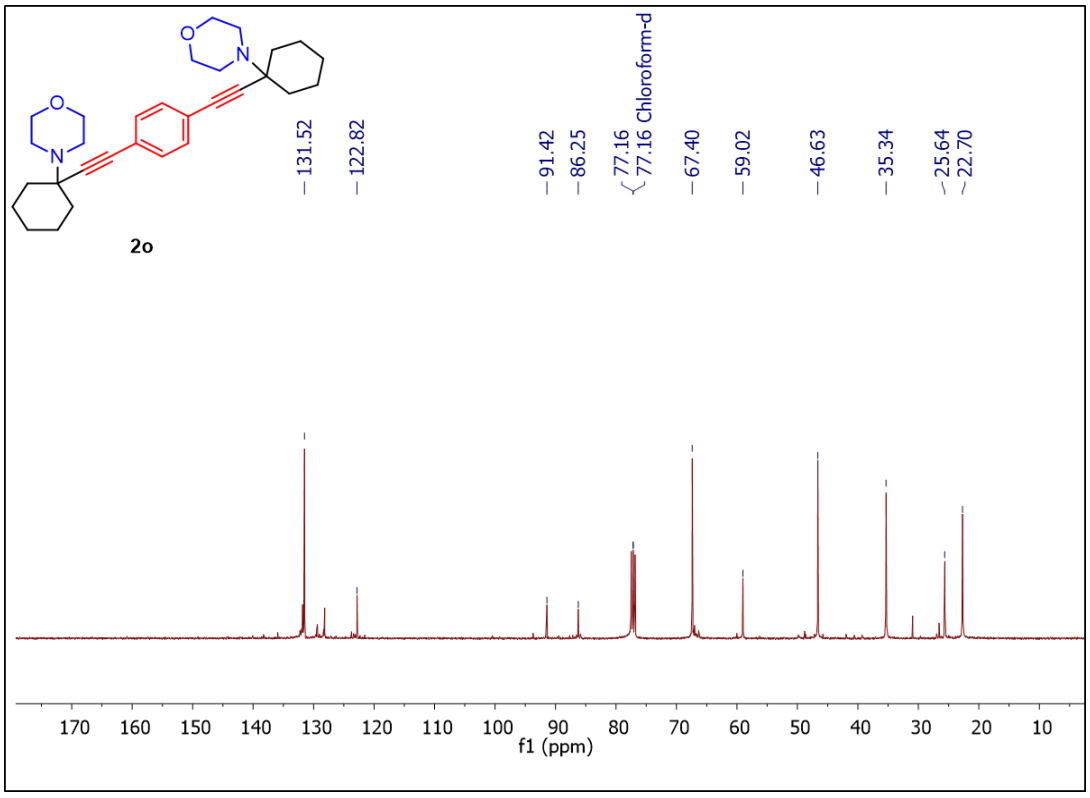

Figure 66: $^{13}C\{^{1}H\}$ NMR spectrum of **2o** in $CDCl_3$.

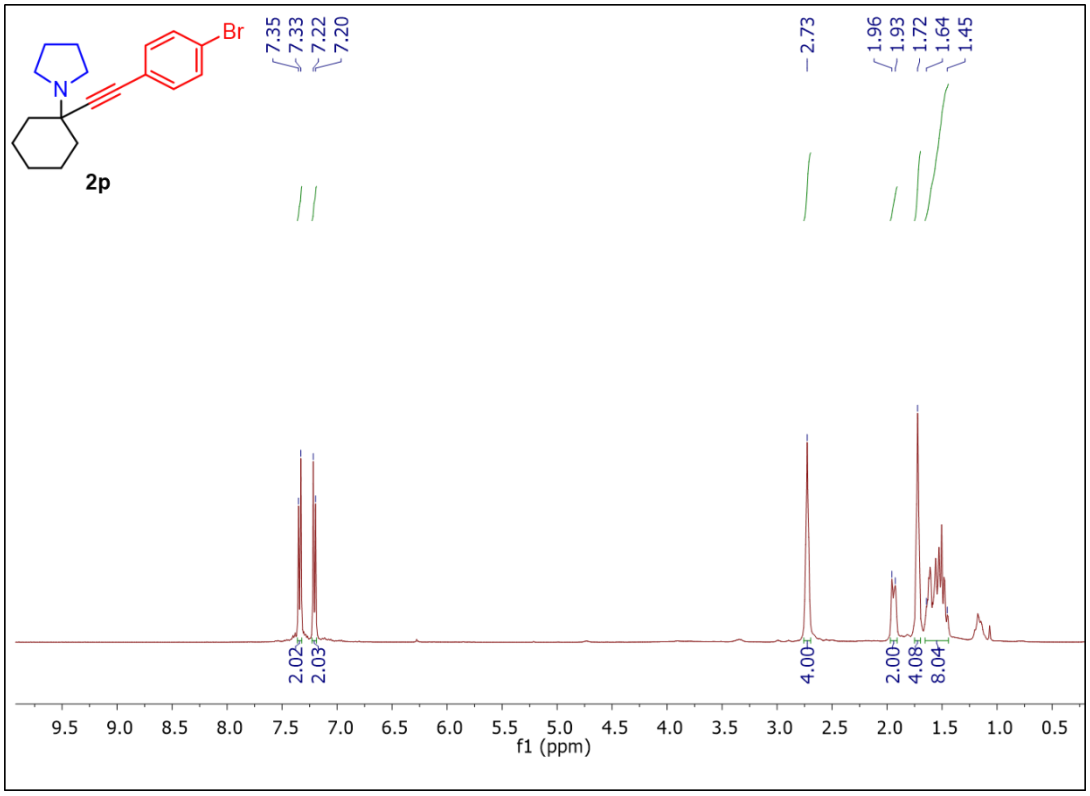

Figure 67: ^{1}H NMR spectrum of **2p** in $CDCl_3$.

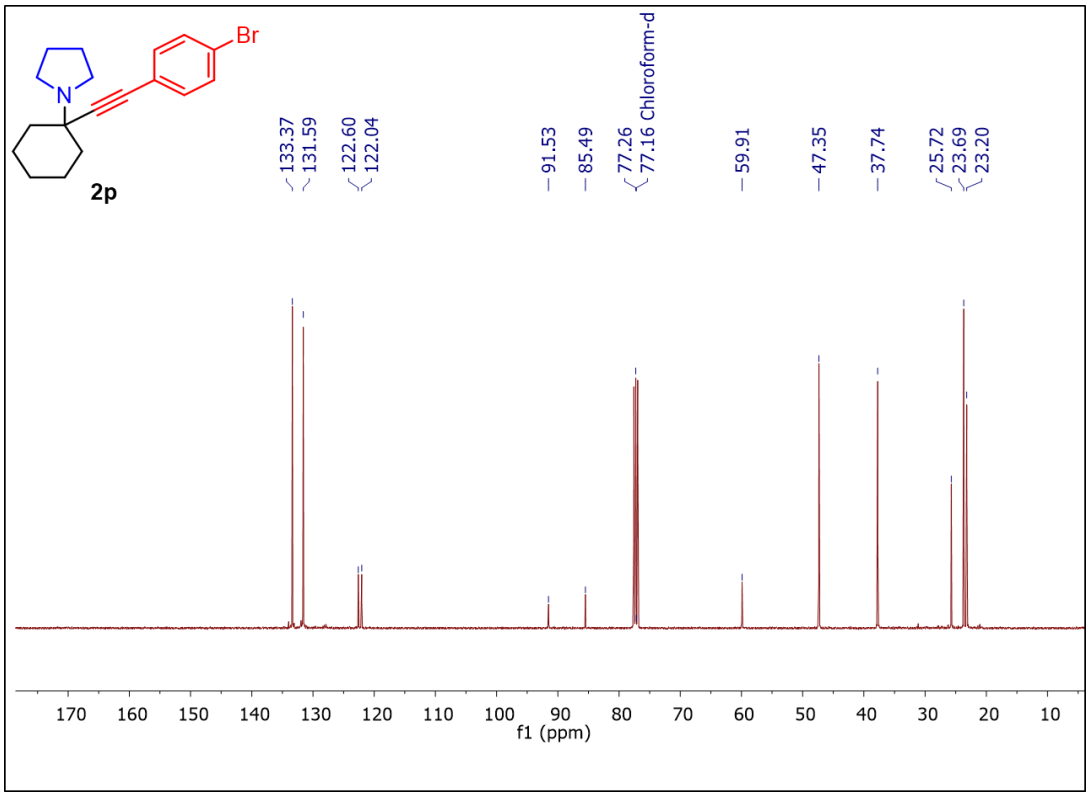

Figure 68: $^{13}C\{^{1}H\}$ NMR spectrum of **2p** in $CDCl_3$.

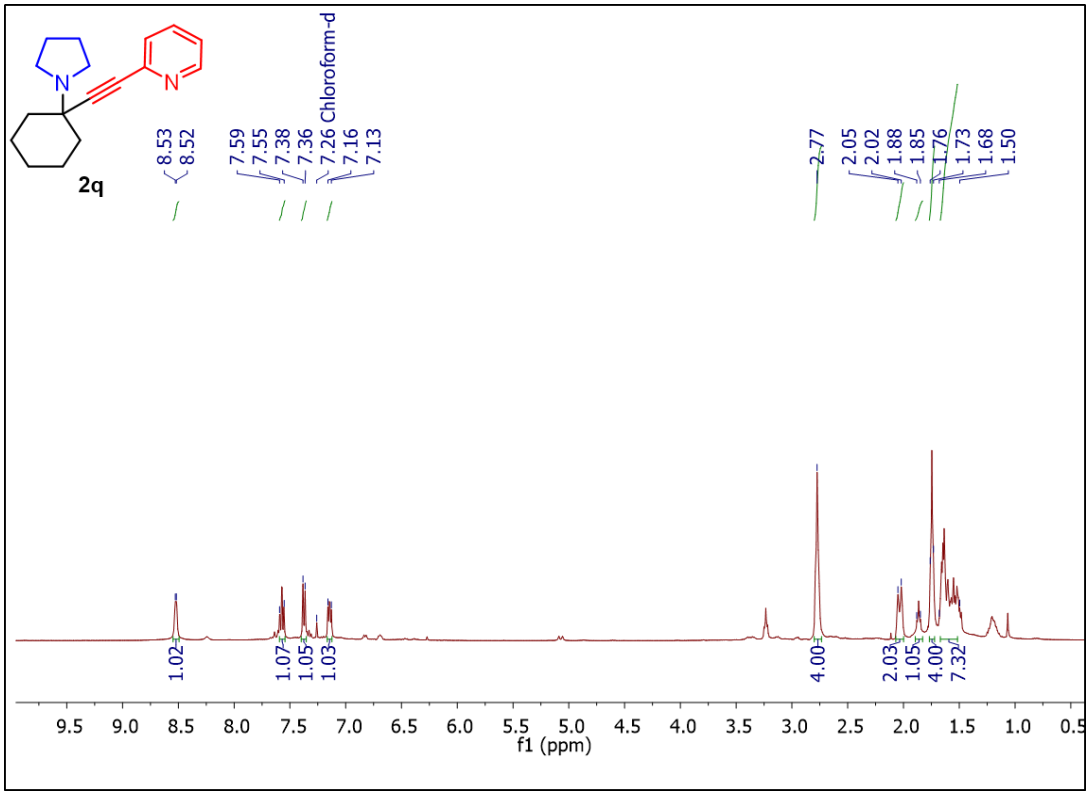

Figure 69: ^{1}H NMR spectrum of **2q** in $CDCl_3$.

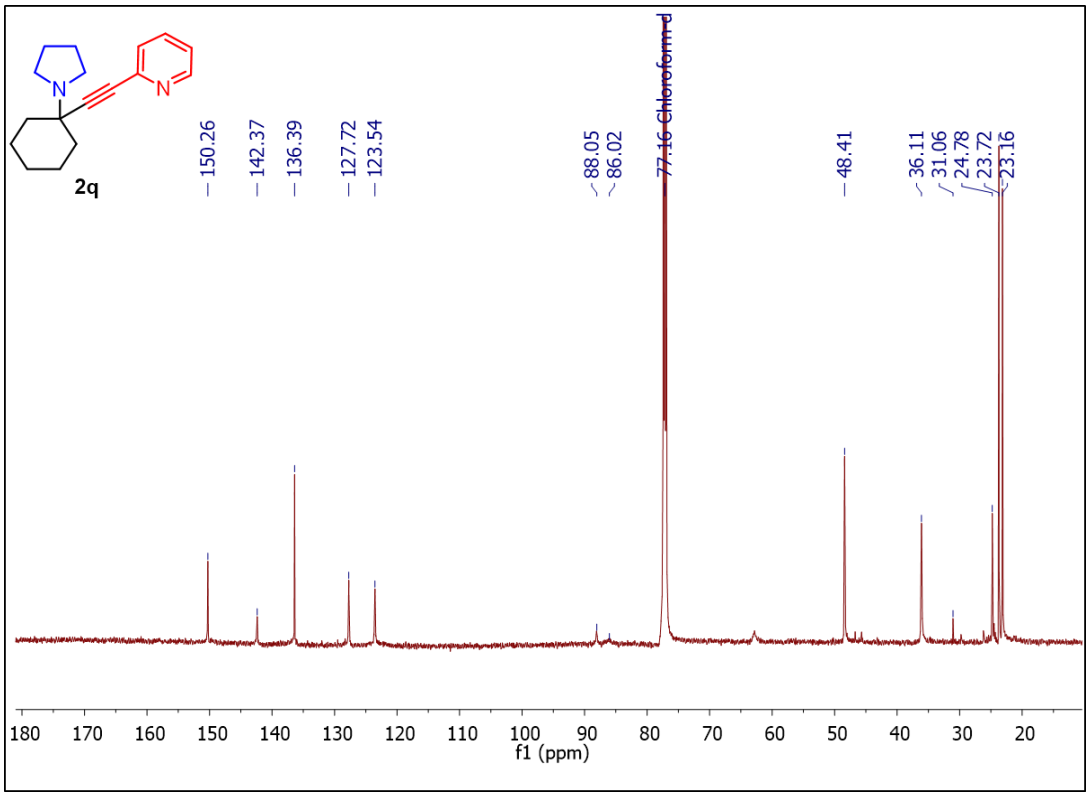

Figure 70: $^{13}C\{^{1}H\}$ NMR spectrum of **2q** in $CDCl_3$

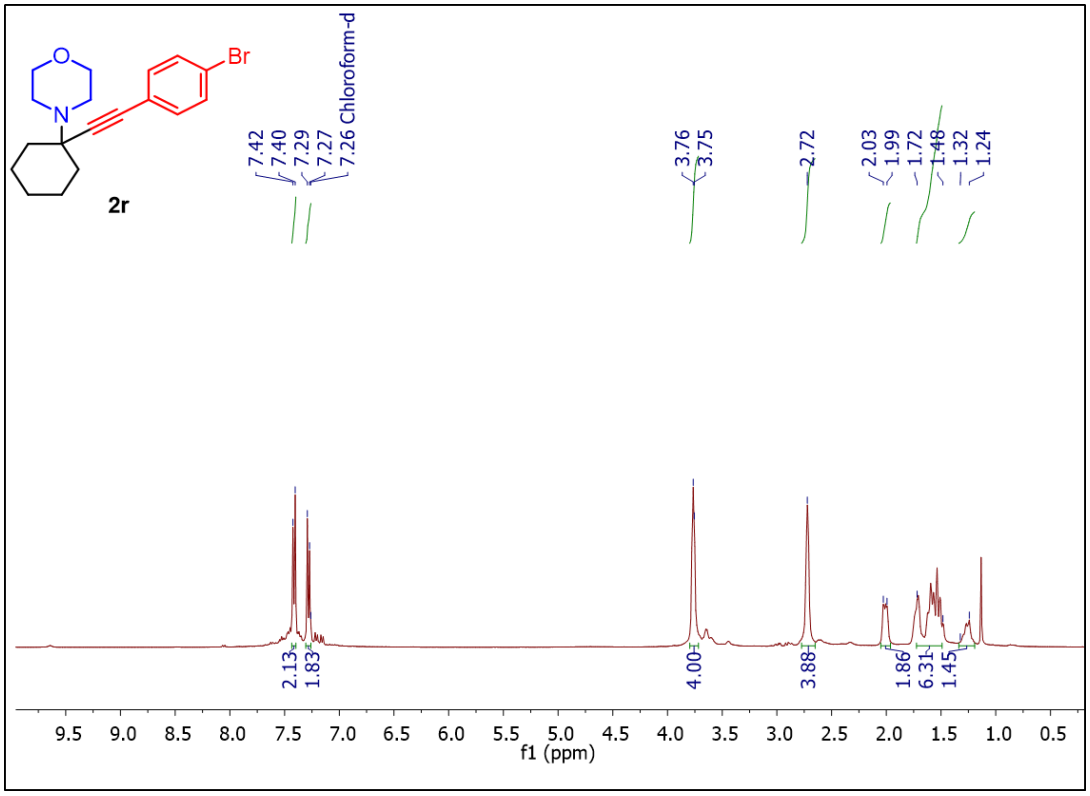

Figure 71: ^{1}H NMR spectrum of **2r** in $CDCl_3$.

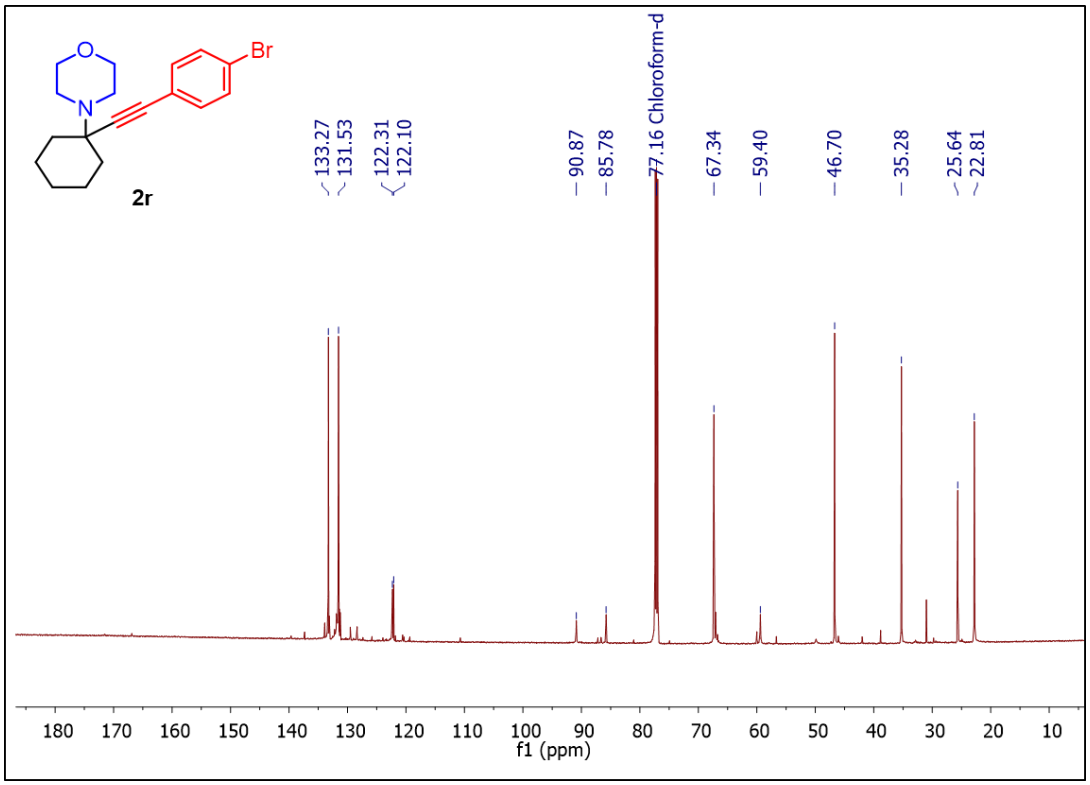

Figure 72: $^{13}C\{^{1}H\}$ NMR spectrum of **2r** in $CDCl_3$.

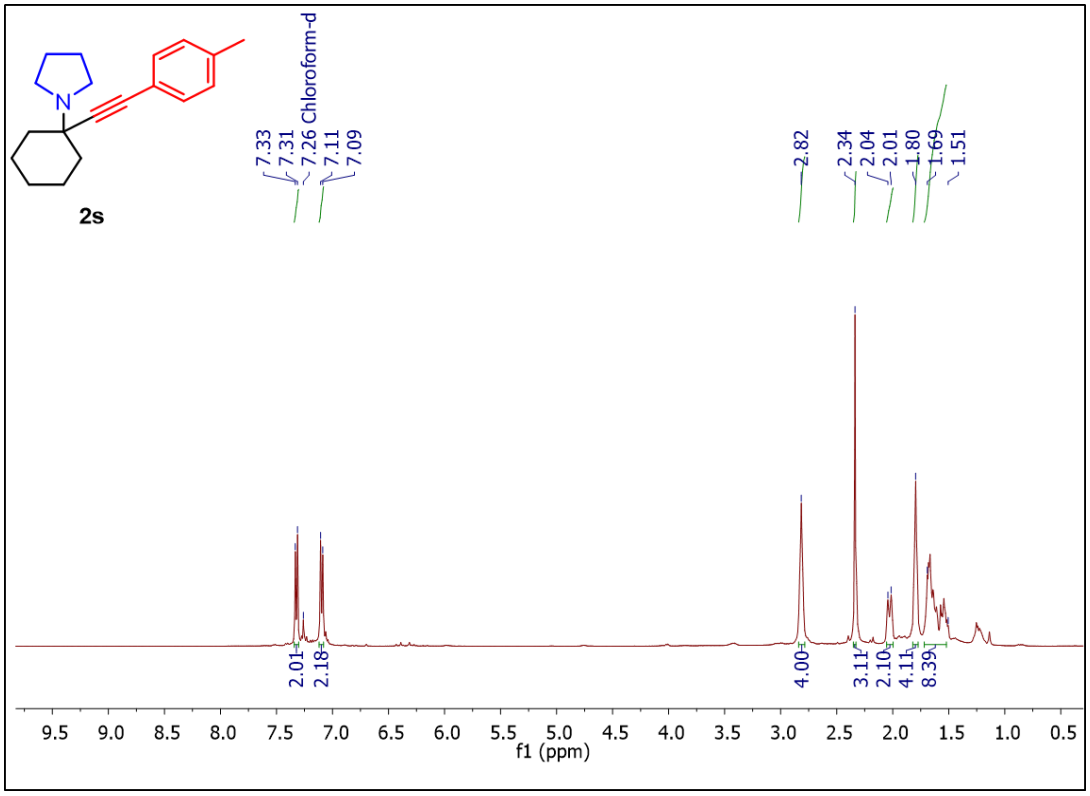

Figure 73: ^{1}H NMR spectrum of **2s** in $CDCl_3$.

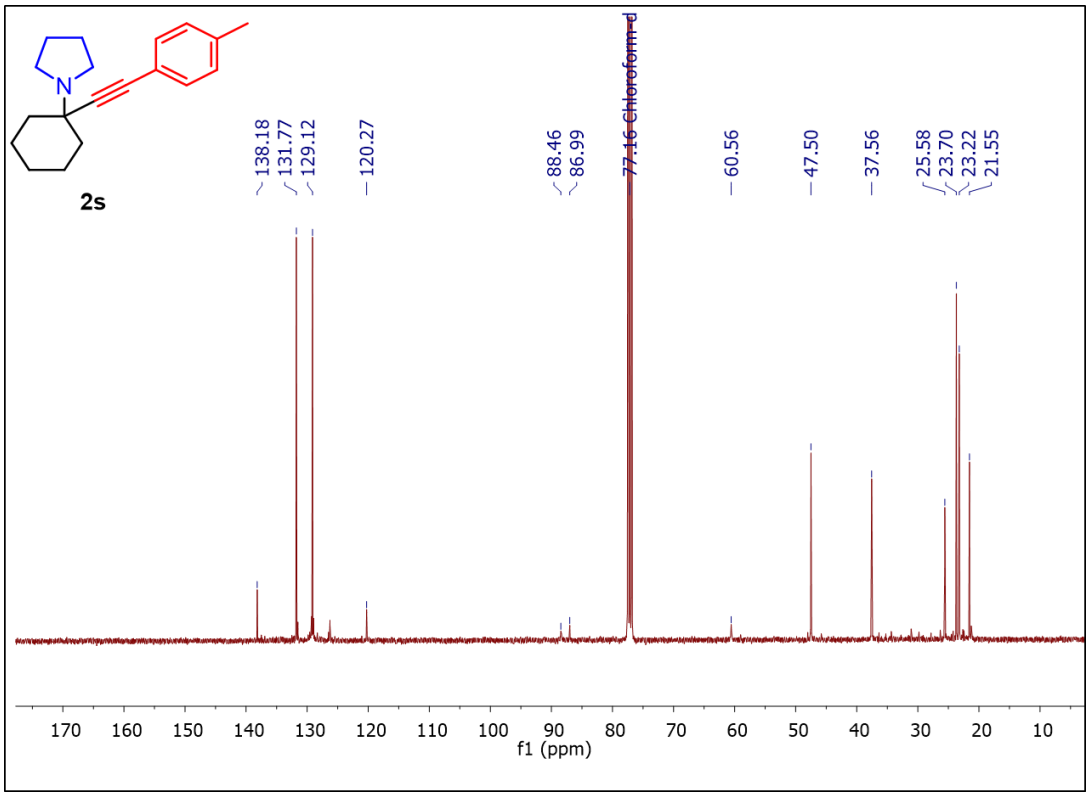

Figure 74: $^{13}C\{^{1}H\}$ NMR spectrum of **2s** in $CDCl_3$.

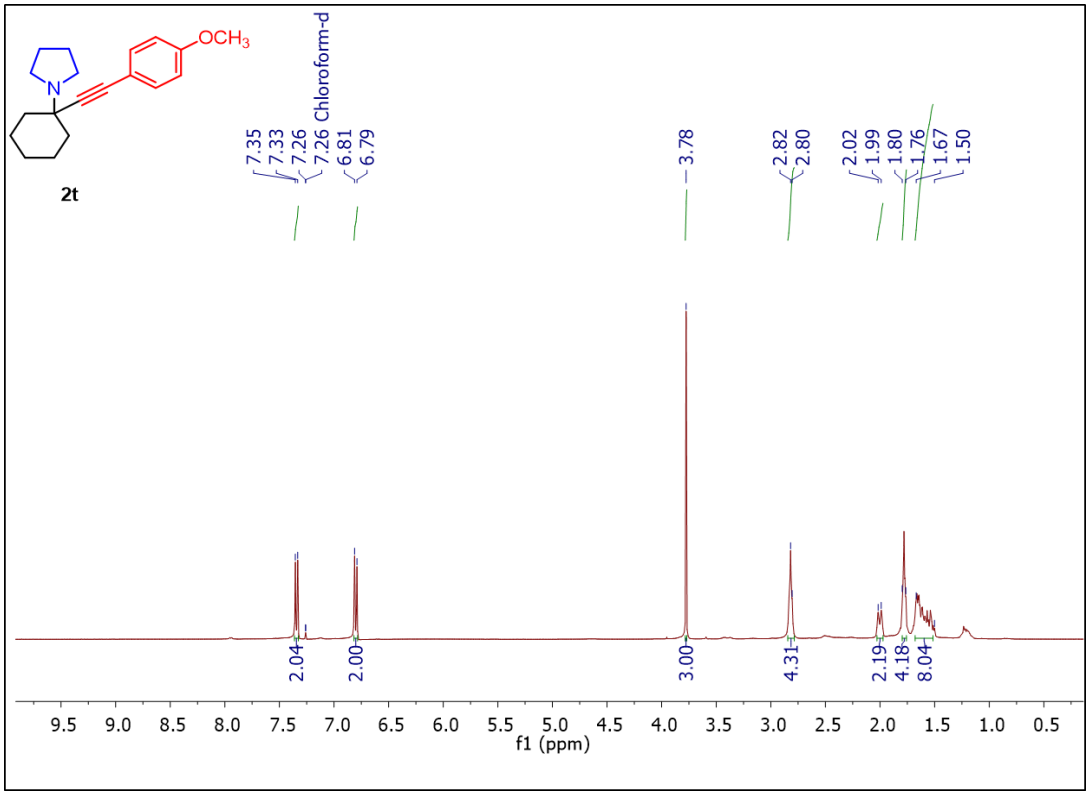

Figure 75: ^{1}H NMR spectrum of **2t** in $CDCl_3$.

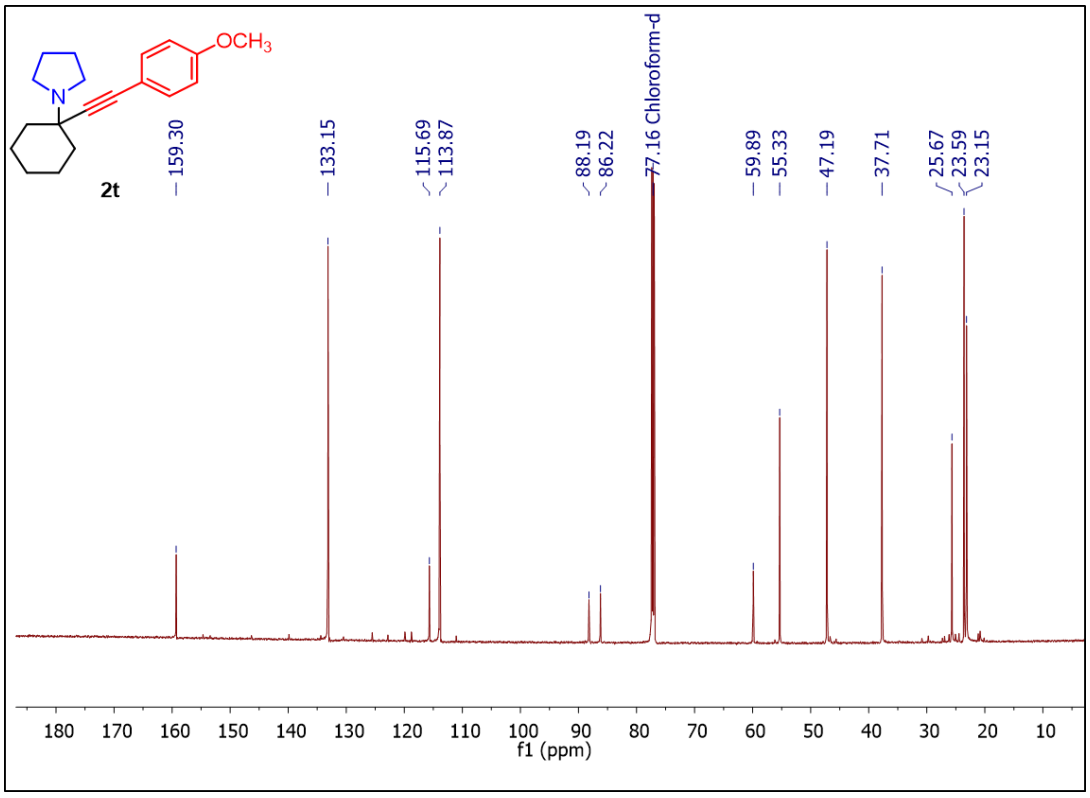

Figure 76: $^{13}C\{^{1}H\}$ NMR spectrum of **2s** in $CDCl_3$.